
UNIVERSITY OF PARMA

DiFeST, DEPARTMENT OF PHYSICS AND EARTH SCIENCE


PhD IN

INNOVATIVE MATERIAL SCIENCE AND TECHNOLOGY

XXV Cycle

---

# KEY DEVELOPMENTS IN $CuInGaSe_2$ THIN FILM PRODUCTION PROCESS FOR PHOTOVOLTAIC APPLICATIONS


DANIELE MENOSSI


YEAR 2013

# UNIVERSITY OF PARMA

DiFeST, DEPARTMENT OF PHYSICS AND EARTH SCIENCE

PhD IN

INNOVATIVE MATERIAL SCIENCE AND TECHNOLOGY

XXV Cycle


---

# KEY DEVELOPMENTS IN $CuInGaSe_2$ THIN FILM PRODUCTION PROCESS FOR PHOTOVOLTAIC APPLICATIONS


DANIELE MENOSSI

Coordinator:

Prof. ENRICO DALCANALE

Supervisor:

Prof. ALESSIO BOSIO

Prof. NICOLA ROMEO



YEAR 2013

# CONTENTS

# Introduction

## World energy situation

So far, conventional fossil fuels have dominated the world energy production scenario. Nevertheless their reserves are not unlimited, and even if these are very big, they continue to decrease day by day.
It is clear that, not very far away in future, it will be necessary to rely on alternative resources, for fulfilling the continuous increasing energy demand.
Since the early years of the 20$^{th}$ century, in fact, it has been started looking for alternative energy sources, with respect to coal, oil and natural gas, whose prices continued to increase and in addition, a new "cost" of the produced $CO_2$ started to be taken into account.
For these reasons, renewable energies began to obtain high consideration, also because, as the words say, they are special energy sources which can "regenerate" and this makes them have a very long, almost infinite, time existence.
From then on, the world renewable-electricity production has had the fastest growth, among the others, reaching in 2010 the 19.6% share of the total (Figure 1).

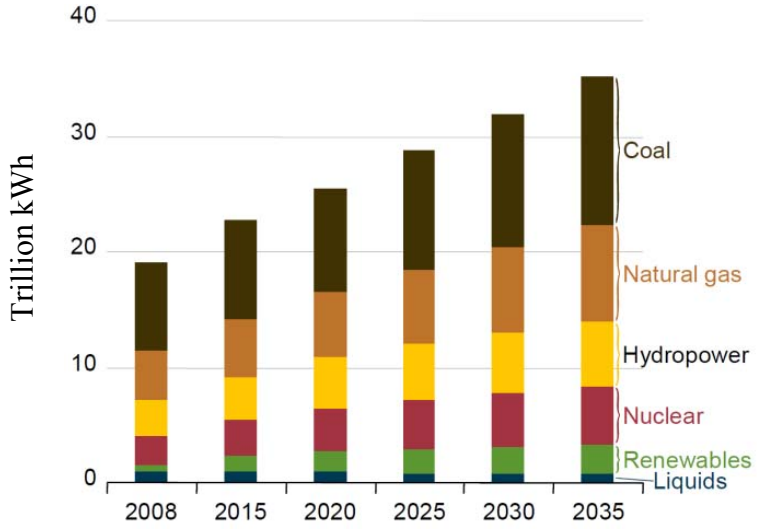


*Figure 1. World net electricity generation by fuel type, 2008-2035 expectation in trillion kWh [1].*

Among renewables, the photovoltaic (PV) technology is considered one of the best energy resources, to fulfill the world demand.
Every square meter of land on Earth, in fact, on average is exposed to enough sunlight irradiation to generate about 1.7 MWh of energy every year, considering of using the currently available technology.
If it was possible to collect the total solar energy that reaches the Earth's surface, it could be produced such a high amount of electric energy to overcome the existing global energy consumptions 10,000 times over (Figure 2).

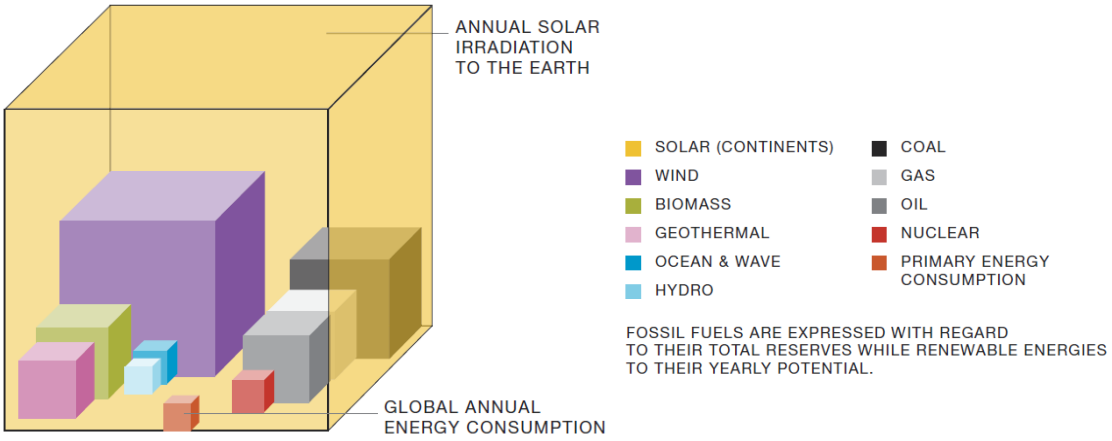


*Figure 2. Solar irradiation potential versus established global energy resources [2].*

Considering this, it can be easily understood that the solar irradiation has the highest potential, among all the global energy resources, to cover completely the world electric energy needs.

Unfortunately, the incident solar irradiation can't be fully converted into electricity by photovoltaic devices and, at the same time, not all the Earth's surface can be used to collect it. Nevertheless, International Energy Agency (IEA) calculations show that if just the 4% of the world's very dry desert areas were used for PV installations, the world's total primary energy demand could be however met [2].
It is clear then that the overall solar power really usable and convertible into electricity is still much higher than the total needs.
This is the major reason which has driven the constant development of photovoltaic technology during the time.
In fact, over the last decade PV technology has shown the potential to become the global major source of power generation, growing all around the world faster than anyone had expected.
For example, at the end of 2009, the world's PV cumulative installed capacity was about 23 GW, while one year later it was 40 GW. In 2011, even more than 69 GW were globally installed.

During last ten years, the photovoltaics growth rate has been on average of about 40%, reaching in 2011 an expansion of almost 70%, an exceptional level among all renewable technologies.
PV is now, after hydro and wind power, the third most important renewable energy, in terms of globally installed capacity and provides 0.2% of total global electricity generation.
This is still a low value, but it is expanding very rapidly due to effective supporting policies and recent dramatic cost reductions of PV energy.
It is estimated that PV is projected to provide 5% of global electricity consumption in 2030, rising even to 11% in 2050 [3].

Another important aspect of PV technology is represented by its remarkable environmental advantages for the electricity generation, over conventional technologies.
During their working operation, PV devices do not produce any noise, toxic-gas emissions, nor greenhouse gases.
In this way, it is possible to meet the electricity demand, safeguarding at the same time the environment.
For example, every gigawatt-hour of electricity generated by photovoltaics would prevent the emission of about 10 tons of $SO_2$ , 4 tons of $NO_x$ , 0.7 tons of particulates (including 1 kg of Cd and 120 kg of As) and up to 1000 tons of $CO_2$ , with respect to the burning of coil.
In addition, the amount of material requested to produce PV devices is extremely low, about 1 gram of semiconductor material per MWh, which is about the same order of magnitude of a breeder reactor, with fuel recycling of 50% (4 g of uranium/MWh) [4].
These reasons further confirm that PV technology is one of the best energy resources for replacing fossil fuels.
Moreover, most of the hazardous materials processed in PV technology, like for example Cd, Te, Pb, Se and S are used however in form of more stable compounds; doing so their dangerousness can be “reduced”, also because many of them are usually waste materials, coming from mining works, which otherwise would be left in the ground.
During last few years even the recyclability of PV modules started to take place, adding other environmental benefits, which enhance the market support.

Despite the many advantages described about PV technology, at the same time it is necessary to take into account the cost needed to produce the final electric energy.
The production of PV devices has, of course, a cost, which constantly decreased over the time, but however modules’ prices are still higher, about 0.8-1 €/Wp (0.16-0.35 €/kWh in Europe), than the cost to produce electricity from fossil fuels, which is about 0.4 €/Wp (0.1-0.2 €/kWh in Europe) [5, 6].
With regard to this, it has been introduced the term of grid parity, which is traditionally defined as the point in time where the generation cost of solar PV electricity equals the cost of conventional electricity sources, like fossil fuels.

It can be easily understood that when PV modules' price will be comparable, or even lower than the price of electricity obtained from fossil fuels, the grid parity will be reached and in this situation renewable energies will be completely equivalent to the conventional fossil ones, or even more competitive.
Since the beginning, the grid parity has been the major challenge of PV technology.
In some countries this condition has been already obtained, mainly due to the local fuels prices policy, but it is still a challenge for all the rest of the world.

All these reasons have constantly led the photovoltaic world to study and develop devices with more and more high efficiencies, in order to reduce the energy production cost.
After Becquerel discovered the photovoltaic effect in 1839, by the action of light on an electrode in an electrolyte solution, the first photovoltaic technology needed to wait many years to take place and has been represented essentially by "bulk" devices, made of mono and poly-crystalline Silicon (c-Si) wafers.
First Si junction based solar cell, in fact, was produced in 1954 and had a conversion efficiency of 6%. From that year on, the technology improved in an outstanding way, reaching nowadays the record conversion efficiency of 25%, for a mono-crystalline Si based solar cell [7].
Nevertheless, the process for producing this kind of cells was very expensive and not properly suitable for a large scale production point of view.
For this reason, another way to produce c-Si based solar cells has been developed, the poly-crystalline technology, which is a bit cheaper and allows to obtain devices with about 20% conversion efficiency [8].
Even if Silicon is a quite cheap and abundant material on Earth and it permits to obtain high conversion efficiency devices, the c-Si based solar cells production process requires a lot of preliminary steps, like first of all the high-temperature purification, the further growth into very big crystalline ingots and their cut into wafers, which are still quite expensive and time consuming.
In addition, in order to obtain a module, the final electrical interconnection of many devices is needed and, since it is hand-made, this represents a limiting factor in the large-area process scalability.
Moreover, Si has a "low" absorption coefficient in the visible part of the solar spectrum, so c-Si based solar cells require a certain amount of material to absorb most of the incident light and, due to the wafers handling and processing restrictions, it sets for the moment about 200 μm thickness.
Even other materials with higher absorption coefficient, like GaAs, have been studied for producing crystalline solar cells, and even if they demonstrate higher efficiencies and good space applications they result having a too low efficiency/cost ratio.

Considering that a large part of the final cost of a PV module is related to the amount of material used, it is clear that using less material it is possible to reduce the PV device cost per Watt.
To solve this problem it was developed the thin film technology, by which materials can be deposited into very thin layers, on the micrometer average thickness scale.
In 1954, for example, the first all-thin film solar cell was produced using a $Cu_xS$/CdS, with a 6% conversion efficiency.
A real large-scale production of this technology started only in 1980s, producing amorphous Silicon (α-Si) devices.
This material, differently from the crystalline one, has a direct energy gap and can absorb most of the incident light just in 1-2 μm thickness, allowing so a consistent decrease in amount of used material.
α-Si based solar cells reached so far efficiencies of about 10% [9], but modules are still demonstrating low time stability problems.
However, since thin film deposition processes are much more cheap and scalable with respect to the Silicon ones, considering their big potential, the photovoltaic world's research has been strongly driven to find out new materials to be used with this technology.
A much more efficient and stable material has been found in Cadmium Telluride (CdTe), which, having a direct energy gap too, but an even higher absorption coefficient, it can allow to produce solar cells with higher efficiencies, up to 17% [10, 11].
Its development has been greatly increased during last years, representing today more than 45% of thin film PV production and the 13% share of total PV production.
Also $CuInSe_2$ has resulted to be another very good PV material.
The $CuInSe_2$/CdS has been the sixth system, along with junctions based on Si, GaAs, CdTe, InP and $Cu_xS$ to show energy conversion efficiencies up to 10%.
For example, in 1974 a $CuInSe_2$/CdS heterojunction solar cell, made up by depositing a CdS film onto a *p*-type $CuInSe_2$ single crystal was presented.
That solar cell exhibited a photovoltaic conversion efficiency of 12%, which was a very high value for that period [12]. Some years later, in 1985, the first all-thin film solar cell based on the *n*-ZnCdS/*p*-$CuInSe_2$ heterojunction was produced by Boeing laboratories, which exhibited a conversion efficiency of about 11.9% [13].
These promising starting results led the PV research to study new methods for the preparation of $CuInSe_2$ based solar cells and even to develop new processes to fabricate $Cu(In,Ga)Se_2$ , with the purpose of producing devices with higher efficiencies, in a reproducible way.
Adjusting the Ga concentration into this material, it has been possible to produce $Cu(In,Ga)Se_2$/CdS based thin film solar cells with conversion efficiency up to 20.3% [14].
This latest result is, so far, the highest value of photovoltaic energy conversion efficiency for an all-thin film solar cell.

Nevertheless, c-Si technologies have dominated the market for the last 30 years and today still represent about 80% of the market, but, thanks to these high results, the thin film technology have been boosted with an impressive growth rate, reaching nowadays the 20% of total share (Figure 3).

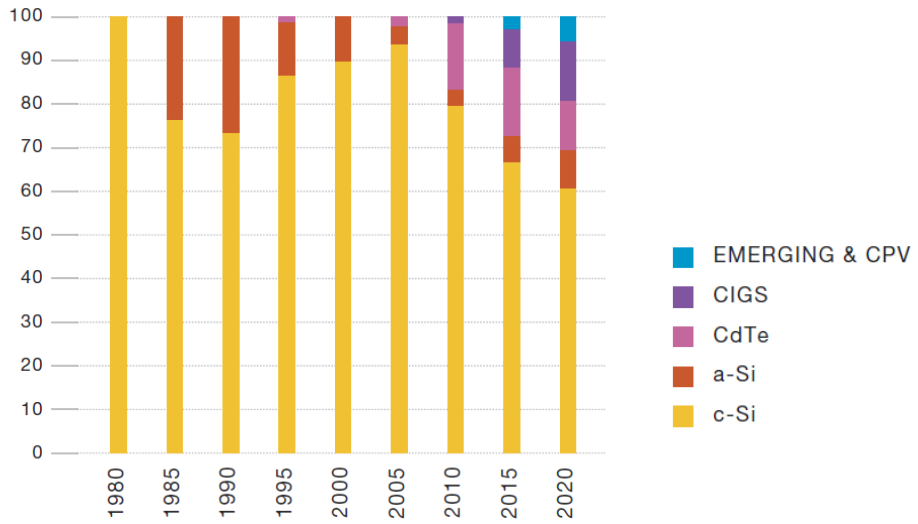


*Figure 3. Evolution of the technology market share and future trends in % [2].*

Technologies such as concentrator PV, organics and dye-sensitized solar cells are starting to enter the market just now.
However, they are expected to achieve significant market share in the next few years, gaining around 5% of the market by 2020.

## Advantages of thin film technology

In thin film (TF) technology, as already said, materials are deposited into very thin layers (films) of about few micrometers in thickness; in this way the average amount of material used, to produce solar cells, can be reduced up to 90% with respect to c-Si technology, permitting a considerable reduction of its contribute to the final cost of the module. This represents the major advantage of TF technology.
The cost of PV systems has been constantly decreasing over time and over the past 30 years the price of PV modules has reduced by 22%, each time the cumulative installed capacity (in MW) has doubled.
Depending on cell technology, the energy pay-back times (periods after which the cost of PV modules is recovered by using them and in some cases even by selling the exceeding energy produced) are now between 1 and 2 years for a Southern-European locations and between

1.7 and 3.5 years for Middle-European locations. Thin film technology is at the very lower edge of this range [15].
The other major advantage is that thin film technologies are also cheaper and more scalable than the c-Si ones, since they allow to build up almost fully-automated in-line processes, at the end of which it is possible to obtain a complete module and not only an assembly of smaller cells, like for mono or polycrystalline-Si based modules.
Recent innovations, like laser scribing, permit to divide a module into single solar cells (which are all deposited onto the same substrate) and to electrically connect them, during the in-line fabrication process, by interconnections fully integrated into the module itself.
This is a very important time-saving aspect into the production process, which doesn't need any further use of manual and external metal connections.

At the same time, films so thin can't stand alone only by themselves, but need a more mechanical resistant substrate.
Since the "active" part of a TF solar cell is constituted by these thin materials layers and not by the substrate, this last one can be made of much more cheap materials (with respect to Silicon wafers) like window-panes glass, without influencing too much the production costs.
Moreover, TF techniques have demonstrated to be very reliable for the materials deposition onto large-area substrates, even on other different kind of materials like metal foils, polymers and even commercial ceramic tiles, resulting then suitable for the large-scale production.

Again due to their small thickness, thin films are not too much stiff, but they can even "follow" different substrate geometries, like curved ones.
In fact, thin films can be also deposited on curved surfaces, where it would be impossible for monolithic and almost flat c-Si based ones and this further enhances their usage potential and market range.

With TF techniques it is even possible to produce solar cells in different "configurations", letting the incident solar light pass through the substrate (superstrate configuration), or not (substrate configuration).
In this last case a "new world" has been opened.
Since in substrate configuration it is no more necessary to use transparent substrates, even opaque ones now can be adopted.
Using for example thin metal foils, or resistant polymer sheets and thanks to thin films' mechanical properties, it is possible to produce flexible solar cells, which have the advantage of adapting to almost all possible installation conditions, far beyond the restrictive flat ones.
Combining these last features, TF technology can improve then the so-called photovoltaics building integration (BIPV), which consists in introducing PV devices into an already existing and, most of all, un-modifiable architectonic system, without altering the building standards.

Finally, despite all, at this moment prices of photovoltaic modules are quite similar for both thin film and c-Si technologies and in some cases c-Si based modules are even cheaper.
This is due to the fact that, despite the many advantages of TF technology, c-Si has been experienced for a longer time and being its production much wider, it leads to reduce part of the industrial production costs.
A the same time there is to take into account that, in the case of CdTe and majorly of $Cu(In,Ga)Se_2$ , thin film solar cells have reached conversion efficiencies values of 17% and 20.3% respectively, quite close to the 25% world record c-Si one and with a very high speed rate, much higher than c-Si.
Considering, then, the constant fast technological evolution, which is happening into the thin film photovoltaic world, and the fact that its production processes tend to be further simplified day by day, it is easy to foresee that within next few years (2020) thin film modules could be produced with much lower costs, about 0.5-0.6 €/Wp, permitting to reach sooner the grid parity condition [11, 16].
The European Industry Photovoltaic Association (EPIA) expects that by 2020 Silicon wafer-based technologies will account for about 61% of sales, while thin films will increase up to 33%. In this way, thin film modules will soon be able to compete with conventional modules based on Silicon wafers and even to be more profitable from the efficiency/cost ratio point of view [17].

Even if $Cu(In,Ga)Se_2$ is a photovoltaic material with a very big technological potential, able for example to absorb 90% of the solar spectrum just in a 0.5 μm [18] thickness layer, nevertheless, because of its difficult preparation, it still seems to be quite complicated to be produced on large scale with the optimal characteristics.
At the same time, $Cu(In,Ga)Se_2$ based modules have showed to be able to keep high performances for long time, more than 20 years and also to stand the atmospheric agents without damaging, making these devices very competitive into the photovoltaic market.

Considering all the features described above, $Cu(In,Ga)Se_2$ has resulted to be, so far, the most promising thin film photovoltaic material able to compete with crystalline-Silicon.
For this reason, the aim of this PhD thesis work is to develop an innovative process for growing $Cu(In,Ga)Se_2$ thin films, starting from precursors obtained by new materials, like Indium Selenide $In_2Se_3$ and InSe, Gallium Selenide $Ga_2Se_3$ and GaSe and Copper, suitable for producing in a reproducible way high-efficiency solar cells.

# The photovoltaic effect theory

## 1.1 The photovoltaic effect

The solar cell is a device able to convert the incident light power into electric power.
Its working principle is based on the photovoltaic effect, which consists in the absorption of incident optical photons by the device constituent materials and the consecutive generation of electron-hole couples inside them.
When a particular material, like a semiconductor, is hit by an incident photon, this photon can be absorbed only if its own energy $h\nu$ is bigger than the difference, in energy, between the valence (V.B.) and conduction band (C.B.) of that material, known as the forbidden energy gap $E_G$.
In this case, the photon's energy can be transferred to an electron inside the valence band, which having received enough energy is excited and is now able to make a transition from the valence band to the conduction one.
This electron is now an "almost free" carrier, which is responsible of the semiconductor electric conduction and as a consequence of the transition, it has left a positive charge, a hole ($h^+$), into the valence band which is responsible of the semiconductor hole conduction.
In this way an electron-hole couple has been generated.
Once this conduction electron has been generated, it has a specific period, called mean life time $\tau$, before relaxing coming back to the starting valence band.
When the electron is back in the valence band, it combines with the hole left, restoring the charge neutrality; this mechanism is called recombination.
If the photo-generation of these charge carriers happens inside a region in which there is an enough strong electric field, this last one will be able to separate the generated electrons from holes and even to drift them to the external contacts of the device, in such a way to produce a current flux between the contacts.
A suitable electric field can be produced inside a solar cell by building the ***p-n* junction**.
This is a structure made up putting in contact two layers of the same material (homojunction), or of different materials (heterojunction), but in both cases doped in a different way, one with an excess of electrons (*n*-type) and the other one with an excess of holes (*p*-type).

The doping mechanism of a semiconductor is produced by forming specific defects inside its crystal lattice, which modifies the whole electronic configuration of the lattice itself.
For example, these defects can be introduced by producing vacancies of reticular atoms, interstitial atoms inside the lattice or substitutions in reticular sites with other kinds of atoms.
In this latest case, if a reticular atom is substituted by another one with one plus electron in the outer shell, the lattice will locally have one plus electron, with respect to the necessary. This will result in supplying the lattice of one "almost free" electron carrier (***n*-doping**), which will contribute to its electronic conductivity.
On the contrary, if a reticular atom is substituted by another one, with one electron less in the outer shell, the effect consists in giving the lattice a lack of one electron with respect to the necessary. This will result in supplying the lattice of one "almost free" hole carrier (***p*-doping**), which will contribute to its hole conductivity.
It's easy to understand that the higher is the number of similar dopant defects into the material, *n* or *p*-type, the higher is the number of corresponding charge carriers which will contribute to the semiconductor conductivity.
By putting in contact a *n*-type with a *p*-type semiconductor, a diffusion process of carriers happens, as a consequence of their concentration gradient.
Then, it starts an injection of minority carriers (electrons from the *n*-type towards the *p*-type material and holes from the *p*-type towards the *n*-type one) through the junction region, which causes respectively an accumulation of charges into these materials and consequently the formation of a region, at their interface, without free carriers. It is called **space charge region SCR**, or depletion region and its width is denoted with W (Figure 4).
Furthermore, the width of this region, in each of the two constituent materials, results to be reverse proportional to their respective carrier concentration, depending on the concentration gradient of the charge carriers and on the diffusion mechanism.
Since at the sides of the junction the same number of carriers should be collected, the zone with less charge carriers will empty more, in comparison with the other side of the junction.
For this reason, the carrier diffusion length into both the materials depends on the concentration gradient, that is established at the two sides of the junction.
For two materials with a very big difference in the concentration of a specific charge carrier type, the junction side with the higher concentration will be little depleted, but it produces a great diffusion of charge carriers into the other side of the junction, causing a depleted zone as wide as big is its lack of the same type of charge carriers.
In this way, into the *n*-type part of the junction, an accumulation of positive charges, holes left by the electron migration, will be formed, while into the *p*-type part negative charges will be accumulated.

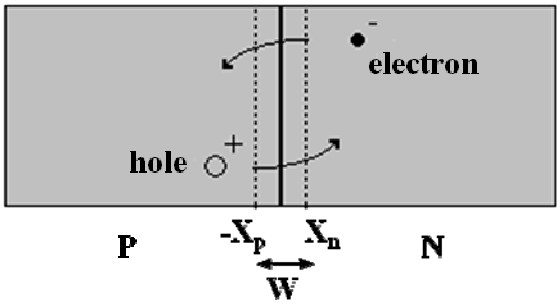


*Figure 4. p-n junction and formation of the space charge region.*

As the carriers diffusion goes on, the charges accumulation into the two materials tends to produce a potential difference across the junction acting like a barrier for the carriers, with a corresponding growing electric field, whose electrical force is opposite to the diffusion transport. In this way the diffusion process continues until the potential barrier is high enough to produce an electric field able to stop any further movement of carriers through the junction; now an equilibrium situation is reached and the potential barrier, which stops the diffusion, is the so-called built-in potential ($V_{bi}$).

From the energy band diagram point of view, this equilibrium is obtained when the charge transfer balances the two materials leading the junction structure to have an unique Fermi level $E_f$ , defining a stationary condition with an unique energy value for its carriers.
As a consequence of this unique Fermi level formation, a bending of the two materials' bands edges must happen, promoting a continuum of their valence and conduction bands across the junction.

Then, in order to promote a good photovoltaic effect most of the incident light must be absorbed into the junction region, where the electric field is present.
Depending on the absorption coefficient α, most of the incident light can be absorbed into a material within a distance from the surface equal to 1/α and in some cases this distance can be even wider than the SCR.
Carriers generated outside the SCR can however diffuse into it and then be accelerated by the electric field thanks to the material thermal energy, but only within a specific distance from it. All the carriers photo-generated too far from the junction in fact can't reach it in time; in this case they will easily recombine, without contributing to the photo-current and so they will be lost.

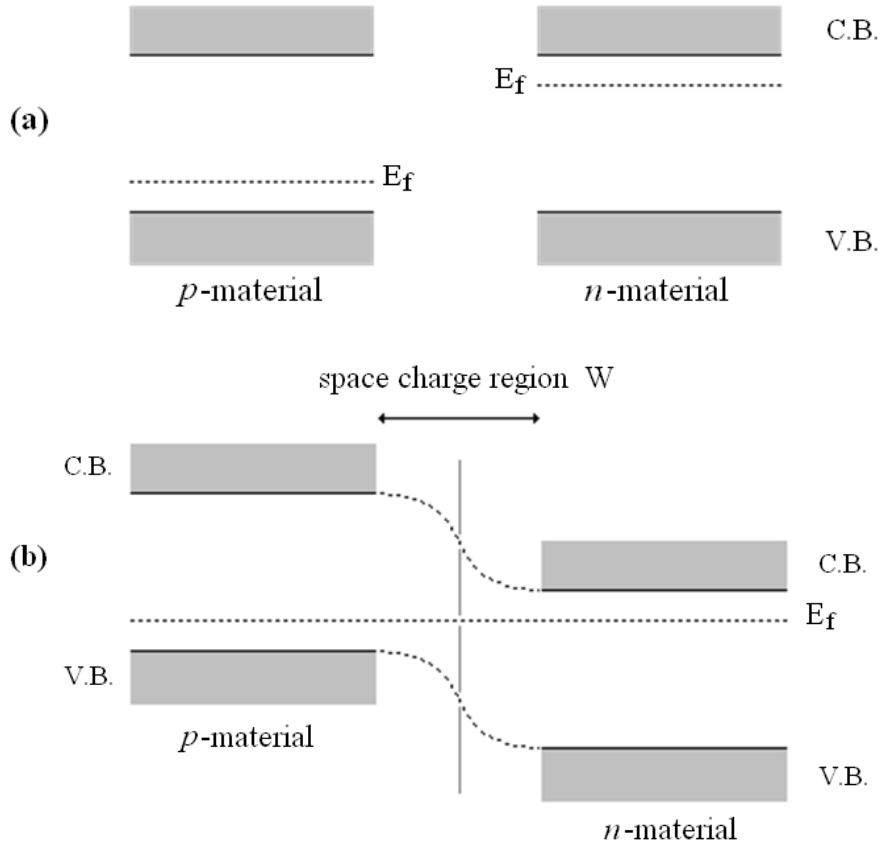


*Figure 5. Energy band configuration for* ***(a)*** *separated semiconductors and* ***(b)*** *homojunction of the two materials.*

This limit distance from the junction, which allows the carriers to diffuse across the semiconductor, is called diffusion length *L*. This is a specific characteristic of each material and it depends on the mobility and on the mean life time of the carriers.
Hence, carriers transport is promoted by the sum of the material's thermal energy, outside the SCR and of the electric field (which depends also on the charge carrier concentration), into the SCR and however happens within a maximum distance *L* from the junction.
It is clear that in order to avoid this problem it is necessary to produce inside the *p-n* junction an electric field wide enough to cover completely the light absorption region, in order to collect most of the generated carriers.
Nevertheless, the width of the SCR is limited by the maximum difference in doping level producible into the materials and in general it results difficult to produce a very wide SCR.

At the same time, if carrier generation extends much beyond the diffusion length, all these carriers will not be collected.
For this reason it is preferable to use materials with higher absorption coefficients, which can absorb the incident light in a smaller thickness; in this way a narrower SCR is required to cover all the light absorption region and carriers can be generated all within their diffusion length area.
A the same time, for a **homojunction** solar cell, it is necessary to remember that the materials which form the junction are equal (but not in carrier type) and have the same "good" absorption coefficient.
Then, to avoid that the incident light is absorbed into the material which comes before the junction, it is very important that the junction itself is formed as near as possible to the surface exposed to the incident light and, depending on the absorption coefficient, in general at a maximum depth of about some tenths of nanometres.
Making layers of mono- or even poly-crystalline materials in form of thin film is quite difficult to obtain the above condition, since these thin layers tend to be affected by a bad crystallinity and a high concentration of surface-state defects, which introduce energy levels deep into the of the material forbidden gap, which are able to trap and so to reduce the amount of photo-generated carriers.

To solve this problem, it is better to produce the junction using two different materials: a first one, the **window layer**, with a wider energy gap, higher than 2 eV in order to let the incident light pass through itself and reducing so its absorption and a second one, the **absorber layer**, with an energy gap of about 1-1.5 eV in order to absorb most of the incident solar radiation, promoting then a higher electron-hole couple generation.

At this point, it is necessary to remember that the photovoltaic effect is based on the transport of minority carriers across the junction, keeping also in mind that electrons have in general a mobility about two order of magnitude higher than the holes.
For these reasons, in order to promote an efficient photovoltaic effect, it is very important to use the *p*-type material like an absorber; in this way, once the carrier couples are formed, thanks to the electric field the electrons will go immediately towards the *n*-type material, with a speed much higher than the recombination mechanism's one, minimizing the carriers lost.
Having chosen the *p*-type material as the absorber, to guarantee a good separation of carriers the electric field must cover almost all the absorption region; for this purpose it is necessary that at least 90% of the electric field falls into the *p*-type part of the junction.
Considering for a while electrons and holes with the same mobility and reminding also the relation which links the material electronic conductivity $\sigma$ to its carriers mobility $\mu$ , $\sigma = \mu * q * N$ ,

in order to have a SCR more shifted into the *p*-type part it is necessary that the *n*-type material has a number of majority carriers *N* (electrons) much higher than the one (holes) of the *p*-type, resulting in an electronic conductivity of the *n*-type material at least one order of magnitude higher than the *p*-type one.

## 1.2 The ideal device

Introducing some approximations, like:

a) the "abrupt" junction (net separation of *p* and *n* layers without any intermixing),
b) complete charge depletion into the SCR,
c) presence of only weak electric field into the junction,
d) low injection mechanisms,
e) stationary conditions,
f) any carrier generation from outside,

it is possible to describe the behavior of a *p*-*n* junction considered "ideal".

Applying a forward bias V to the junction, the diffusion of minority carriers across it can be induced and this transport can be described by the next ambipolar equation:

$$\Delta p(x) = p_0(x_n) * (e^{qV/KT} - 1) * e^{-(x-xn)/Lp} \qquad (1) \qquad \text{(for the } n\text{-type material)}$$

where $x_n$ is the edge of the SCR into the *n*-type material and $L_p$ is the holes' diffusion length

$$L_p^2 = (KT/q) * \mu_p * \tau_p$$

From equation (1), the hole current density can be defined as

$$J_p(V,x) = (KT * \mu_p/L_p) * p_n^0 * (e^{qV/KT} - 1) * e^{-(x-xn)/Lp}$$

and, in the same way, also the electronic one as

$$J_n(V,x) = (KT * \mu_n/L_n) * n_p^0 * (e^{qV/KT} - 1) * e^{(x+xp)/Ln}$$

where $p_n^0$ and $n_p^0$ are respectively the minority carriers densities into the *n*- and *p*-type materials, at the equilibrium and far away from the junction.

The total current density, which crosses the junction, can hence be obtained

$$J(V)_{TOT.} = J_p(V) + J_n(V) = J_s^0 * (e^{qV/KT} - 1) \qquad (2)$$

where $J_s^0$ is the reverse saturation current density of the junction.

If the device is now illuminated, a constant photo-generation of carriers with a rate $G_{est.}$ can be considered; it is then necessary to introduce a new term into the previous equation (2):

$$J(V)_{TOT.} = - J_s^0 * (e^{qV/KT} - 1) + qG_{est.} * (L_n + L_p)$$

Since the carrier photo-generation happens even into the W region (width of the SCR), the equation becomes

$$J(V)_{TOT.} = - J_s^0 * (e^{qV/KT} - 1) + qG_{est.} * (L_n + L_p + W) \qquad (3)$$

The J-V relationships are represented, either in normal dark conditions, or under illumination, in the next figure (Figure 6).

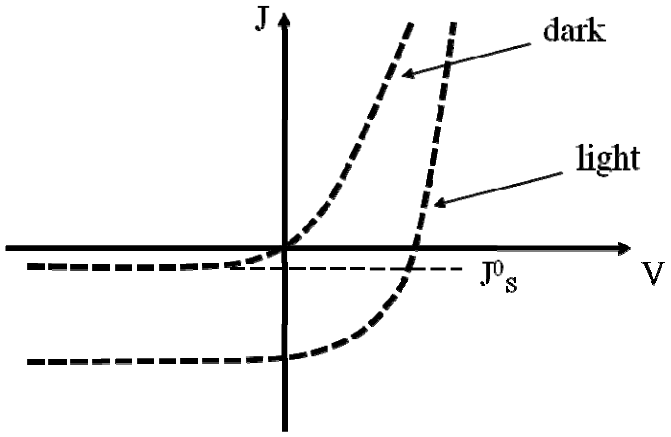


*Figure 6. J-V characteristic of an "ideal" photovoltaic device.*

Under illumination, such an ideal device can be represented also by this electric circuit:

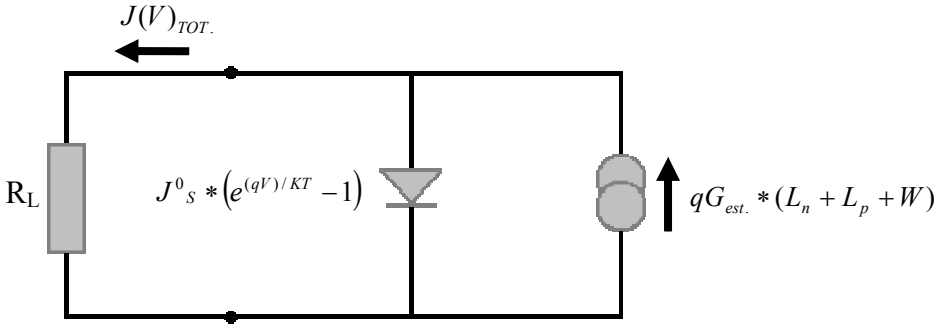


*Figure 7. Equivalent electric circuit of an ideal photovoltaic device, connected to an external load with a resistance $R_L$ .*

If this circuit is closed onto a load with a very small electric resistance (near to zero), it can be considered in a short-circuit condition and in the circuit can flow the so called **short-circuit current density $J_{SC}$** , which corresponds to the all light photo-generated current.

$J_{SC}$ can be described starting from equation (3) and setting V = 0 :

$$J_{SC} = qG_{est.} * (L_n + L_p + W) \qquad (4)$$

On the other hand, for a load with a very high electric resistance (considered infinite) after separation the carriers tend to accumulate at the external contacts of the device; this accumulation produces on its own an increasing forward polarization of the junction, which tends to oppose to the motion of the photo-generated carriers and so their transport continues until the direct current produced by the forward applied bias is equal and opposite to the photo-current.
In this condition, the total current flux which crosses the junction under illumination is zero and the corresponding voltage difference between the external contacts is called **open-circuit voltage $V_{OC}$** , which can be described starting from equation (2) and setting J(V) = 0 :

$$V_{OC} = (KT/q) * \ln(1+ qG_{est.} * (L_n + L_p + W) / J_s^0) \qquad (5)$$

Then, it is clear that for an intermediate load resistance the device can be set at values of voltage and current, $V_M$ and $I_M$ respectively, which correspond to the maximum power $P_M$ which the device can supply

$$P_M = I_M * V_M$$

## 1.3 The real device

For a real device, it is necessary to take into account also all the resistive terms probably present in it (Figure 8).
The **series resistance $R_S$** for example, can be due to :

a) the intrinsic electrical-resistivity of each material which compose the solar cell and which is crossed by carriers,
b) the not perfect ohmicity of contacts and also to the carriers recombination mechanisms which happen into the device.

The **parallel resistance $R_P$** (or shunt resistance $R_{Sh}$) can be caused by :

a) the presence of spurious phases inside the materials,
b) by grain-boundaries, for polycrystalline materials, with an electrical-resistivity lower than the rest of the material.

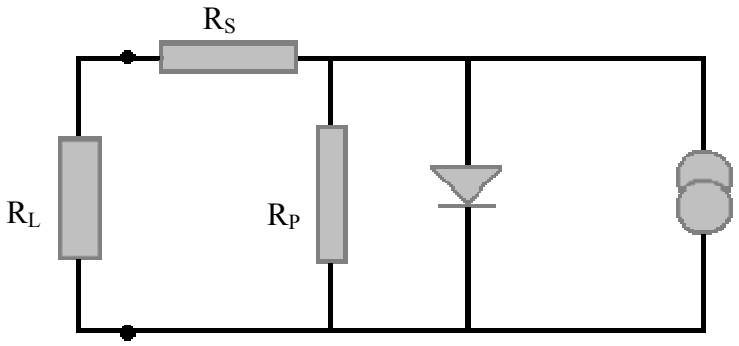


*Figure 8. Equivalent electric circuit of a real device.*

Considering now these new resistive terms, the equation (3) becomes:

$$J(V)_{TOT.} = - J_s^0 * (e^{q(V+I*Rs)/KT} - 1) - V/R_P + qG_{est.} * (L_n + L_p + W) \qquad (6)$$

Finally, it is possible to describe the two main photovoltaic parameters, by which it is possible to characterize a solar cell and they are the **fill-factor FF** and the **energy conversion efficiency η**.

The fill-factor represents the "squareness" of the solar cell J-V characteristic, the difference in the cell behavior from the ideal condition and can be defined in the following way:

$$FF = (V_M * J_M) / (V_{OC} * J_{SC}) \qquad (7)$$

The conversion efficiency is instead the ratio between the maximum power supplied by the solar cell and the light power incident on it:

$$\eta = P_M/P_{inc.} = FF * (V_{OC} * I_{SC}) / P_{inc.} \qquad (8)$$

A part from the solar cell ability in separating the generated carrier couples and in allowing the photo carriers to be extracted from contacts and to be collected, it can be noticed that the main limiting factor which influences the conversion efficiency of a solar cell is the very light power which the device can convert with respect to the whole incident one that arrives on the Earth surface.

Depending on the material used, solar cells can convert only a small portion of the whole incident solar power and so it is clear that in order to increase their efficiency in the electric conversion process, it is necessary to study and to research ways to optimize their carrier photo-generation mechanism.
Improving the photovoltaic properties of each of the materials used to produce the solar cell as well as the ones of its whole structure, it is possible to reduce the carrier generation losses mechanisms and to increase the energy conversion efficiency.

# The $CuInSe_2$

## 2.1 Photovoltaic properties

Copper Indium Diselenide $CuInSe_2$ (CIS) is a semiconducting material with excellent photovoltaic properties, that make it very suitable to be used as an absorber material in solar cells.

First of all, it has a forbidden energy gap of 1.04 eV, which allows it to absorb a quite big portion of the incident solar spectrum (Figure 9).
Moreover, its energy gap is a direct one and it allows photo generated carriers to have the fastest possible energetic transitions between valence band and conducting band of the semiconductor. In fact, these energy transitions will occur in a "vertical" way, without any help by lattice phonons or other slow second order mechanisms.
For this reason, using an absorber material with a direct energy gap assures a higher efficiency in the carrier couple generation process, reducing the probability of carriers recombination.

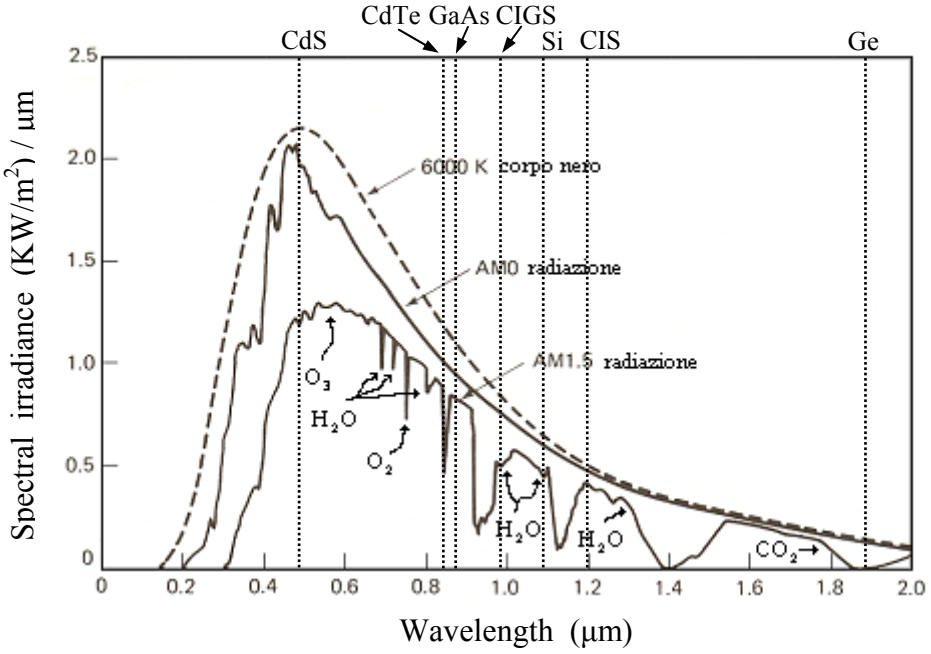


*Figure 9. Solar light spectral distribution. AM 0 and AM 1.5 radiations and their absorption by different materials are shown in comparison with the 6000°K black body spectrum [19, 20]. For example a $CuInSe_2$/CdS based solar cell can absorb and in case convert the portion of spectrum between the absorbing lines of the two materials used for the junction*[1].

CIS has also a very high absorption coefficient, $3\text{-}6*10^5$ $cm^{-1}$ , which is the highest value among all semiconductors (Figure 10), taking always into account the portion of the solar spectrum that solar cells can generally convert into electric energy.

This material can be also prepared both with a *n*- or a *p*-type electrical-conductivity and in case of the *p*-type conductivity it exhibits a minority carrier diffusion length $L_n$ approximately of 1 µm, an electron mobility in the range of about 200-300 $cm^2V^{-1}s^{-1}$ and a hole mobility between 5-20 $cm^2V^{-1}s^{-1}$ [21].

1 Air Mass (AM) is the thickness of atmosphere crossed by the solar light, before it reaches the Earth's surface. The AM 0 solar spectrum is related to the outer space, the AM 1 at the Earth's surface when the Sun is in the zenith position and the AM 1.5 at the Earth's surface, at 48.2 degree.

CIS results to be also very suitable for producing a good heterojunction with CdS, thanks to the small 1.2% lattice mismatch existing between the CIS chalcopyrite structure and the CdS wurtzite (hexagonal unit cell) one.

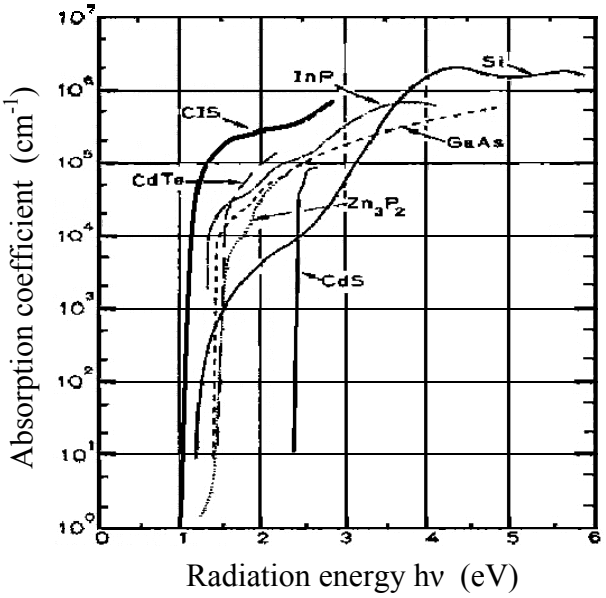


*Figure 10. Absorption coefficients of the main photovoltaic materials versus the energy of incident radiation [22].*

Finally CIS can be well grown and deposited in polycrystalline thin films, using a large number of techniques and in general it doesn't suffer from stability problems at the operating conditions normally used in solar cells production processes.

## 2.2 Crystal defects

As already said, $CuInSe_2$ has a chalcopyrite structure, with a face centered tetragonal unit cell. Such a crystal structure is shown in the next figure (Figure 11).
Inside this kind of cell, each atom of Selenium represents the center of a tetrahedron, made by two atoms of Copper and two of Indium, while each one of the metallic atoms is surrounded by a tetrahedron of Selenium atoms.

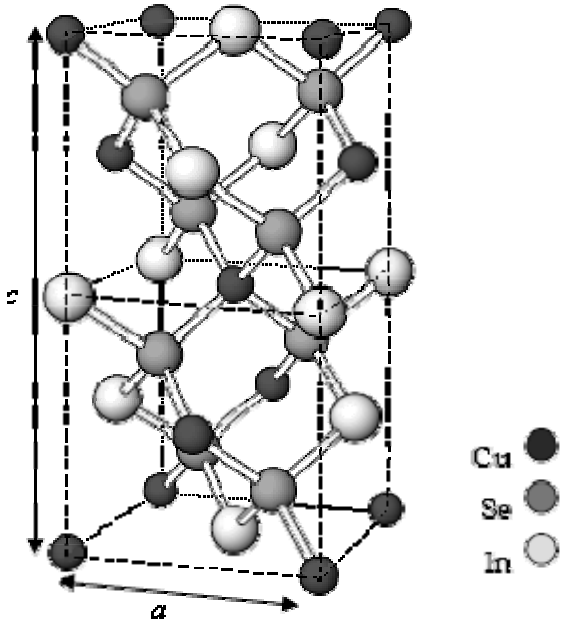


*Figure 11. Unit cell of the CIS crystal lattice.*

Since CIS is a ternary compound, it is quite difficult to establish its structure and composition, varying the thermodynamic conditions of the system. Nevertheless, a help can be given using the Cu-In-Se ternary phase diagram (Figure 12).

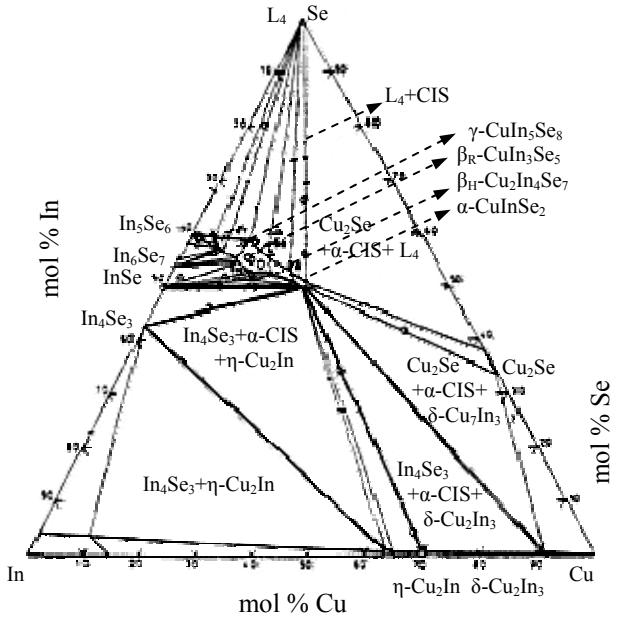


*Figure 12. Cu-In-Se ternary phase diagram [23].*

Is has been noticed by experiments that the electronic conductivity of CIS is very sensitive to the presence and concentration of native defects, donor (*n*-type) or acceptor (*p*-type), introduced for example varying the Cu/In ratio during the preparation of the material, or changing the Selenium concentration during its growth or as a consequence of later thermal treatments needed to obtain the desired stoichiometry.
The presence of these defects allows this structure to be considered constituted by three different sub-lattices:

$$(Cu, Vacancies, In)_1^{I}\ (In,Cu)_1^{II}\ (Se,Vacancies)_2^{III}$$

Differing from many other materials, $CuInSe_2$ can be therefore obtained either *n*- or *p*-type by producing correctly these native defects, even without the need to introduce extrinsic impurities. This characteristic represents an important advantage, since it is possible to produce with $CuInSe_2$ either hetero- or homo-junction devices without doping the material with external species, limiting so the problems related to the defects which normally are produced during the doping process.
Moreover, these native defects can be distinguished in three main different types: vacancies, interstitials and substitutionals.
By photo-luminescence measurements it has been possible to classify these native defects among which the most frequent ones are:

a) **Selenium vacancies $V_{Se}$** : this defect acts like a double donor (2 electrons supplied by In and Cu to the lattice for each Selenium atom missing), giving in this way two "free" electrons, as showed in the following mechanism

$$V_{Se} \rightarrow V_{Se}^{2+} + 2e^{-}$$

b) **Copper vacancies $V_{Cu}$** : this defect acts like a single acceptor (introducing one single acceptor level into the $E_G$) , since for each Cu atom missing there is a lack of one electron into the lattice.

This causes the formation of a positive charge near the vacancy site, which corresponds to a "free" hole and the mechanism by which it happens is the following mechanism

$$V_{Cu} \rightarrow V_{Cu}^{-} + h^{+} \quad \text{with } \Delta E = 0.63 \text{ eV}$$

c) **Indium substitutional to Copper $In_{Cu}$** : in this case the defect represents a double donor, (Indium has 3 electrons in the outer shell and it substitutes Copper which has only one) and the reaction mechanism is described below

$$In_{Cu} \rightarrow In_{Cu}^{2+} + 2e^{-} \quad \text{with } \Delta E = 1.85 \text{ eV}$$

d) **Copper substitutional to Indium $Cu_{In}$** : this defect acts like a double acceptor (Copper has one electron in the outer shell and substitutes Indium which has instead two other more).
The mechanism can be explained as follows

$$Cu_{In} \rightarrow Cu_{In}^{2-} + 2h^{+} \quad \text{con } \Delta E = 2.41 \text{ eV}$$

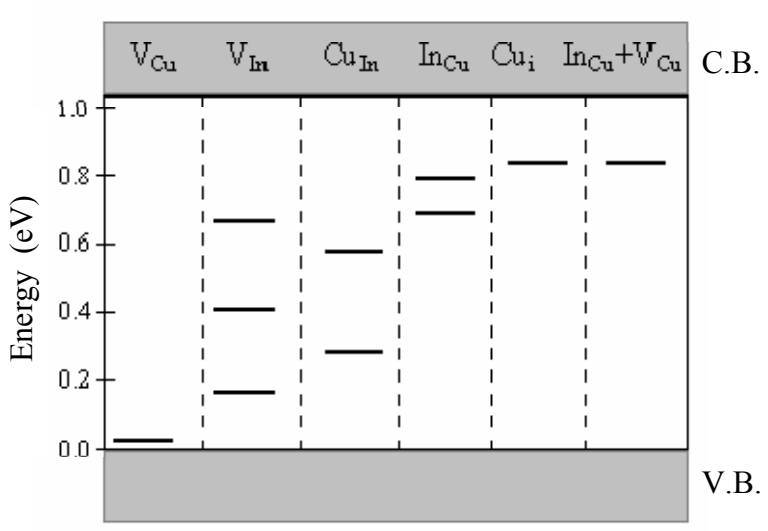


*Figure 13. Energy levels inside the CIS energy-gap produced by native defects.*

The excellent *p*-type self-doping behavior of CIS can be attributed to the presence of many Cu vacancies into its lattice, due to their low formation energy and so they are able to promote the introduction of a shallow acceptor level into the CIS forbidden band gap [24].

In addition, it is thought that into CIS there is also a high concentration of coupled defects, which are able to modify the material electronic properties too.
Among these, the most common ones are $In_{Cu}$ defects associated to $V_{Cu}$ vacancies.
This kind of defects has been useful in explaining the existence of the many Cu-In-Se based Ordered Defect Compounds (ODCs), like $CuIn_5Se_8$ and $CuIn_3Se_5$ since they can be considered composed by the repetition of *m* $(2V_{Cu}^{-} + In_{Cu}^{2+})$ units for each *n* $CuInSe_2$ unit (Figure 14).

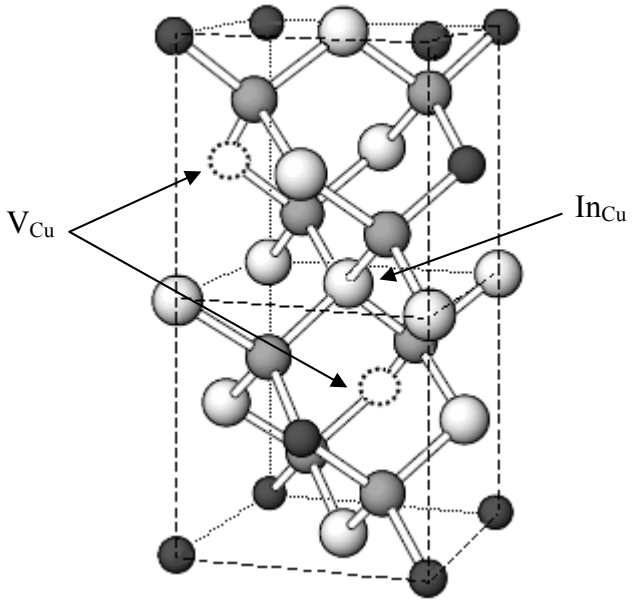


*Figure 14. Coupled defects ($2V_{Cu}^{-} + In_{Cu}^{2+}$) into the unit cell of CIS crystal lattice.*

# Thin film $CuInSe_2$ conventional growth techniques

Along years many methods have been developed for the growth of $CuInSe_2$ thin films, based for example on the vapour phase deposition processes, like flash evaporation, sputtering and molecular beam epitaxy, or on liquid phase processes, like spray-pyrolysis and electro-deposition.
In this case only the vapour phase based techniques will be described, since the techniques used in this work are part of this group.

First technique ever used for this purpose had been the **single source deposition** or **flash evaporation**, which consists in heating up to its sublimation point the target source, made by a powder of the material to deposit.
This technique didn't get much success, because it was very difficult to keep constant the material stoichiometry and from this the concentration of Se and Cu vacancies often resulted to be uncontrollable. Moreover, the polycrystalline material normally obtained in this way was composed normally by very little grains, less than 100 nm in dimensions, and for this reason the material was not suitable for being used like an absorber in solar cells.

After that, another technique was adopted, the **double source deposition**.
In this technique in addition to the CIS source also a second Selenium source was used.
In this way it could be possible to compensate the intrinsic lack of Se, which occurs during the deposition process. With this technique, satisfying results had been obtained; in fact it was possible to grow films of good quality, with grains of about 2.5 μm in dimension.

The maximum precision in controlling the material stoichiometry could be obtained instead using the **three different sources deposition** technique, in which the three elements constituting the CIS material are deposited independently and in this way it is possible to achieve very good results.

Alternative to the previous techniques has been the **selenization of metallic films** previously deposited.

Once metallic In and Cu layers are deposited by electron gun or sputtering system, a thermal treatment in presence of Se based species is performed, using gases like $O_2/H_2Se$ at a 400°C temperature (Verma et all.) or using a pure Se flux at temperatures between 150 and 400°C (Talieh and Rockett). In this way the growth of a good CIS material can be obtained too.

Some attempts have been performed also by depositing the CIS even by **radio frequency magnetron sputtering** in an Ar atmosphere, using *p*-type poly-crystalline $CuInSe_2$ ingots or sintered $CuInSe_2$ as target materials.

Some other trials have been performed depositing Cu and In by reactive magnetron sputtering in an Ar + $H_2Se$ atmosphere, but the obtained results showed the presence of many defects into the sputtered material, probably caused by the bombardment by high energy Se charged atoms formed into the discharge.

Using the **molecular beam epitaxy deposition,** it has been possible to obtain nearly stoichiometric $CuInSe_2$ epitaxial films, in a very reproducible way.
Nevertheless, it is necessary to remember that this technique has some considerable disadvantages, which are mainly the very high cost of the instrumentation required for the deposition process and the very slow deposition rates allowed [22].

# Fabrication of a $Cu(In,Ga)Se_2$/CdS thin film solar cell

## 4.1 The heterojunction solar cell

A CIGS/CdS solar cell is basically composed of a *p*-*n* hetero-junction, made by two different semiconducting materials, the first one *p*-type and the second one *n*-type.

First of all, it is necessary to remind that the CIGS/CdS solar cells described in this PhD work have the peculiarity of being produced in the **substrate configuration**. In other worlds the incident solar light comes from the opposite side with respect to the substrate, the cell holder, and as a consequence the solar cell structure is built up starting from the deposition of the back contact.

Moreover, it has been noticed that CIGS solar cells in this substrate configuration normally show higher photovoltaic energy conversion efficiencies with respect to the superstrate ones.
This is mainly promoted by:

1) CdS deposition takes place at a lower temperature with respect to the CIGS one and for this reason, depositing CdS after the CIGS growth, the inter-diffusion and the inter-mixing mechanisms between these two materials can be minimized,

2) CdS window layer deposited onto the CIGS, protects the CIGS absorber itself from the interaction with the external environment and with the next layers, saving so its desired photovoltaic electronic and optical properties,

3) the annealing in Oxygen atmosphere, used to treat the solar cell structure, strongly enhances the cells performances only if the window layer is really deposited on top of CIGS (it will be described later).

More in details a heterojunction solar cell is composed by:

a) a front contact

b) a window layer, transparent to the incident solar light and which lets the light to reach the beneath absorber. It should exhibit the following characteristics:

   1) forbidden energy gap higher than 2 eV
   2) *n*-type semiconductor
   3) low electrical resistivity in the range of about 0.01-1 Ωcm

c) a layer able of absorbing the solar light, with the following characteristics:

   1) forbidden energy gap in the range of 1-1.5 eV
   2) direct energy gap semiconductor, with a very high absorption coefficient in the visible part of the solar spectrum
   3) electrical resistivity in the range of about 1-100 Ωcm
   4) *p*-type semiconductor, with electrons as minority carriers

d) a back contact.

Moreover, the two materials used to form the junction have to satisfy particular requirements, like:

1) the same thermal expansion coefficient, since every thermal stress can introduce at the interface of the junction region some surface-state energy levels into the materials energy gap, which can act as recombination centers for minority carriers and also as deep trap levels for the photo-current flux

2) the same lattice parameter, minimizing their reticular mismatch, in such a way to promote their optimal fitting and avoiding again the formation of interface-state defects

3) The same electronic affinity (energy difference between the energy vacuum level and the bottom of the conduction band).

In case the *p*-absorber material electronic affinity $\chi_p$ is bigger than the *n*-window material one $\chi_n$, putting these materials in contact, a spike forms along the junction conduction band profile, acting as a potential barrier which limits the minority carriers motion through the junction itself and hence the photo-current flux.

On the contrary, if $\chi_p$ is smaller than $\chi_n$, another discontinuity forms into the band profile, this time along the valence band profile. This energy cliff limits the carrier diffusion through the junction and hence the formation of the built-in junction potential (Figure 15). As a consequence of this, a weaker electric field is formed at the junction, which is able to separate just a small number of charge carriers and which causes then a reduction in the open-circuit voltage $V_{OC}$ of the device.

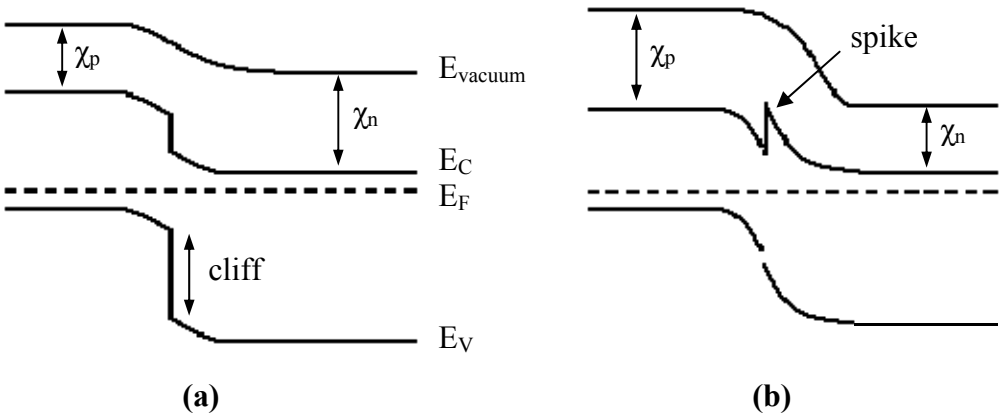


*Figure 15. p-n junction band diagram for* ***(a)*** $\chi_p < \chi_n$ *and* ***(b)*** $\chi_p > \chi_n$.

## 4.2 The Cu(In,Ga)$Se_2$/CdS thin film solar cell

The production process of a thin film solar cell consists in the deposition of several thin layers, made by different materials, onto a suitable substrate.

The structure of a Cu(In,Ga)$Se_2$/CdS based thin film solar cell is illustrated by the following scheme (Figure 16).

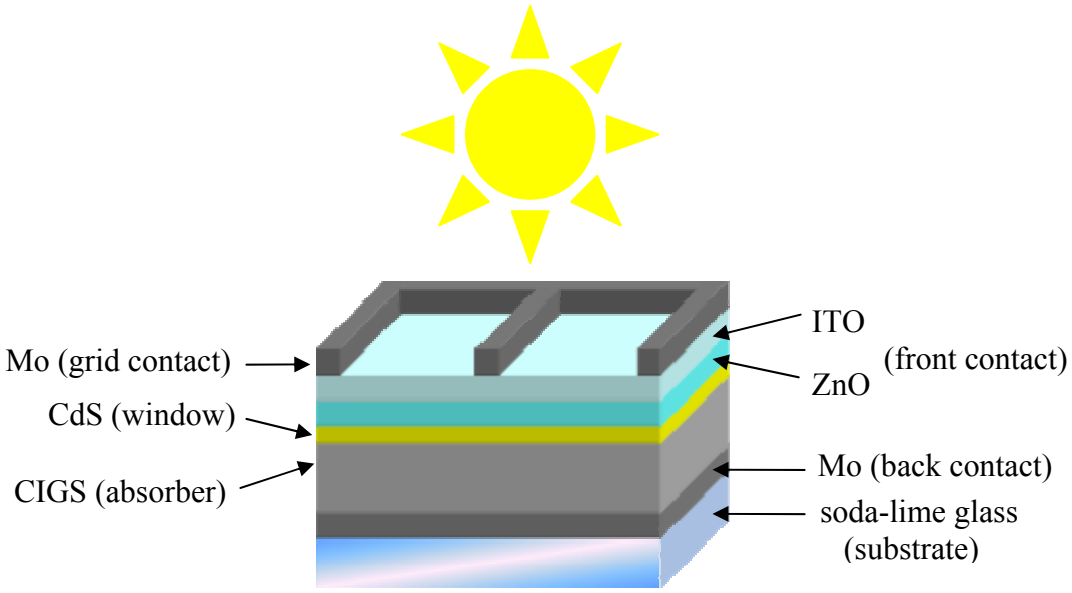


*Figure 16. CIGS/CdS based thin film solar cell structure.*

### 4.2.1 The substrate

Before describing the properties of all the materials used and the specific techniques adopted to deposit them in thin films, it is necessary first to focus on the substrate to be used.
In fact, the substrate, the base on top of which all the device structure will be produced, must satisfy precise requirements:

1) it doesn't have to suffer from neither chemically, nor physically alterations at the operating conditions at which the layers are deposited

2) it must have a perfectly smooth and clean surface

3) it doesn't have to promote unwanted reactions with the materials to be deposited

In case it is needed to deposit a mono or poly-crystalline film, with grains tilted in a particular crystallographic direction, it would be necessary to use a specific substrate with the same crystal structure of the further film itself, since growing in epitaxial conditions, this layer will tend to reproduce the same substrate crystal structure.

Finally, one other important parameter to be taken into account during the deposition of a thin film is the lattice mismatch existing between the substrate and the film, which in general must be limited in the range of 1% or less, in order to guarantee a good adhesion of the film, a limited concentration of structural defects in it and then its good crystalline quality.
In this PhD work, the substrate used to produce solar cells is the soda-lime glass (SLG), the common window pane glass.
Moreover, a part from its easy availability, soda-lime glass is the most common and cheap glass substrate and so it results to be also the best choice in order to partially limit the final cost of the devices.

## The substrate cleaning

Before the soda-lime glass can be used as a substrate, it must be cleaned in a very careful way. There are two main ways, which have been adopted to clean these glasses.
In the old and classic one, the glass is first cleaned in acetic acid ($CH_3COOH$) and wiped with lens-paper in order to remove in this way the protective salts, deposited on it by the glass producers.
Then, it is kept for some minutes in an ethylic alcohol ($C_2H_5OH$) and nitric acid ($HNO_3$) solution bath, in about a 1:5 ratio. This solution produces a very exothermic chemical reaction, which is very useful to remove the dust and the organic compounds from its surfaces.
Finally, the glass is washed in an acetone ($CH_3COCH_3$) and isopropyl alcohol ($CH_3CH(OH)CH_3$) solution, able to eliminate any residual products remained in case from the previous bath.

On the other hand, the second and new way consists in cleaning the glass with the same acetone and isopropyl alcohol solution of before, wiping it with the usual lens-paper always in order to remove most of the material present on its surfaces.
Then, the glass is put into a plasma cleaning machine.
In this machine, after having reached the desired vacuum condition, a constant pressure of about $5*10^{-1}$ mbar is kept, introducing a stable flux of the external normal air.

At this point, a plasma discharge is turned on and ions formed into the discharge can bombard the glass surfaces in a very uniform way, removing from them most of the residuals left during the previous step.
In addition, being present a high amount of Oxygen into the air used as plasma gas, a lot of O ions can be formed into the discharge and since they have a very good oxidizing power, they can really oxidize the glass surfaces. In fact, these O ions tend to bond especially with the organic compounds present, which are in general quite difficult to be removed.
The combination of heat produced during the bombardment and the presence of Oxygen ions provokes the oxidation of these compounds and hence their burning and transformation into volatile phases, which leave the glass' surfaces and so they can be pumped away by the vacuum system.
It is easy to understand that this last cleaning method is preferred, since neither dangerous chemicals need to be used, nor hazardous vapours are produced as a consequence of chemical reactions. Moreover, this process would be even much more scalable from an in-line production point of view, since it can be better automatized and doesn't require any storage or selling off of hazardous chemicals.

After the cleaning step, the glass is then annealed in vacuum at 500°C temperature for about 30 minutes. In this way the glass tends to expel the gases probably adsorbed during its previous cleaning (degassing).
If these gases would remain into the glass, they could pollute the film material during its growth, or could even provoke the lift-off of the deposited films from the glass' surface.

It has been experimented that solar cells produced with this kind of substrate normally show better performances with respect to those produced on substrates without alkali elements (alkali free).
It is thought that Sodium, coming from the soda-lime glass, during the material depositions can diffuse through the back contact and even modify the photovoltaic properties of the upper CIGS material.
In fact, a moderate diffusion of Na can improve the *p*-doping of CIGS, by increasing the amount of acceptors and consequently promoting an increase in the hole density of about 1-2 orders of magnitude and hence its *p*-type conductivity.
This phenomenon can be explained considering that Na, substituting $In_{Cu}$ antisites, inhibits the formation of these donor-like defects.
Nevertheless, this "passivation" mechanism becomes less effective as the amount of Cu reduces into CIGS material down to Cu/In concentration lower than 50%, because in such materials the probability of $In_{Cu}$ defects formation tends to increase [25].

In addition to this, thanks to the Na presence some $Na_2Se_x$ based compounds can be formed. These compounds seem to act like a surface Se "reservoir", preventing the establishment of $V_{Se}$ donor defects into the CIGS material and helping so to increase its hole density, as well as its *p*-type conductivity [26, 27].
On the other hand, an excessive diffusion of Na from the substrate causes the growth of a high electrical resistivity material layer at the Mo/CIGS interface, mainly as a consequence of the reaction with the atmosphere during the in-air annealing step.

Some experiments put also into evidence that the Na presence into CIGS-based solar cells can even prevent the In-Ga inter-diffusion, mainly at high substrate temperatures, while it can strongly limit the Cu diffusion at low substrate temperatures.
It is not to be excluded that Na could also block the Se diffusion into the forming absorber material.
In such a way it would delay the overall transformation of the CIGS phase, because of the unsuccessful inter-diffusion of constituents elements, mainly considering deposition processes using low substrate temperatures in the range of 370°C.
In these circumstances there is the possibility to extend the range in which CIGS material can transform, towards more favourable temperatures and compositional conditions.
In fact, Sodium is able to increase the activation energy barrier related to the diffusion of these elements and for this reason at low substrate temperatures this mechanism is very limited; instead, as the substrate temperature increases the atoms start to acquire more energy, enough to be allowed to overcome the barrier and to promote their inter-diffusion. In this way the formation of a better quality CIGS is enabled, characterized by grains bigger than 1 μm, by a smaller film surface roughness and finally also by a better passivation of its grain boundaries. With this kind of material it has been possible to produce solar cells with higher fill factors and conversion efficiencies.
It has been noticed also that the ability of Na of delaying CIGS formation is really effective after the deposition of all the constituent elements, reacting with them during the CIGS formation [28].

On the contrary, in solar cells produced onto alkali free substrates it has been noticed an increase in the space charge region width at the junction and a lower *p*-type conductivity of their CIGS absorber material.
This can be explained again in terms of the lack of Na, which couldn't promote the increase of acceptors density into CIGS, taking into account that in a semiconductor the SCR width is reverse proportional to its majority carriers concentration [27, 29].

In some cases CIS films grown in absence of Na and with a Cu-poor stoichiometry (Cu/In lower than 30%) have even resulted to undergo a changing in majority carriers type, from *p* to *n* (type inversion) [30].

### 4.2.2 The back contact

In order to produce a good back contact for solar cells, the use of a metal with a high electrical conductivity is of course the right choice.
For example, Molybdenum has an electrical resistivity of $10^{-6}$ Ωcm and with such a material contact the device total series resistance can be easily limited.
Remembering that, in order to produce an ohmic contact between a metal and a *p*-type (*n*-type) semiconductor it is necessary to use a metal with a working function higher (lower) than the semiconductor, in the case of *p*-CIGS a working function near 5 eV is needed, which is the working function of Cu(In,Ga)$Se_2$ .
Even if Molybdenum has a working function of about 4.6 eV, a bit lower than CIGS, it provides however a quite good ohmic behaviour for the Mo/CIGS contact.
Moreover, being a high melting point metal and with a very little thermal expansion of about 4 μm/mK, Mo results to be very suitable for being used in CIGS solar cells production process.
Normally, the CIGS production needs process temperatures higher than 500°C and for example, if in these conditions the CIGS material would grow on top of a high thermal expansion metal, a lot of lattice defects will be introduced at their interface, caused by the mechanical stress generated during the heating and cooling steps of the process.
During the solar cell fabrication stages Mo doesn't undergo any changing and so this allows the future CIGS material to grow on it free from thermal stress and then with less defects.
Anyway, putting Mo in contact with CIGS some lattice defects are however introduced into the absorber material, since the difference in lattice parameters between CIGS and Mo is not negligible.

Nevertheless, during the CIGS deposition a thin layer of $MoSe_2$ normally tends to form at Mo/CIGS interface.
This $MoSe_2$ enables a more gradual variation of the lattice mismatch between the two materials, promoting their better adhesion and so limiting also the formation of interface-state defects.
$MoSe_2$ has also a high *p*-type conductivity and it is able to improve the ohmic contact with the CIGS, since without this intermediate material there would be a Schottky metal/semiconductor junction, characterized by a more resistive and rectifying electrical contact and for these reasons, it wouldn't be suitable for solar cells [31-36].

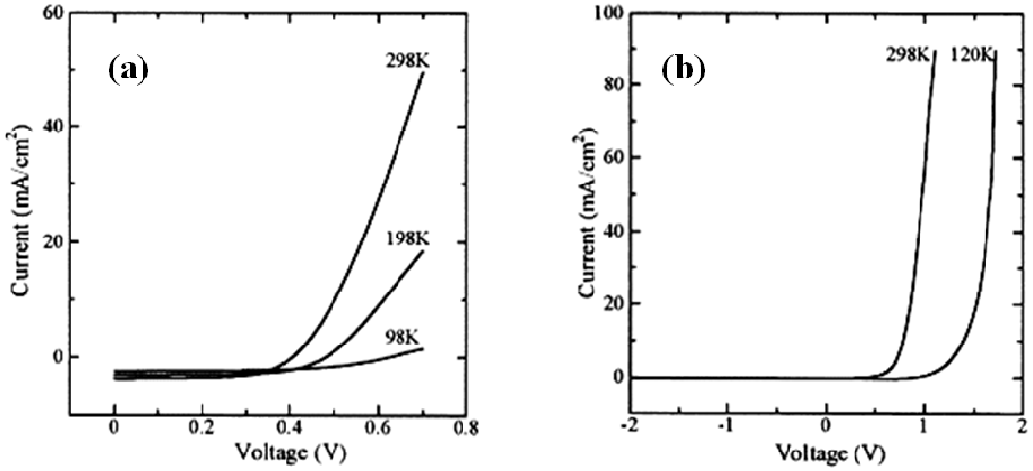


*Figure 17. Temperature dependence of the dark J-V character of solar cells with:* ***(a)*** *the CIGS/Mo/$SiO_2$/glass structure (without $MoSe_2$) and* ***(b)*** *the CIGS/Mo/glass standard device structure (with $MoSe_2$).*

This effect has been seen for example in solar cells produced with a Mo back contact but paying attention in avoiding the $MoSe_2$ formation (Figure 17a). Studying their J-V characteristics at different temperatures, it has been noticed that the J-V curves slopes decreased as the temperature decreased in the forward current region (positive voltage applied to the device back contact). This suggested that the Mo/CIGS contact without the $MoSe_2$ interlayer had a really rectifying behavior, since its ohmic quality increased with the temperature and this is typical of a rectifying metal/semiconductor contact.

On the other hand, for solar cells produced with a Mo/CIGS contact and with the $MoSe_2$ interlayer (Figure 17b), the J-V curves resulted to have the typical *p-n* junction character and moreover they kept the same slope in the forward current region also at different temperatures, indicating the ohmic type of such a contact [29].

It has been also noticed that modifying the Mo deposition conditions, it is possible to obtain layers with different morphological and electrical properties.

In fact, when Mo is deposited by sputtering at high Argon pressure, at about $10^{-2}$ mbar, it grows with a porous columnar structure, with even some inter-granular voids and in these conditions it is found to be under tensile stress forces.

This is due to the fact that at high pressures, multiple gas-phase collisions reduce the energy of the sputtered atoms and in addition the angle at which they impact the substrate becomes more oblique.

In this way the sputtered atoms don't have enough energy and superficial mobility to optimize their disposal but tend instead to condense onto the substrate almost immediately and so in a not regular and not uniform arrangement.
The observed increase in resistivity of Mo films deposited at higher sputtering pressure is a direct result of this porosity induced into them.
On the other hand, decreasing the deposition pressure down to about $10^{-3}$ mbar, the scattering of the sputtered species decreases and so the film becomes less porous and more tightly packed. This results in both an increase in the in-plane tensile stress and a decrease in film resistivity (Figure 18).

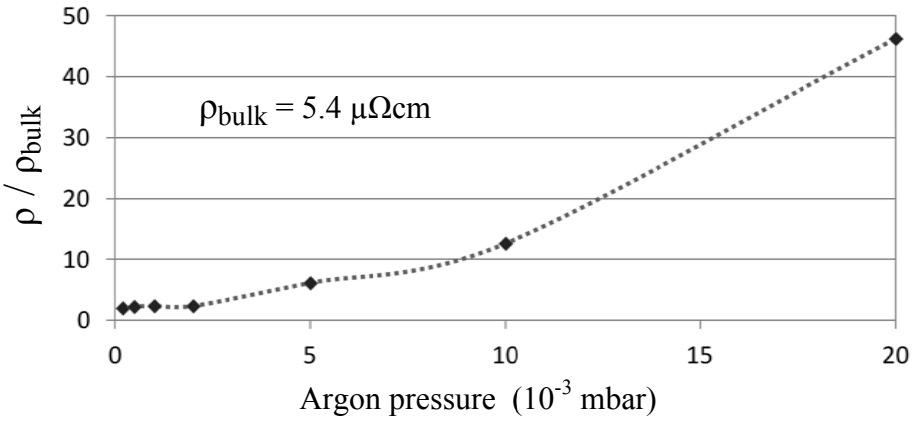


*Figure 18. Normalized resistivity $\rho/\rho_{bulk}$ of Mo thin films versus Ar sputtering pressure.*

Moreover, when the sputtering pressure becomes too low the inter-granular film spacing decreases so much that grains start to touch.
At this point compressive forces begin to exceed the tensile ones and in this condition the lattice mismatch between the substrate and the Mo film starts to increase, reaching the limit at which the Mo layer is no more able to have a good adhesion onto the glass substrate and this causes its delamination.
On the contrary, thanks to their particular structure, the porous Mo films adhere very well, because their porosity reduces the lattice mismatch forces with the substrate.
Since the final will is to obtain a Mo layer with a good adhesion to the glass substrate and, at the same time, with a very low electrical resistivity, the solution results in growing a Mo double layer structure, in which the first one must be deposited at high pressure, for the adhesion and the second one at low pressure, for the good electrical conductivity [37].

Finally, since Mo is a metal with big dimension atoms, it normally hardly diffuses into the next layers made of smaller atoms materials. It prevents in this way the formation of low electrical resistivity paths into the active layers, which can short-circuit the device and forbid it to work correctly.

For these reasons, Mo represents the best choice for producing the metal back contact in CIGS-based solar cells.

### 4.2.3 The Cu(In,Ga)$Se_2$

As said above, in order to obtain CIS based photovoltaic devices with conversion efficiencies higher than 17%, it has been thought to modify its optical and electronic properties, but keeping its good structural ones unchanged.

In fact, if an appropriated concentration of Gallium is introduced into the $CuInSe_2$ material, Ga will properly partially substitute In into the lattice, promoting the transformation of CIS into a new compound, the $CuIn_{1-x}Ga_xSe_2$ Copper Indium Gallium Diselenide (CIGS).
This is again a semiconducting material, but whose forbidden energy gap can vary from 1.04 eV for $x = 0$ ($CuInSe_2$), to 1.68 eV for $x = 1$ ($CuGaSe_2$).
This is due to the fact that the Ga atoms are smaller than the In ones, so during their substitution a changing in the inter-atomic distances happens, causing even a variation in the lattice bond forces.
This results in stronger bond forces, which make atoms keep electrons more close to their nuclei, reducing their "freedom".
Because of this, more energy is needed to promote the electronic transitions in this new lattice: hence, the material energy gap is increased.
The CIGS energy gap $E_G$ can be calculated in advance as a function of the Ga concentration present in that material and it is described by the following equation:

$$E_G\,(\text{eV}) = 1.02 + 0.67 * x + 0.24 * x * (x - 1) \qquad (9)$$

where $x$ represents the Ga/(In + Ga) concentration put into the starting CIS material [38].

It is necessary to remind also that the open-circuit voltage $V_{OC}$ of a solar cell is proportional to the characteristic built-in voltage $V_{bi}$ of the *p-n* junction produced. This last one depends on the majority carriers concentration and hence on the electrical-conductivity of the junction materials used. It is also limited by the difference in energy between their Fermi levels and at maximum it can be equal to the energy gap of the absorber material (divided by the carriers charge).
Then, it is easy to understand that absorber materials with higher energy gap permit the photovoltaic devices to reach higher $V_{OC}$.
On the other hand, the short-circuit current density $J_{SC}$ is dependent from the quantity of electron-hole couples generated by the incident solar radiation, taking always into account that only incident photons with an energy higher than the absorber energy gap will be really absorbed and will generate these couples.
For these reasons, as the energy gap of the absorber material increases, the quantity of incident photon which can be successfully used in the photovoltaic conversion process reduces too; in these conditions only solar cells with lower $J_{SC}$ can be obtained (Figure 19).

In order to produce solar cells with the best performance, it is unavoidable to make a compromise between the $V_{OC}$ and the $J_{SC}$, which can be obtained from a solar cell for a specific value of the absorber energy gap.

From equations (3) and (9) it can be found that for CIGS the energy gap sets in an optimal value range of 1.1-1.2 eV, corresponding to a Ga concentration *x* between 25% and 35%, in order to produce solar cells with such $V_{OC}$ and $J_{SC}$ to reach 20% conversion efficiencies.
This hypothesis has been even confirmed by experiments, in fact best CIGS based solar cells are produced with a Ga/(In+Ga) ratio into the CIGS material of about 25-35% [14, 39].

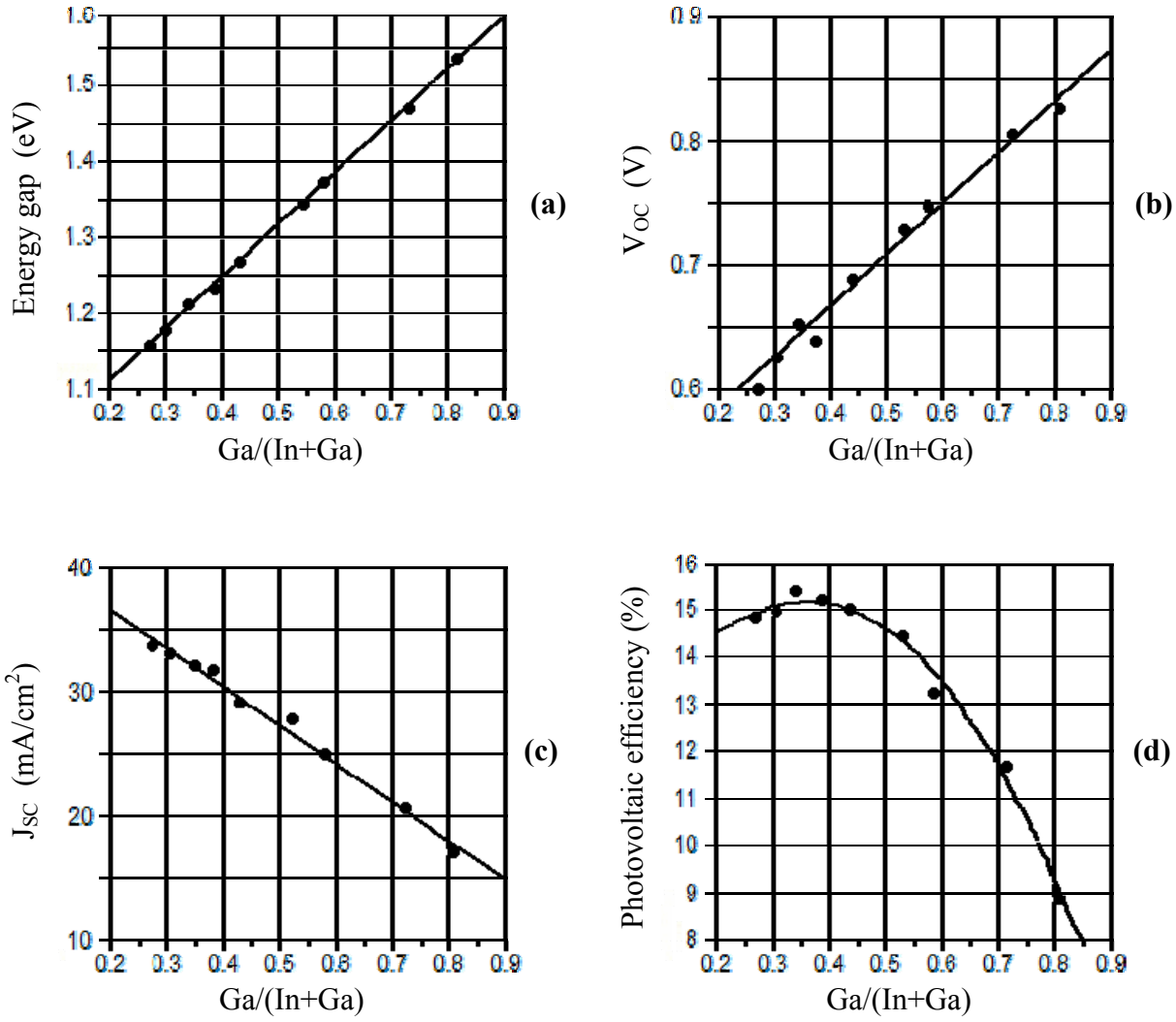


*Figure 19. Variation of CIGS based solar cells photovoltaic parameters as a function of the Ga concentration introduced:* ***(a)*** *energy gap,* ***(b)*** $V_{OC}$ *,* ***(c)*** $J_{SC}$ *and* ***(d)*** *photovoltaic efficiency [22].*

Nevertheless, as it can be noticed in the graphic below (Figure 20), which shows the theoretical conversion efficiency of solar cells versus their absorber energy gap, a CIGS material with an energy gap of 1.1-1.2 eV permits however to produce solar cells with efficiencies quite far from the theoretical maximum reachable.

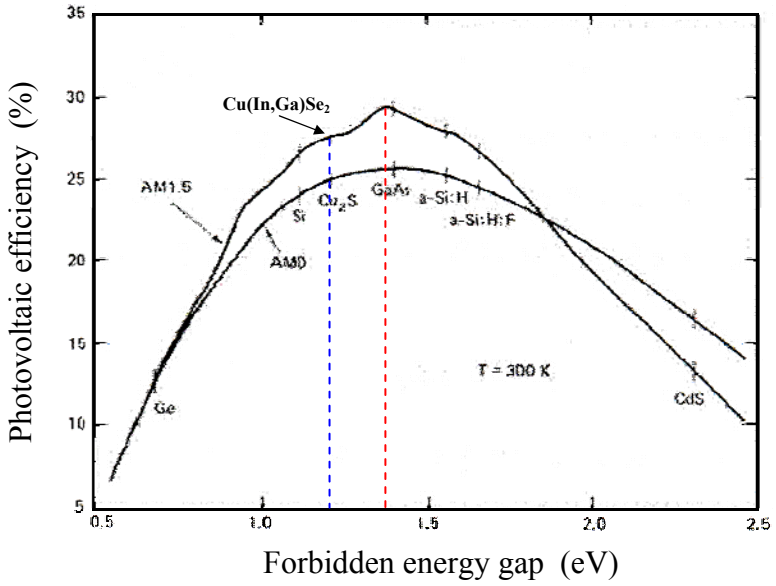


*Figure 20. Theoretical conversion efficiencies of solar cells produced with different kind of absorber material versus their energy gaps. The theoretical efficiency of a solar cell made of a GIGS with 1.2 eV $E_G$ in blue line, while the maximum of the curve in red line [19].*

This maximum efficiency sets about 1.45 eV, like the value of the GaAs energy gap and for CIGS it would correspond to a Ga/(In+Ga) ratio higher than 65%.

In order to reach the 1.45 eV energy gap, the first thought would be that of increasing the Ga concentration into the $CuInSe_2$ material much more than 35%, but as already said there are some drawbacks in doing it.
In fact, the transformation of CIS into CIGS improves the electronic properties of the CIGS/CdS hetero-junction only if the Ga concentration is correct.

For a too little Ga concentration, the absorber material will remain CIS and the junction will be affected in the band diagram by a detrimental spike at the interface with CdS (Figure 21). On the contrary for an excessive Ga concentration, the $CuGaSe_2$ material will be obtained instead of the $Cu(In,Ga)Se_2$ and in this case the junction will show a cliff in the band diagram at the CIGS/CdS interface (the effects of these mechanisms have been already explained above).

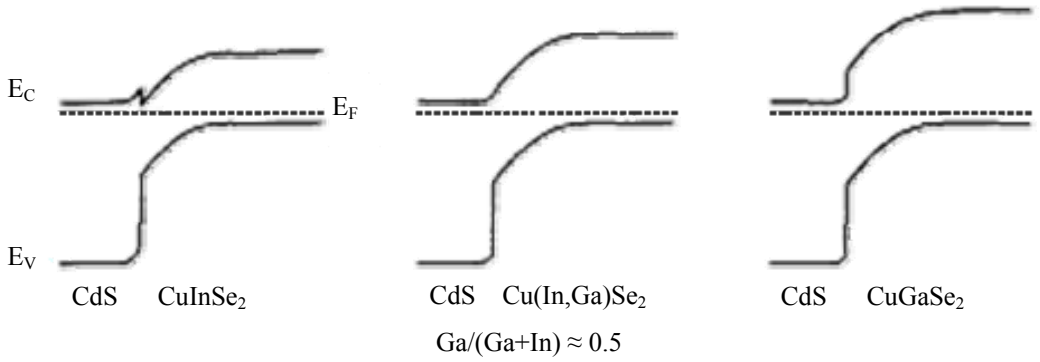


*Figure 21. Band diagram of the CIGS/CdS junction, for different Gallium concentrations into the material [40].*

Only for an appropriate concentration of Ga introduced into the $CuInSe_2$, the spike at the interface can be reduced and the cliff can be avoided, allowing the transport of minority carriers through the junction to happen in an easier and efficient way.
In addition, for In-rich $Cu(In,Ga)Se_2$ materials, a strongly Cu-depleted surface made of a $Cu(In_{3-x}Ga_x)Se_5$ based material tends to form and it is characterized by a Fermi level position just below its conduction band.
Hence, near the surface an inversion in the CIGS electrical type conductivity happens.
In fact, $Cu(In_{3-x}Ga_x)Se_5$ is a *n*-type ODC and it is able to produce near the surface a *p*-*n* pseudo-homojunction with the beneath *p*-CIGS, which allows so the electrical *p*-*n* junction to be pushed back deeper into the absorber bulk.
This prevents the junction from being damaged by the usual interface-state defects, which act like carriers traps and so its electronic behavior is improved.

In fact, in general, a homojunction is less affected by interface-state defects since the lattice mismatch between the two junction materials is negligible and in this case the minority carriers transport can be well described by only diffusion and recombination.
On the contrary, into a heterojunction the difference between the two materials always introduces some discontinuities in the bands alignment and this makes the minority carriers be involved in different and more complicated transport mechanisms, mainly related to the interface region.

Promoting the formation of this pseudo-homojunction has resulted to be the key point for obtaining the highest efficiency solar cells.

$Cu(In_{3-x}Ga_x)Se_5$ tends also to segregate into the polycrystalline film grain boundaries, which can act as conduction inversion centers and as barriers for carriers confinement into the columnar CIGS grains; in this way the carriers recombination mechanism (into grain boundaries) is reduced, leading to higher photovoltaic parameters of the devices [41, 42].

On the contrary, for Ga/(In+Ga) ratios higher than 40%, going towards $CuGaSe_2$ , the absorber material suffers from a considerable reduction in carrier mobility (Figure 22), caused by stronger recombination mechanisms and, as a consequence, by a shorter photo-generated carrier mean lifetime. This condition decreases the photo-carrier collection efficiency and it worsens the solar cell performance.

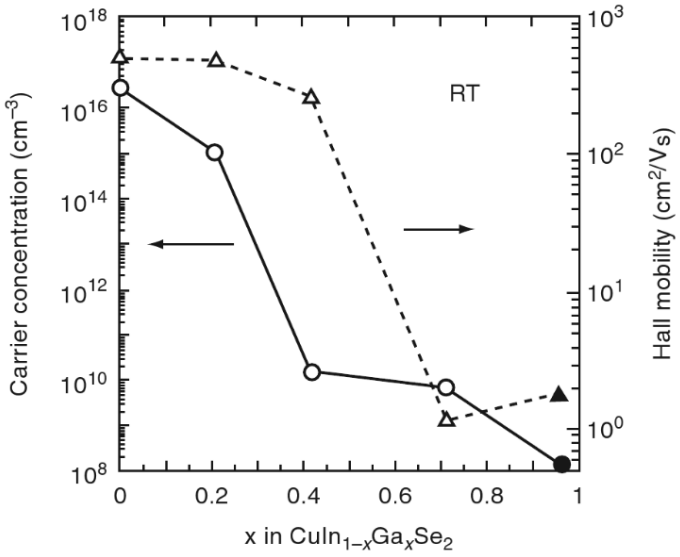


*Figure 22. Carrier concentration and Hall mobility of $CuInGaSe_2$ crystals, as a function of the Ga concentration [43].*

For these reasons the approach of increasing the Ga concentration into the whole CIGS material, for obtaining better photovoltaic efficiencies, can't be followed.

However, another strategy has been studied.
Modifying the Ga concentration into the CIGS layer, a local variation in its band profile happens and mainly in conduction band. Increasing the Ga concentration (and hence the CIGS energy gap) towards the back contact, with a **single grading**, it is possible to form an additional electrical field into that region of the absorber material (Figure 23).

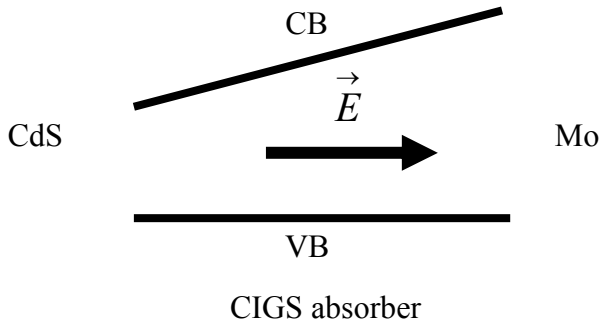


*Figure 23. Band diagram of a Ga single graded CIGS absorber material*

Such an electric field is able to push the electrons, eventually generated in that region, towards the space charge region of the CIGS/CdS junction. Into the CIGS, these electrons (minority carriers) feel, in addition to the concentration gradient, also a second force due to this new electrical field; in this way more carriers are collected at the depletion region's edges, so the $V_{bi}$ and hence the $V_{OC}$ increase and consequently also the probability that these minority carriers contribute to the photo-generated current can be enhanced. At the same time, since electrons are pushed away from the back contact but towards the *p-n* junction, the recombination at the back contact is minimized and this mechanism is called "mirror effect".
In order to have a stronger electrical field for better drifting the carriers and then to have a higher carrier collection at the depletion region (higher $V_{OC}$), the slope of this Ga grading needs to be increased towards its maximum.
To keep the good electronic properties of CIGS it is convenient however not to exceed about 60-65% Ga/(In+Ga) concentration at the back of the absorber layer; this leads to have a top CIGS with the smallest $E_G$ possible.
To have a real and consistent gain in $V_{OC}$, it is very important to build the gradation in such a way to introduce this electric field "extension" outside the space charge region. At the same time it is necessary to preserve also the low-$E_G$ CIGS (absorption edge) inside this region, in order to enable the best carrier photo-generation and hence the best $J_{SC}$.
Doing this the total effect for $V_{OC}$ is limited, but however higher $J_{SC}$ are normally obtained, as described above.
To further improve this configuration, it has been thought to introduce a second Ga graded profile near the CIGS/CdS interface, but this time the profile is inverted. In this superficial region the Ga concentration increases towards the *p-n* junction, resulting in total a **double graded distribution** (Figure 24).

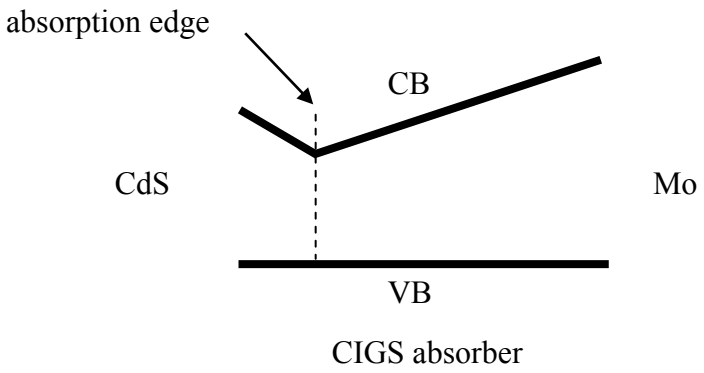


*Figure 24. Band diagram of a Ga double graded CIGS absorber material.*

In this way, with this higher energy gap CIGS material in contact with the CdS window layer it is possible to further increase the device $V_{OC}$ .
Nevertheless, passing from the lower to the higher-$E_G$ region, the rising of the conduction band near the CIGS/CdS interface normally acts like a potential barrier, hindering the carriers transport through the junction. The higher is that energy gap at the CIGS/CdS interface, the more intense will be this effect and moreover if this superficial grading is too extended it will make the absorbing edge go outside the space charge region, causing a loss in $J_{SC}$ .

The solution consists in producing a modest superficial grading region thin enough, well below 200 nm, to let carriers overcome this barrier or pass through it by a tunnel mechanism [18, 44]. In fact, for moderate superficial $E_G$, of about 1.2-1.25 eV and for thin reverse grading regions, carriers can tunnel the barrier; in these conditions the photo-generated current is preserved and at the same time, using a higher $E_G$ CIGS material to form the CIGS/CdS junction, higher $V_{OC}$ are guaranteed.
To permit at the same time that most of the incident light is really absorbed inside the space charge region, it is necessary to produce a quite extended low-$E_G$ region into the CIGS layer, of about 1 μm thickness, which is so able to increase the long wavelengths absorption and hence to supply a higher amount of photo-generated carriers (Figure 25) [45].

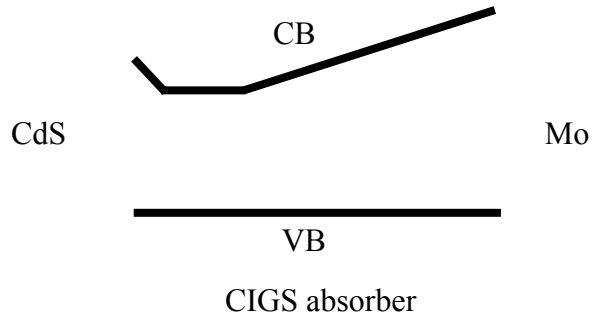


*Figure 25. Band diagram of an optimized double graded CIGS absorber material.*

In total, with the correct Ga double graded profile, solar cells can exhibit higher $V_{OC}$ up to 720-740 mV, thanks to the high-$E_G$ CIGS top and bottom regions and also higher $J_{SC}$ up to 35-36 mA/cm$^2$ ,thanks to the low-$E_G$ middle region and again to the bottom one [14].

The Cu(In,Ga)$Se_2$ keeps also the same high absorption coefficient of CIS, of about $10^5$ cm$^{-1}$, and this enables to produce very thin absorber layers for photovoltaic devices.
In fact, a material with an absorption coefficient α is able to absorb, on average, almost all the incident radiation within a depth equal to 1/α ; it's easy then to understand that the higher is the absorption coefficient of a material, the smaller will be the thickness of that material layer needed to absorb most of the incident light.
This feature is very important in the field of photovoltaic thin film technology since, using such materials, it is possible to produce very thin absorber films, whose thickness must be however on average at least equal to 2/α , in order to limit failures caused by the intrinsic defects present into a polycrystalline material. For CIGS this thickness sets in the range of 2-3 μm.

The CIGS suitable to be used as a solar cell absorber material, in analogy with the CIS, has a chalcopyrite crystal structure, whose unit cell has dimensions varying as a function of the Ga concentration $x$ in it: $a(x) = 5.812 - 0.332 * x$ , $c(x) = 11.650 - 0.438 * x$ [46].
Such a structure, similar to the diamond one, would let think that it is built up by covalent bonds, but, since its constituent atoms have quite different electro-negativity, it's feasible to foresee the existence of mixed ionic-covalent bonds.

The formation of this material can be seen as the result of different chemical reactions, which happen in particular conditions of temperature and, most of all, between perfect and appropriate ratios of the constituent atomic species In, Cu, Ga and Se.

In the case that the CIGS is grown by using the "metallic" precursors selenization method, by studying the binary phase diagrams Cu - Ga, Cu - In, and Ga - In (Figures 26-28), it's possible to determine which can be the most favourable conditions for the formation of the desired precursors, taking into also account the possible compounds and secondary phases which can coexist.

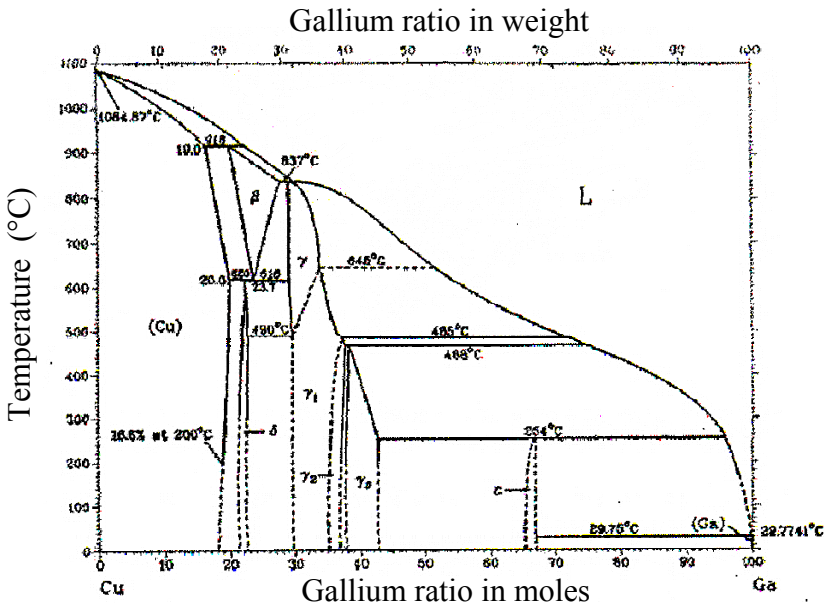


*Figure 26. Copper - Gallium phase diagram [47].*

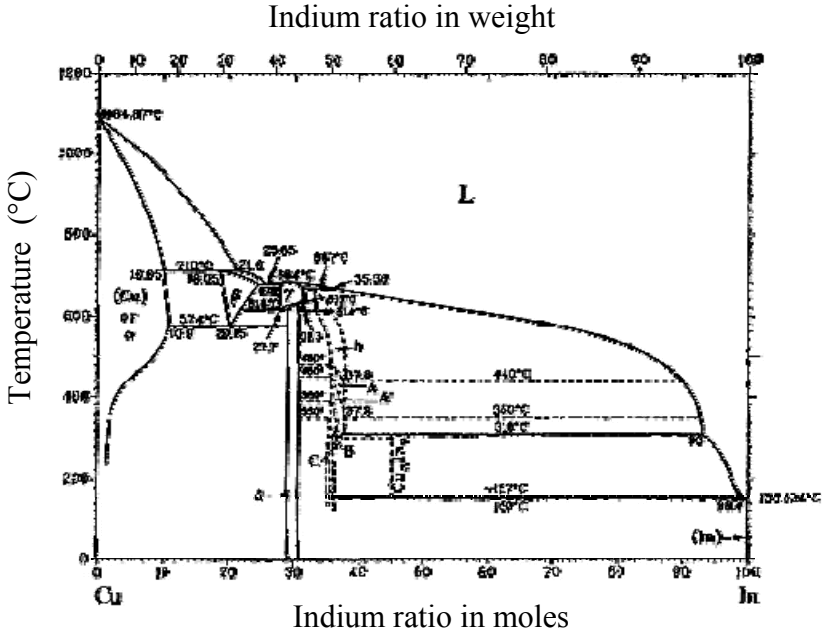


*Figure 27. Copper - Indium phase diagram [48].*

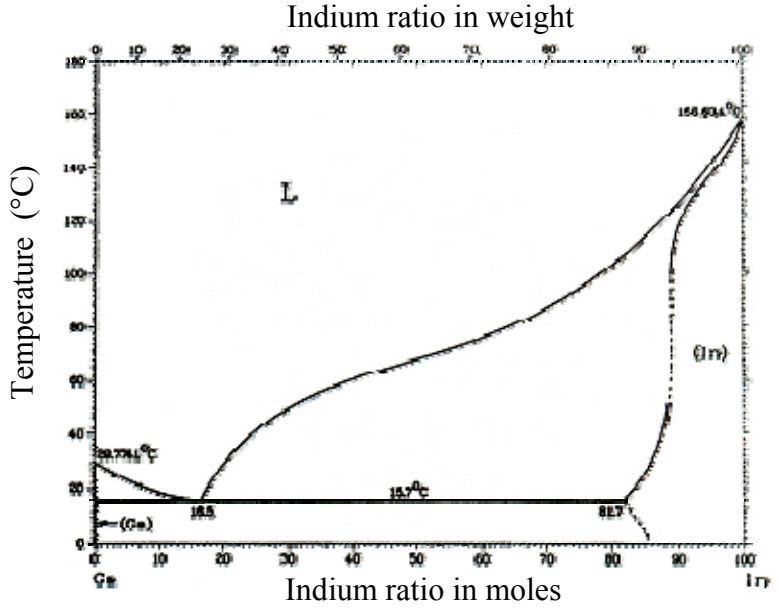


*Figure 28. Gallium – Indium phase diagram [47].*

Once In-, Cu- and Ga-based "metallic" precursors are formed, it is feasible to foresee that, at temperatures of about 500°C, an equilibrium condition can exist between a solid phase (the precursor) and a Ga-rich liquid one.
At this point, if the system temperature is risen up to about 520-530°C and an appropriate concentration of Selenium is added to this system, the solid phase composed of Cu-In-Ga (Indium plus Gallium in a small concentration) tends to melt. This Cu+In-rich liquid-like phase, reacting immediately with Se, promotes the formation of the most reactive compounds, like $CuInSe_2$ which will grow from the Ga-rich liquid-like phase.
In fact, both Cu and In are more reactive than Ga in presence of Se and for this reason their interaction is promoted and hence it happens first. Being Cu and Indium in a liquid phase , Ga helps them to mix and to combine with Se, before bonding properly in the lattice of the growing material.
Moreover, since Ga melts continuously other Cu and In present into the precursor which didn't react before, with the help of Se these latest constituents enable the formation of new CIS, transforming most of that precursor and even combining with this CIS-based precursor that Ga can form some CIGS material, depending on the amount of Ga introduced.

Even in the case that the Ga introduced into the precursor wasn't sufficient to substitute enough Indium, in order to form a CIGS material with the desired stoichiometry, its presence into that material is fundamental for the good interaction between Cu, In and Se.
In fact, forming for example $CuGa_2$ , Gallium is able to delay the reaction between Cu and In, preventing them from going into their phase diagram up to 250°C and allowing their interaction to happen in better thermodynamic conditions.
Moreover, in part Ga bonds with Cu to form also $Cu_9Ga_4$ compounds which are even more stable; in this way the stoichiometry of the CIGS material can be controlled and then the interaction with Se is well regulated.

In a too little concentration, Ga is not able to melt enough Cu and In to transform most part of the precursor into CIS. In this case the reaction mechanism between constituents stops earlier and hence the precursor, being at high temperature (more than 500°C) but in a wrong stoichiometry, tends to exit from the optimal thermodynamic conditions for its correct transformation.
Because of this, a small amount of $CuInSe_2$ will grow and at the same time a lot of unwanted spurious phases will be formed.

On the other hand, taking into account that Gallium is more reactive with Cu with respect to In, Ga in excess provokes normally the growth of a In-rich material affected by segregations.

Taking a look to the pseudo-binary $Cu_2Se$ - $In_2Se_3$ and $Ga_2Se_3$ - $Cu_2Se$ phase diagrams (Figures 29, 30), it's easy to understand how any variation in stoichiometry, even if small, can lead to obtain a material different from the desired one and the formation of secondary compounds, like $Cu_{2-x}Se$ , $Cu_xSe$ , $In_2Se$ , $CuIn_2$ , $CuGa_2$ or even the sphaleritic CIS (with a random arrangement of Cu and In atoms in the lattice).

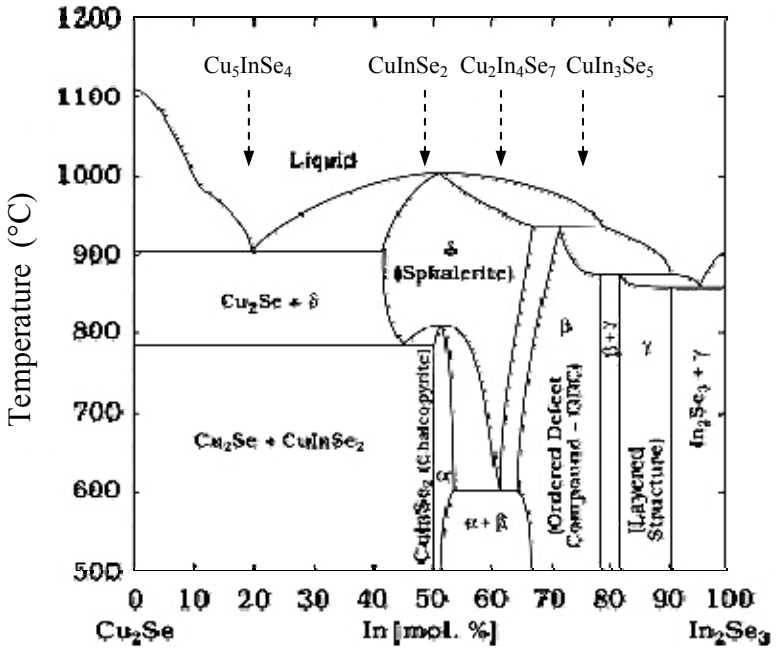


*Figure 29. Pseudo-binary $Cu_2Se$ - $In_2Se_3$ phase diagram [49].*

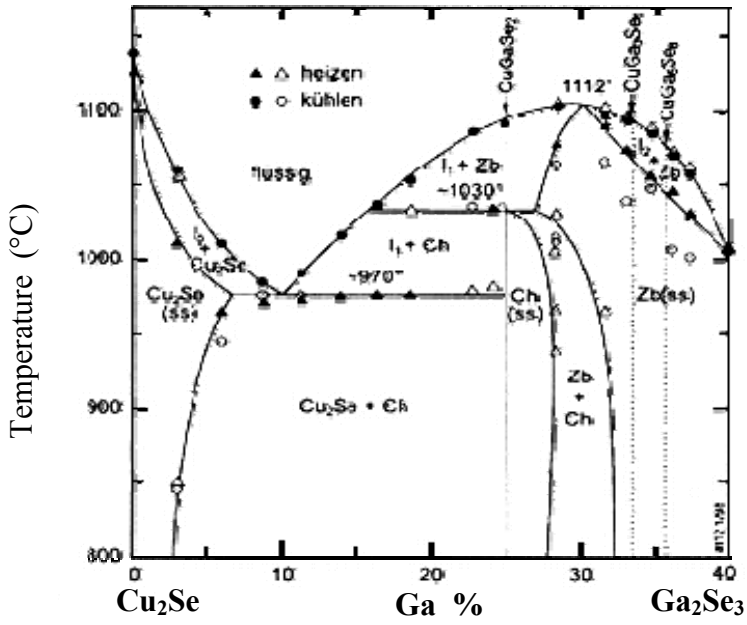


*Figure 30. Pseudo-binary $Cu_2Se$ - $Ga_2Se_3$ phase diagram [50].*

About Cu-Se based compounds, the $Cu_{2-x}Se$ is for sure the most dangerous one for the correct working of a solar cell, since it has a high tendency to grow during the stage of selenization (addition of Se at high temperature) and which tends to increase as the Cu concentration increases.

$Cu_{2-x}Se$ is in fact a material with a low electrical resistivity of about $10^{-3}$ Ωcm and besides it is an unstable material able of easily setting Cu atoms free, which are very quick diffusers.

Cu atoms can move then into the grain boundaries of the absorber layer, reaching even the junction region and the CdS layer.

$Cu_{2-x}Se$, segregated also into the grain boundaries near the junction, causes then short-circuit of the junction introducing a low shunt resistance $R_{Sh}$ , which enables the reverse current flow and reduces the device $V_{OC}$ .

In addition to this, as a consequence of the $Cu_{2-x}Se$ compound cracking at high temperature, some Cu diffusing into the CdS layer can even dope it. In this case Cu introduces deep energy levels into the energy gap of CdS, which act as carriers traps increasing the material electrical-resistivity and also the series resistance $R_S$ of the device.

Indium-based compounds, like $In_2Se$ o $In_2Se_3$, are instead more insulating and their presence into the grain boundaries of the absorber material normally doesn't damage the devices performances.

Finally, in the case that some sphaleritic CIS is formed, there would be again problems related to the presence of $Cu_2Se$, which in fact tends to form simultaneously with that, in addition to the fact that this CIS material is also quite unstable and can cause other kind of segregations during next high temperatures stages.

To obtain a complete Cu(In,Ga)$Se_2$ absorber layer it's necessary then to add an appropriate concentration of Ga to the system, in order to promote a specific partial substitution of In by Ga into the whole CIS layer.
To summarize, it's easy to understand how much important is to find and to develop a process to grow this material, that enables to control and to modify in a precise way all the needs required by the system.

### 4.2.4 The CdS

Cadmium Sulphide (CdS) is a *n*-type semiconductor characterized by an energy gap of 2.42 eV. It is transparent for the most part of the convertible solar radiation, which can reach the beneath CIGS absorber layer. The CdS layer represents for this reason the solar cell "window layer". Since the *p*-*n* junction between CdS and CIGS is strongly dependent from their interaction, the techniques used to grow these materials are very important for the device performances.

The CdS film is introduced into the cell structure in order to have the *n* part of the junction and also to have a buffer layer, which can protect the CIGS one.
In fact, since CdS is deposited between the CIGS layer and the front contact, it can avoid the diffusion of metallic atoms coming from the upper TCO layers, during the deposition of the front contact or during the next heat treatment.
Diffusing towards the absorber layer, these metallic atoms can damage the correct working of the junction by normally shunting it.
A part from CdS, also other buffer layers have been investigated by the photovoltaic world along the time, like (Cd,Zn)S , ZnS and $In_2S_3$ which have even a higher energy gap. With these materials it was thought that it was possible to produce higher efficiency solar cells, but for reasons related to the mismatch with CIGS the best results have been obtained however with CdS [51].

This material promotes in fact a good intermixing of both materials at CIGS/CdS/TCO interfaces, enabling to obtain a structure with the least possible concentration of defect caused by lattice mismatch.
Moreover, CdS provide a better band alignment in the device structure and this reduces the carrier recombination probability into the SCR, promoting so their better transport [52].

CdS is also thought to act as a Cadmium source, at temperatures higher than 200°C.
Diffusing from the CdS film, Cd is able to reach the beneath absorber layer and to dope *n*-type its surface. Doing this, Cd promotes the formation of a *p*-CIGS/*n*-CIGS pseudo-buried - homojunction, which is extremely important for the good performances of the solar cells [53-55].
Considering this, it's easy to apprehend that into this homojunction there is also an almost intrinsic *i*-CIGS layer, due to the gradual decreasing in the diffused Cd concentration towards the deeper CIGS, balancing the two different doping (Figure 31).

For this reason it would be better considering the junction a *p*-*i*-*n* pseudo-homojunction, and not a simple CIGS/CdS *p*-*n* heterojunction.

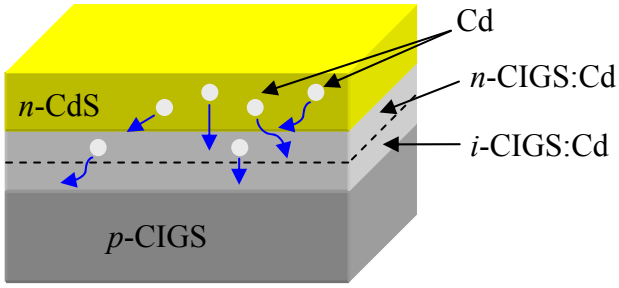


*Figure 31. Cadmium diffusion from CdS layer and formation of the pseudo-buried-homojunction near CIGS layer surface.*

In fact, CIGS based solar cells with high conversion efficiencies have revealed a behavior similar to the homojunction devices. This phenomenon has revealed that the highest efficiencies can be obtained when a homojunction-like transport mechanism for photo-carriers happens and this must necessary occur at the *p*-CIGS/*n*-CdS interface, otherwise a pure heterojunction effect would be seen.

Hence, this pseudo-homojunction must be between an *n*-type material and the same but *p*-type one like the *n* and *p*-CIGS and in this condition the CdS layer represents no more the real *n*-part of the solar cell *p*-*n* junction, but its presence is however fundamental for promoting the best electronic behavior of the device and also for the buffer action.

Nevertheless, at the same time as Cd diffuses towards the CIGS there is a gradual and continuous "consumption" of the CdS layer and so the provided protection tends to decrease.

In this way of thinking, it can be expected that depositing thicker CdS layers there would be less possibilities for the junction to be short-circuited. Instead, generally as the window layer thickness increases, even the optical absorption of a part of the incident light increases (Figure 32) and also the thickness of residual semi-insulating CdS layer increases too, causing a decrease in the solar cell $J_{SC}$.

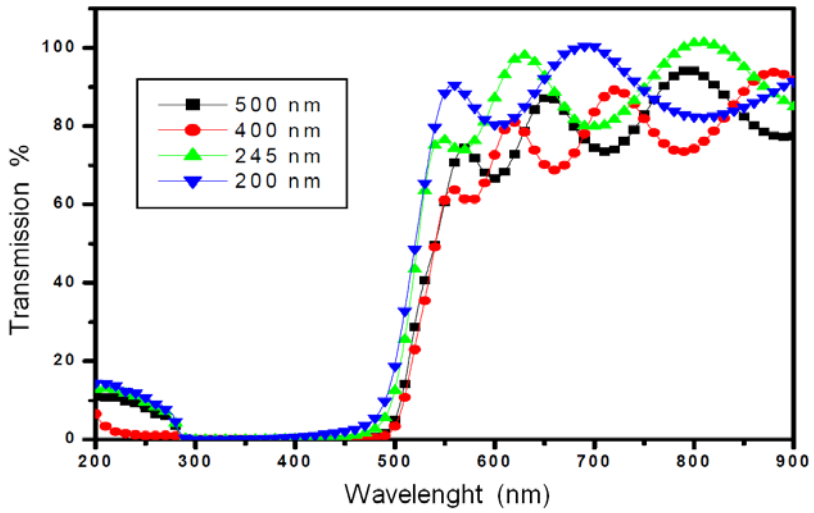


*Figure 32. Transmission spectra of CdS thin films of different thickness [56].*

On the other hand, a too thin and then not properly uniform CdS layer doesn't provide a sufficient or homogeneous amount of Cd for the formation of a homojunction extended on the whole CIGS layer surface, but it causes instead just a decrease in the device shunt resistance $R_{Sh}$ and it leads to obtain low fill-factor, because of the worsening in the device band alignment caused by the CIGS/ZnO interface.

The conventional technique used for depositing CdS thin films in CIGS solar cells is the Chemical Bath Deposition (CBD).
This technique consists in using a liquid aqueous solution kept at temperatures from about 60 to 90°C, containing CdS based compounds and in deeping the substrate in this bath many times, in order to promote the deposition of a uniform layer.
It has been noticed that the CBD positively affects the device performance and in fact the highest efficiency CIGS solar cells have been produced depositing the CdS layer by this technique.
It seems that the CBD process promotes the cleaning of the CIGS surface, etching it and removing its superficial oxide compounds; in addition it is thought that an intermixing probably happens at the absorber surface enabling so the formation of intermediate compounds which gradually reduce the mismatch at the interface. Finally, since the addition of the CdS layer happens by a chemical solution, the CIGS coverage is considered to occur in a more uniform way, providing then a further more homogeneous Cd diffusion and a better establishment of the homojunction extended on a larger area [52].
By using the CBD technique, good CdS films can be obtained already in 50-80 nm thick layers, allowing to obtain high efficiency solar cells.

Also other techniques for the CdS deposition have been tested, someone even more simple and cheaper like the sputtering, but similar results to the CBD best ones have not been obtained yet. In addition, in the sputtering case, in order to guarantee the proper film uniformity and the CIGS surface coverage, normally thicker layers of about 80-120 nm are needed.

A possible solution for depositing by sputtering thinner CdS layers is presented in this PhD thesis work and it will be described more in details later.

However, even if CBD is a wet process and it suffers from problems related to the large production scalability, so far best results are still being obtained with this technique and for this reason it is the main one to be used.

### 4.2.5 The front contact

In order to produce a suitable *n*-type front contact for solar cells, it is necessary to have materials characterized by a high optical transparency, at least 90% in the visible region of the solar spectrum, together with a good electronic conductivity. In fact, these materials must be transparent, for letting the incident light pass through them and reach the beneath *p*-*n* junction and, at the same time, they are required to have a low electrical resistivity, for allowing a good extraction of photo-generated carriers.
Such materials can be obtained by producing an electron degeneracy in wide-gap oxides, with energy gap higher than 3 eV , by introducing in their lattice suitable non-stoichiometric defects and/or proper dopants.
In general, the electrical properties of oxides critically depend upon the oxidation state of their metal components (oxide stoichiometry) and on the nature and quantity of impurities incorporated into the films.
Perfectly stoichiometric oxides are either insulators or ionic conductors. These latest ones are of no interest as transparent conductors due to the high activation energy required for ionic conductivity.
The way to obtain good conducting oxides is doping them with dopants, which must have the same size as, or be smaller than the host ions replaced and don't have to form compounds with the host oxide.

In particular, Indium oxide $In_2O_3$ is a semiconductor oxide with an energy gap of 3.5 eV.
As grown, it generally lacks stoichiometry because of Oxygen vacancies $V_O$ into the lattice, which act as double donors and each one provide two electrons to the material electrical conductivity. This material can be represented like $In_2O_{3-x}$ where x is the $V_O$ concentration and should be a mixed conductor, having both electronic and $O^{2-}$ ion conduction.
The donor carriers can be generated in it by doping this material with elements of the group IV, like Tin. In fact, Sn dopes *n*-type the $In_2O_3$ by substituting In, since In has three valence electrons while Sn has four, providing so an "almost free" electron into the material lattice per each substitution.
Increasing the amount of Sn concentration into the material, it is possible to increase the *n*-doping up to very high values of carrier concentration, on the order of $5\text{-}10*10^{20}$ $cm^{-3}$ .
At these high doping levels, the material has so many free carriers that a donor level, full of electrons, starts forming near the bottom of the conduction band, or even into the conduction band itself.

In this condition the material is called "degenerated" and since its donor energy levels are already into the conduction band, they need a very small energy to contribute to its electrical conduction. This is the reason of the metal-like high electrical conductivity of this material.
The $In_2O_3$:Sn, Indium Tin Oxide (ITO) has also a very high transparency, more than 90%, in the range of light which can be normally converted by photovoltaic devices (visible and near infra-red) and so, because of its very good optical and electrical properties, it is one of the most interesting material among the Transparent Conducting Oxides (TCOs) suitable to be used as front contact in solar cells.

Nevertheless, for a too high doping level the carrier concentration of ITO films decreases; this implies that a part of Tin remains electrically inactive, because, for an excessive Sn concentration, there is a compensation of such donors and also a strong scattering of free charge-carriers. The high impurity amount introduced into the material results also in a distorted crystal lattice, which contribute to reduce either the concentration or the mobility of carriers. This problem can be solved increasing the material deposition temperature.
It has been seen that, as the substrate temperature increases, the material carrier concentration increases too and this phenomenon may be due to an enhancement in the Sn atom diffusion and their better distribution into the $In_2O_3$ lattice. Giving them more energy, they are allowed to thermalize reaching the best energetic conditions, like donors from interstitial locations and grain boundaries into the proper In location sites.

At the same time, an increase in carrier mobility normally happens and it is regarded as the result of a better crystalline quality of the film deposited at higher temperatures, of about 400-450°C, which promote the enlargement in its grains size and reduce the grain-boundary scattering mechanisms. In this way the electrical-resistivity of the film decreases (Figure 33).

Quite similar effects have been observed also performing an annealing of ITO films at high temperature, even if they had been deposited at lower temperatures.

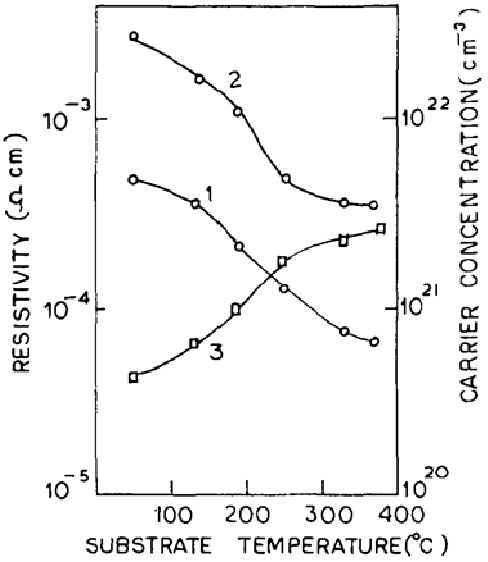


*Figure 33. Resistivity and carrier concentration of ITO films as a function of the substrate deposition temperature. Curves:* ***1)*** *resistivity as deposited,* ***2)*** *resistivity after annealing in air and* ***3)*** *carrier concentration of as deposited films [57].*

The desired optical and electrical properties of ITO films can be obtained mainly depositing them by the sputtering technique.
Using metal In-Sn targets and pure Oxygen like sputtering gas, it's easy to grow thin films of $In_2O_3$ and $SnO_2$ onto the target material surface and as a result of the difference in vapour pressure and sputter rates of these oxides, an In-enrichment of the deposited film can be observed.
Therefore, the film composition easily deviates from the target one and, for this reason, the control on the oxidation state of the target surface is very important.
On the other hand, using oxide targets, a better control on the film stoichiometry can be obtained and also the intrinsic diffusion problems can be minimized.

With ITO targets composed of 90% $In_2O_3$+10% $SnO_2$ it has been possible to grow films with electrical resistivity values of about 1.46 x $10^{-4}$ Ωcm (Y. Shigesato et all.), which is an optimal value for a transparent contact to be used in solar cells. Also in this case, heating the material allows its structure to re-arrange, promoting a better distribution of the dopants and this effect has been noticed depositing also these ITO films at high substrate temperatures, more than 350°C and in fact they have demonstrated lower electrical resistivity and high carriers mobility [58, 59].

Even if ITO is considered an excellent transparent electrical contact, the high doping level makes this semiconductor degenerate, implying a near-infrared light absorption by its free carriers.
In fact, the material normally shows a band edge, in the UV spectral range, which is determined by its energy gap electronic transitions; instead, within the visible region its transmittance is very high and exhibits such extremes of minimum and maximum which are due to interference effects.
More characteristic is the infrared region, in which the film material enters into a reflecting regime with metallic-like properties. The strong enlargement of this absorption and reflection region, called **plasma edge**, is associated to the excitations of the many free electrons present into the conduction band (Figure 34).

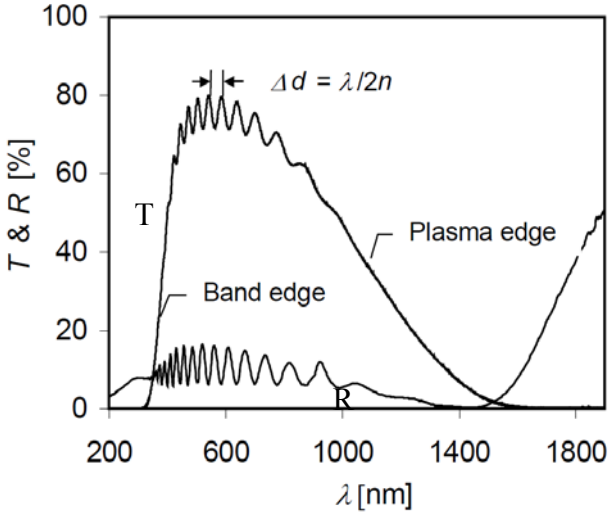


*Figure 34.* ***T)*** *transmittance and* ***R)*** *reflectance of the ITO film with thickness of 1.656 μm [60].*

To overcome this drawback, Zirconium doped ITO could be used, since it was discovered that for dielectric oxides, their permittivity can be increased by the addition of higher-permittivity oxides such as $ZrO_2$ or $HfO_2$ . It is also known that the permittivity of dielectric oxides increases rapidly with even small additions of a higher-permittivity constituent and this is especially true for high-frequency permittivity $\varepsilon_\infty$ . The increase in $\varepsilon_\infty$ due to Zr addition, can shift the plasma resonance wavelength $\lambda_p$ , to a longer wavelength and this makes possible to improve the Near Infra Red (NIR) transmission significantly (Figure 35), without altering the material properties like its carrier concentration or its mobility.

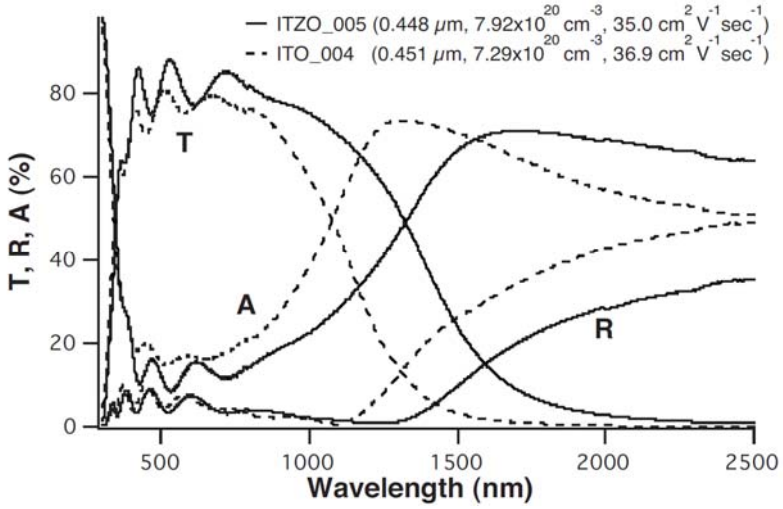


*Figure 35.* ***T)*** *transmittance,* ***A)*** *absorption and* ***R)*** *reflectance of ITO and ITO:Zr (ITZO) thin films [61].*

### 4.2.6 The buffer layer

Since the ITO film contains some In and Sn metallic atoms which are not properly bonded into the lattice and being these atoms good diffusers, it's feasible thinking that they could diffuse into the near layers especially at high temperatures.
These atoms can diffuse into the grains of the poly-crystalline films, contaminating the materials, or segregating into their grain boundaries. In this way short-circuits can be easily formed, causing the failure of the device.
To promote the correct behaviour of the solar cells, it's necessary then to interpose between the CdS and the ITO films a TCO **buffer layer**.

For this purpose, a material which exhibits an optical transparency similar to the ITO one and which is able to stop the possible metallic atom diffusion is needed. A good candidate is Zinc Oxide (ZnO).
The ZnO is a II-VI semiconductor with a direct energy gap of 3.3 eV, it exhibits a high optical transparency near 90% in the visible and NIR solar spectral regions and it tends to grow with a hexagonal Wurtzite crystal structure.

It is known that ZnO electronic and optical properties are extremely dependent on the Oxygen concentration into the material and hence it can be prepared with a wide range of different characteristics, by modifying its stoichiometry.
Like ITO, also ZnO tends to lack stoichiometry as deposited in thin films and this causes its usual *n*-type conductivity.
Its carrier concentration and hence its electrical conductivity are in fact proportional to the typical Oxygen vacancies $V_O$ or Zinc interstitials $Zn_i$, both donor defects, present into the lattice. For ZnO films deposited by reactive sputtering and using a Zn metallic target, clearly the number of $V_O$ or $Zn_i$ decreases with increasing the $O_2$ deposition partial pressure, thus the carrier concentration decreases too and the material becomes nearly intrinsic, or even too much resistive for being used as an electrical contact in solar cells (Figure 36).

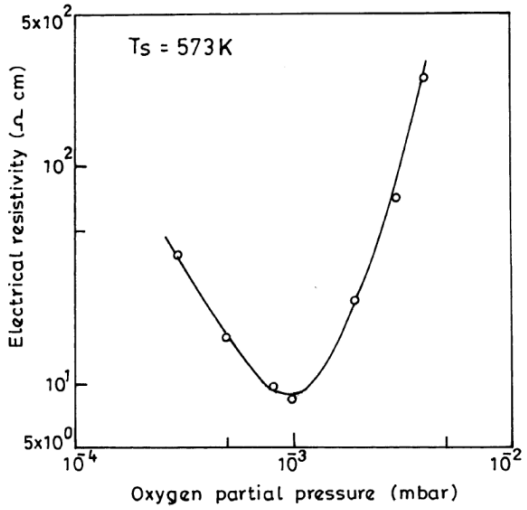


*Figure 36. Electrical resistivity of ZnO films deposited at different Oxygen partial pressures [62].*

On the other hand, with a too little concentration of $O_2$ and depending also on the deposition temperature used, films start becoming opaque, since they contain an excess of Zinc and suffer from different growth kinetics which make the films grow with very small grains (nanometer scale) and so with a more rough morphology.

Instead, using a ceramic target the material can't be grown with as less $O_2$ as wanted, because into the target material there is already a high amount of Oxygen, near to the stoichiometric concentration.
Oxygen, in this case is not a such useful variable for changing ZnO properties; nevertheless, it has been noticed that increasing the substrate temperature from 150°C to 400°C, it is possible to let the material lose some more Oxygen, increasing so its electrical conductivity.
On the contrary, at temperatures higher than 400°C many $V_O$ can be formed, enough to leave a lot of Zn atoms be not bonded in molecules. At these high temperatures and in these conditions even Zn starts to re-evaporate, causing so the erosion of the film.
This material has in fact the characteristic of self-regulating its stoichiometry, limiting any too big defect in stoichiometry.
However, using a proper amount of $O_2$ and the right temperature, the ZnO can be deposited in thin films with a quite high resistivity of $10^2$-$10^3$ Ωcm, which is enough to avoid the increase of the reverse saturation current $J_0$ of the devices, in case there are pin-holes in the beneath CdS layer [63].

In addition to this, ZnO and CdS are both II-VI compounds and, as said before, they grow in a similar hexagonal Wurtzite crystal structure.
For these reasons their lattice mismatch is very small and this condition prevents the CdS/ZnO interface from being damaged by too many defects.

# The innovative process

## 5.1 Deposition techniques

### 5.1.1 The sputtering system

The working principle of the sputtering technique is based on the ignition of a glow discharge. Into a vacuum chamber a target holder and a substrate holder both metallic are installed and by a high-impedance power supply a proper bias is applied between them. They represent in this way the parallel metallic plates of a plane capacitor: the target is the cathode and the substrate is the anode.

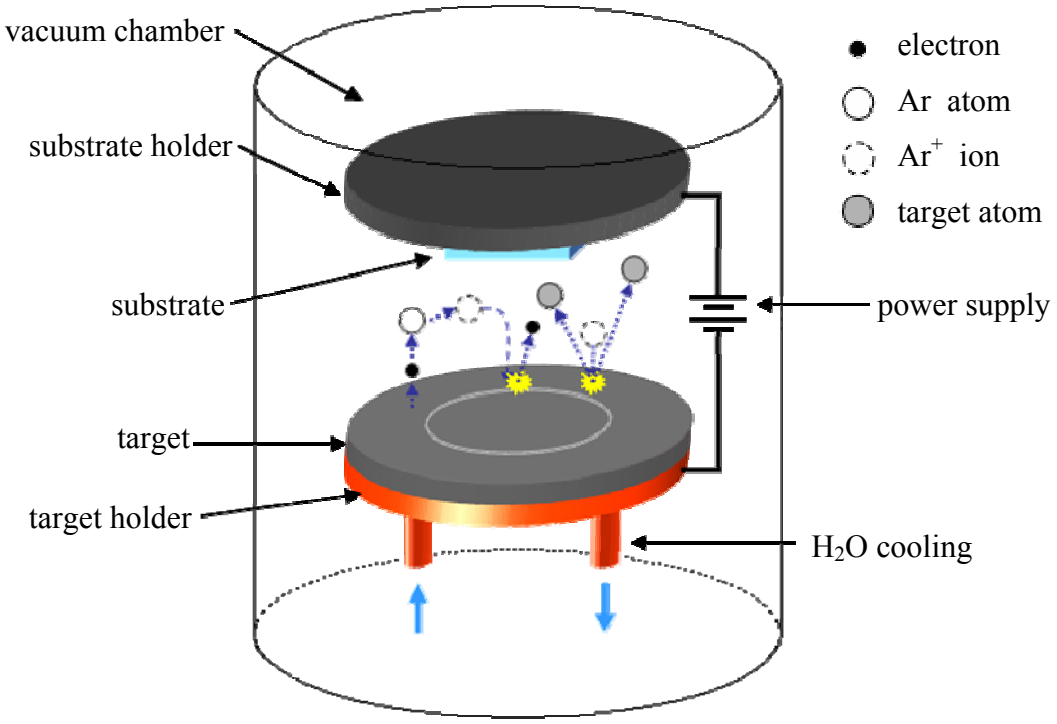


*Figure 37. Working principle scheme of the sputtering system.*

After having evacuated the chamber up to the desired vacuum level ($10^{-5}$ mbar) a high voltage difference of about some hundreds of volts can be applied between cathode and anode and so an intense electric field is generated among them.
Introducing then a controlled quantity of gas into the chamber, thanks to some cosmic radiations which can ionize someone of the gas atoms and thanks also to some ions, which are already present into the gas introduced, it is possible to accelerate these charged particles formed by the electric field produced.

For **Direct Current sputtering** (**D.C.**), during this mechanism a discharge starts and the discharge current increases very quickly while the voltage remains constant, because of the high impedance of the power supply (Townsend discharge regime).
In this configuration, for example positive ions tend to go towards the cathode, bombarding its surface.
Producing a quite intense electric field, by supplying a high voltage bias and by positioning cathode and anode at short distance of about some centimetres and using sputtering gases constituted by high atomic weight species, it is possible to have bombarding particles with energies of about 10-100 eV able to extract atoms, molecules and also secondary electrons from the surface of the target material.
These last ones will be accelerated by the electric field and as a consequence of the scattering with the gas particles they will ionize other gas atoms and molecules, producing an avalanche mechanism.
Then, the discharge can maintain on its own, the so-called “normal discharge”, when the number of the extracted electrons becomes big enough to generate a quantity of ions, which hitting the cathode keep constant the number of those electrons.
At this point the discharge voltage decreases, instead its current increases and the gas starts glowing. In this way a plasma discharge is generated.
Nevertheless, during this stage the target bombardment is not uniform, but it is more intense on its edges and on its surface defects.
If the discharge power is now increased again, the discharge becomes “abnormal”, either the voltage or the current increase and the bombardment finally turns into an uniform configuration, making possible to start the material deposition (Figure 38).

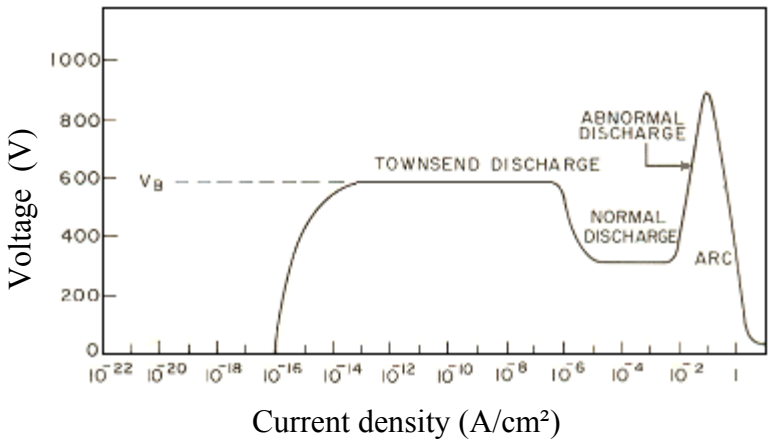


*Figure 38. Formation of the discharge in direct current [64].*

It is very important to cool down the cathode during the bombardment, because, otherwise, the target could locally reach a temperature high enough to obtain a the thermo-ionic emission of electrons, which could increase the avalanche mechanism decreasing the discharge voltage and with a consequent dramatic increase in its current. In this case an “arc discharge” could be generated, able to spoil the target.
In order to improve the target cooling it is possible to stick it to the metallic target-holder, which is water cooled, by using a thermally conductive glue, promoting a better thermal exchange.

The sputtering-gas ions, when neutralized, emit a characteristic light, while the electrons are instead accelerated away from the cathode, producing in this region a negative discharge zone. Moreover, near the target surface a “dark region” tends to form, due to a limited ionization caused by the electrons migration towards the anode; in that region a positive discharge forms, because almost only ions are present there.
Finally there is also a glow discharge region, in which electrons ionize the introduced sputtering-gas atoms and at the end of this region the substrate can be properly mounted in order to have the optimal deposition conditions (Figure 39). The dimension of this region defines the correct target-substrate distance inside the sputtering system.

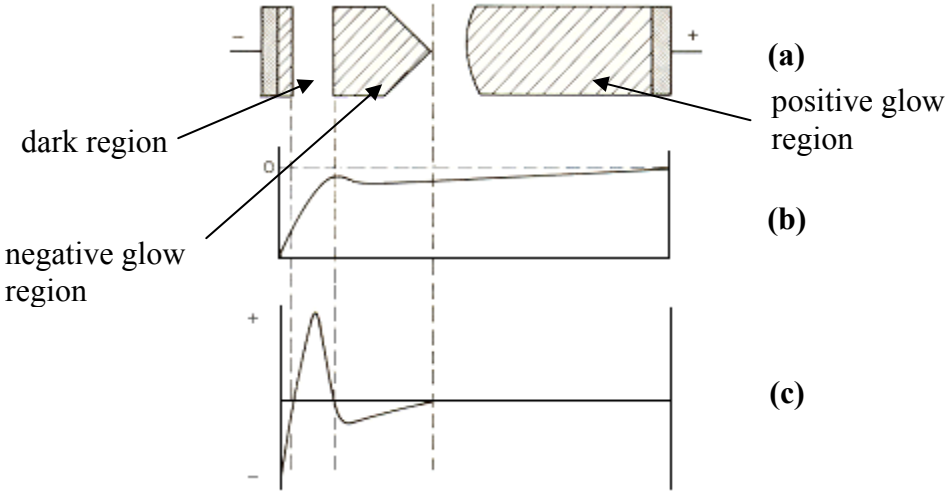


*Figure 39. Position of **(a)** glowing regions, **(b)** voltage, **(c)** charge between cathode and anode [64].*

Nevertheless, with the D.C. sputtering technique it is very difficult to deposit semiconducting materials, or even impossible for insulators, since these materials are not able to exchange the charges accumulated during the ionic bombardment.
Then, on the surface of such a target material a "layer" of charges tends to form, which is able to stop the discharge and hence the whole sputtering process.

To overcome this problem it is possible to use the **Radio Frequency sputtering** (**R.F.**) technique. In this case at each half-period there is an inversion in the system polarization.
As a consequence of this, electrons oscillate into the glowing region, acquiring enough energy to ionize the gas.
This causes an ion bombardment either on the target or on the substrate and in this condition it would be impossible to deposit the film, since part of atoms and molecules condensed onto the substrate would be hit again by ions and then removed (back sputtering).
To avoid this situation it is possible to electrically connect the cathode to the radio frequency power supply by a proper capacitor, in order to increase the negative potential on this electrode.
Doing this, when a radio frequency signal is applied to the system, during the first half-period (positive) there is a high electron current at the anode.
On the other hand, during the second half-period (negative) just a small ionic current instead can flow, because of the lower mobility of the ions which are still near the cathode region.

In this situation a lot of electrons flow towards the cathode, but in the same half-period not an equal amount of ions can reach the anode. So a charge difference between the two electrodes would tend to establish.

However, since through a capacitor a net charge can't be transferred, the anode potential must modify by itself in order that the small positive current could balance the big negative one and this makes the cathode potential even more negative (Figure 40).

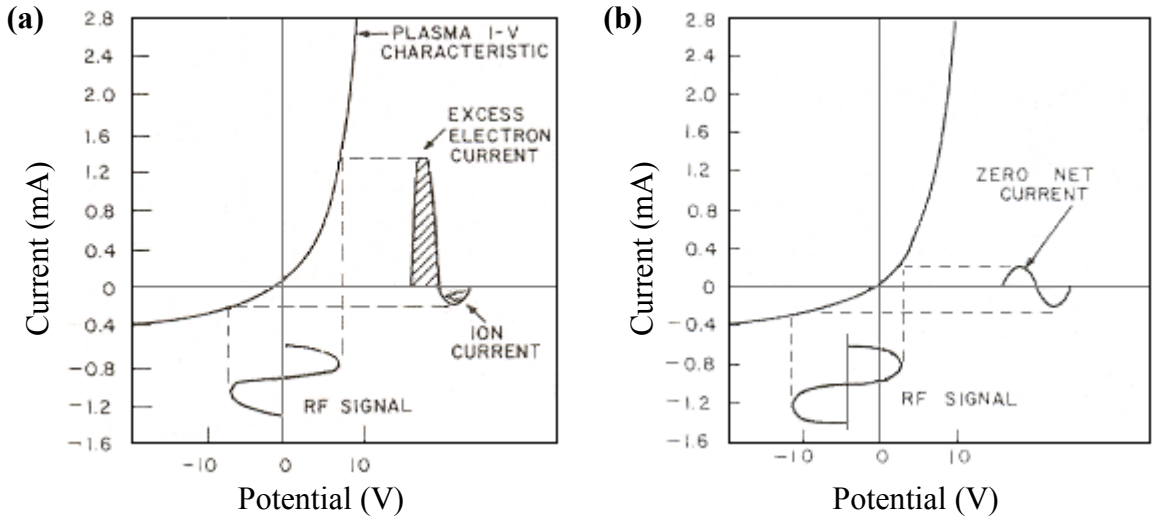


*Figure 40. Discharge current behavior as a function of the radiofrequency potential* ***(a)*** *for electrodes disconnected and* ***(b)*** *for electrodes connected by a capacitor [64].*

With an appropriate capacitor, its characteristic charge and discharge phases produce a total effect that is the real inversion of the system polarization happens only for a very small time during each half-period, like one hundredth of it.
This period will be long enough to allow that a suitable amount of electron can reach the cathode, removing the target superficial charged layer and restoring so its charge neutrality, but at the same time it will be short enough to avoid that the corresponding ions can reach and bombard the substrate, causing the film removal.
In this way it is possible to sputter even very insulating materials without damaging the growing film.

Finally, considering that the electrodes potentials are reverse proportional to the fourth power of their respective surfaces, in order to increase further the cathode negative potential it is possible to electrically connect the anode to the metallic base plate and also to the walls of the vacuum chamber.

It is also possible to add a permanent magnet (constituted by a central cylinder and a concentric ring, for circular targets) directly beneath the target, with the purpose to introduce magnetic field force lines perpendicularly to the electric field.
This variation is called **magnetron sputtering**.
These force lines, together with the electric field, make the electrons arriving near the target do a rotor-translator motion, since they are subjected to a Lorentz force.
In this way electrons are entrapped near the target, enabling then a more efficient gas ionization in this region and increasing so the sputtering efficiency up to three times more than the normal sputtering.

In case it is needed to preserve the composition and the nature of the target material it is compulsory to use sputtering gases which will not react with that material and normally such gases are chosen among the inert gases, like Neon, Argon, Krypton and Xenon.
On the contrary, in some cases there would be the need to modify the composition or to adjust the stoichiometry of the film material, in order to obtain specific film properties.
This is possible by introducing into the deposition chamber a sputtering-gas this time able to react with the target material and to form compounds with it; this procedure is called **reactive sputtering** and it can be performed either in D.C. or in R.F. conditions.
Thinking about compounds which normally tend to lack stoichiometry when deposited, because of the difference in the vapour pressure of their components, using a reactive sputtering-gas it is possible in fact to restore the correct stoichiometry of the growing film, enabling the formation of the desired compound onto the target material surface or into the discharge during the sputtering mechanism.

Finally, to improve the homogeneity and the crystallinity of the growing films, a proper negative bias can be applied to the substrate.
In fact, for low biases applied a small quantity of ions are enabled to bombard the film surface removing its weakly bonded atoms and improving in this way its superficial morphology.
On the contrary, for high biases applied that surface bombardment increases and then it can damage the film or even promote the absorption of gas into the film itself.
For compound materials, these biases can also help to regulate the films stoichiometry, removing mainly their more volatile atomic species.

## 5.1.2 The selenizator

As explained above, to let the CIGS material formation happen it is vital to promote the right interactions, through chemical reactions, between the Cu, In, Ga and Se based "metallic" starting materials.
This innovative process is based on the selenization of precursors, containing the constituent elements. In fact, in this case the starting materials used to form the CIGS are $In_2Se_3$ (or InSe), $Ga_2Se_3$ (or GaSe) and Cu, and by depositing them in a specific structure and promoting their "natural" interaction even at high temperatures it is not possible to obtain directly the desired $CuInGaSe_2$ but another material tend to form.
This is due to the fact that there is normally a too little concentration of Selenium which came from the starting materials, with respect to the stoichiometric one (it will be explained more in details later) and in this condition, if the further annealing of that starting material structure is performed at temperatures near 500°C, the material itself tends to separate into different secondary phases preventing from obtaining the right composition.
To overcome this problem, once the structure made of these "metallic" compounds has been deposited, it is necessary then to perform a selenization of this precursor structure.
The selenization consists in an annealing of the precursor structure at high temperature, in presence of Se based compounds vapours which in this process are made of just pure Se.

The system used to supply correctly the Se needed by the precursor is the **selenizator**.
It consists in a vacuum chamber in which there is a cylindrical graphite effusion cell, similar to a Knudsen cell and this last one is filled with small Se shots.
After having evacuated the chamber down to a vacuum level of about $10^{-5}$ mbar, the cell is heated by a proper coaxial resistive coil up to 300°C, in order to enable the evaporation of Se shots.
The substrate and hence also the precursor structure is kept by a graphite holder, which is mounted exactly on top of the effusion cell, at about 10 cm distance, in the way to face completely the Se-vapour flow produced.
Moreover, it is extremely important to have a high control precision on the substrate heating during the selenization stage, since only a particular range of temperatures (more than 500°C) permits the deposited metallic precursors to mix and to react correctly with the incoming Se for the transformation into a good CIGS material.
It is necessary then to have a heating system which allows to produce a specific substrate temperature ramp, in order to optimize the precursor transformation and at the same time also a uniform heating.

The substrate heating system used is made of heating quartz lamps, placed in the rear of the substrate holder and in this way it is possible to have a very good temperature uniformity on the whole substrate area, which helps the same interaction happen into all the precursor material. Finally the system has also a shutter mechanism, which is very important to stop the early not-uniform Se flow or its deposition once the selenization stage is finished.

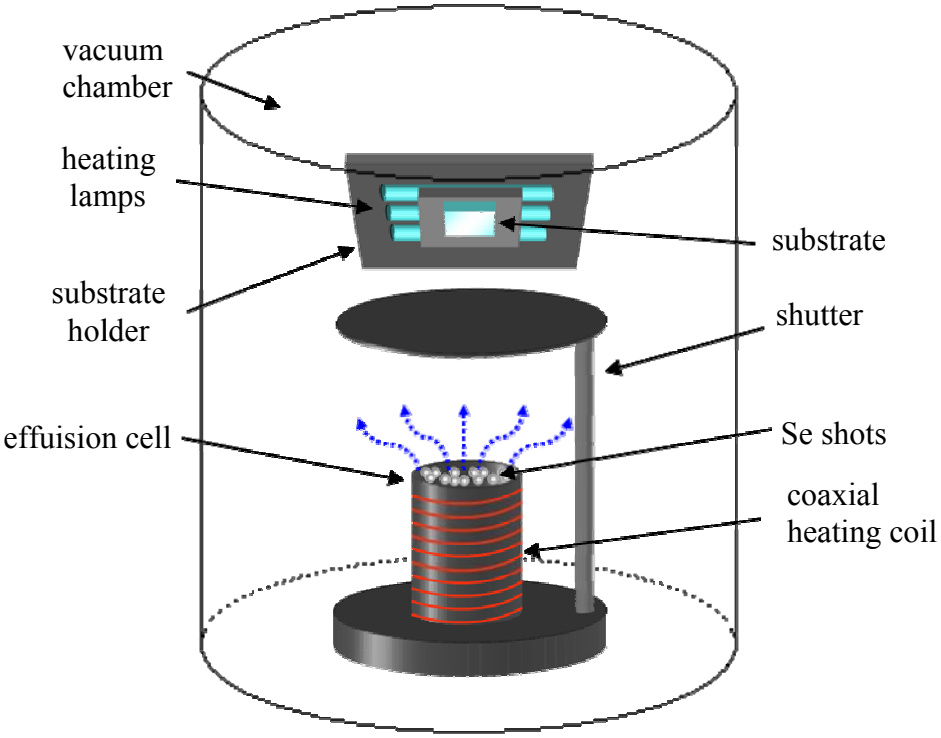


*Figure 41. The selenizator*

## 5.2 The $Cu(In,Ga)Se_2$ growth process

The main subject of this PhD thesis work has been the deposition process focused on the $Cu(In,Ga)Se_2$ growth, purposeful for the production of polycrystalline CIGS thin film solar cells. This process is alternative and innovative with respect to the others used so far worldwide.

The solar cell fabrication starts with the deposition of the back contact.
It is very important keeping in mind that the deposition of the first layer is maybe the most important one, since the morphology and the structure of the whole solar cell will depend on it. For this reason this first deposition must be performed very carefully.
After having cleaned properly the substrate, normally 1 inch square 4 mm thick SLG glass, it is possible to deposit the Mo back contact by D.C. magnetron sputtering in Argon atmosphere.
As explained before, this contact shows better characteristics if it is composed of two Mo films: the first one for the good adhesion to the substrate and the second one for the good electrical conductivity.
Many trials have been performed to find the best deposition parameters; knowing that the deposition pressure mainly affects the Mo adhesion is by, the procedure started depositing this first layer at different Ar pressures.
A good adhesion requires a high deposition pressure, but at the same time it is known that at too high Ar pressures the sputtered Mo films start absorbing the gas, which during the next process steps at high temperatures can even cause the lift-off of the upper layers.

The starting point was set at $8*10^{-3}$ mbar, using a 60 sccm pure-Ar flux.
At the beginning a 30 nm thick Mo film was deposited at room temperature, with a 1.8 $W/cm^2$ power density discharge. In these conditions the Mo film shows a good adhesion to the SLG substrate.
The contact was then completed with a 200 nm thick Mo film, deposited again at room temperature with the same 1.8 $W/cm^2$ sputtering power density, but with a lower pressure of about $5*10^{-3}$ mbar, using a 30 sccm Ar flux, remembering that the film electrical conductivity increases as the deposition pressure decreases.
On top of this contact it was next deposited the precursor absorber material at temperatures of about 400-450°C and then an annealing in vacuum at about 450°C was performed. After this annealing, dismounting the sample from the deposition chamber, it was observed its rapid delamination as soon as it felt the pressure shock, caused by the difference between the deposition conditions and the external environment atmosphere. In this case the substrate remained completely bare and this meant that all the mechanism started hence at the interface between the substrate and the first Mo layer deposited.

It was understood that the pressure for depositing the first Mo layer was not suitable for enabling its good adhesion and to allow it to stand the whole process conditions, in particular the higher temperature annealing stage.
Then, it was deposited the first Mo layer with a lower pressure of about $7*10^{-3}$ mbar, using a 50 sccm Ar flux; again, onto this layer, the second Mo film and the precursor structure were deposited in the same conditions of before and they were further annealed.
This time the structure resisted, so the process was carried out, performing also the selenization of the stacked layers at a temperature higher than 500°C.
Nevertheless, during the selenization stage sometimes it was observed in real time the complete delamination of the deposited structure, with the same result of the previous case.
This meant that the limit situation for depositing a suitable first Mo layer for the whole process was found.
In this way of thinking, the first Mo layer was deposited, reducing more the Ar pressure down to $6.5*10^{-3}$ mbar, using a 45 sccm Ar flux.
Again, the process was carried out as before. This structure resisted even to the selenization stage, which, being the hottest step into the solar cell production procedure, it pointed out that these deposition conditions, for the first Mo film, were suitable for the process.

It was also modified the thickness of this first layer, checking the effects on the whole structure.
For Mo films thinner than 20 nm it was seen, in some cases even before selenization, the lift-off of the precursor structure, leaving the substrate covered only by the first Mo layer.
These layers have been thought to probably be too thin to cover the substrate surface.
In addition, considering a further annealing (the selenization) near the softening point of the SLG substrate, a possible Mo diffusion has to be taken into account.
In fact, after heat treatments, Mo results to have diffused for some hundreds nanometres into the glass substrate as it is demonstrated by Energy Dispersive Spectroscopy (EDS) depth profiling measurement (Figure 50).
In this condition the first Mo layer was easily consumed and the second layer was probably in direct contact with the substrate in some regions.
Remembering some consideration about the Mo deposition conditions, it is obvious understanding why the second Mo layer couldn't keep stuck to the substrate, causing the structure delamination.
Since no effects have been seen for thicker first Mo layers up to 50 nm, it was set the suitable thickness at 30 nm.

Using this preliminary Mo back contact, constituted of a first 30 nm thick layer and a 200 nm thick second layer, some solar cells have been completed.
Neglecting the photovoltaic parameters for this moment, the most important aspect of these solar cells was that their J-V characteristics were affected by the roll-over effect.
In fact, these solar cells suffered from a too electrical-resistive back contact, probably due to a too porous second Mo layer.

The Ar pressure for the deposition of the second Mo film was then decreased down to $2*10^{-3}$ mbar, using a 15 sccm Ar flux, in order to let it grow with a more compact structure.
As foreseen, with this new second layer into the bi-layer Mo back contact, the roll-over in the devices J-V characteristics started reducing.
Since it was not possible to further reduce the Ar deposition pressure, because the sputtering discharge began suffering from stability problems, in order to enhance the back contact ohmic behaviour and to remove completely the roll-over phenomenon, it has been decided to increase the thickness of the second Mo layer, up to 500 nm. Doing this, the roll-over disappeared completely, probably thanks to a really further increase in grain dimensions of the second Mo film and to its more dense and compact nature (Figure 65).

From these results it has been possible to set the right conditions for the deposition of the Mo bi-layer back contact, which can best be done with a first 30 nm thick film and a second 500 nm thick one, both deposited at room temperature with a 1.8 $W/cm^2$ power density discharge and with deposition rates of 0.2 nm/s and 0.4 nm/s respectively.

Once the back contact is completed, it is possible to grow on top of it the CIGS absorber material.
Since the essential idea of this work was a CIGS-based thin film solar cell production cheap and easily transferrable to large scale, it has been decided to develop an innovative process, only established on the sputtering and the selenization (by evaporation) techniques.
In fact, this stage consists in the in-sequence film deposition of the In-, Ga- and Cu-based starting compounds, in order to obtain a precursor material, which can further transform into CIGS during the selenization.
A very important aspect is that the conventionally used Indium and Gallium are low melting point elementary materials, with melting temperatures of about 156.6°C and 29.8°C respectively and with high surface tensile forces. These characteristics in general introduce some problems during the sputtering glow discharge, making these materials quite difficult, or even impossible in the case of Ga, to be deposited by the sputtering technique.

Moreover, it has been found out that, when layers of elemental In, Cu and Cu-Ga alloys are used, in order to obtain the right precursor, suitable for being further selenized, an annealing at quite high temperature and for a long time is normally needed [65].

For these reasons it has been decided to substitute in this process Indium with $In_2Se_3$ and Gallium with $Ga_2Se_3$ . In fact, these last semiconducting materials have both higher melting points (more than 850°C) and they also can stand very well all the operating conditions of the process.
Since all the chosen starting materials can be deposited by the sputtering technique, for their deposition it has been used an unique sputtering chamber, containing four different sources, Mo, $In_2Se_3$, $Ga_2Se_3$ and Cu targets.
In this way the possible contaminations from the external environment between subsequent depositions of these materials are avoided, keeping safer the composition of the future precursor.

### First method using $In_2Se_3$ , $Ga_2Se_3$ and Cu

The first idea was of producing first a $CuInSe_2$ material, for checking step by step the correct working of the process and adding in a second time the needed Ga content for obtaining the desired $Cu(In,Ga)Se_2$ absorber layer (Figure 44).
Knowing that the Cu atom is a very good diffuser and that it is very reactive with In, these properties have used to promote the better Cu-In interaction.
If the Cu film is put over the In-based one, during its diffusion towards the back of this deposited structure it could mix and interact with most of the beneath material. On the contrary, if Cu is deposited under the $In_2Se_3$ film it will be able to diffuse just in a small portion into that material, depending on their deposition temperatures. As a consequence, the probability that some $In_2Se_3$ doesn't react increases, preventing from obtaining a good stoichiometric uniformity.
Hence a precise sequence of the starting materials has to be respected and, for this reason, on top of Mo it is necessary to deposit first the $In_2Se_3$ film.
In order to promote its best crystallinity and morphology, this material needs to be deposited at a high substrate temperature, of about 400°C.
At lower deposition temperatures the In-based film tends to grow with a Se-excess. In fact, in these conditions, $In_2Se_3$ films were characterized by some segregations, represented by superficial Se-rich zones. These segregations are quite dangerous because, reacting with Cu, they can easily form $Cu_2Se$ phases into the absorber material, causing the short-circuit of the future *p-n* junction.

On the other hand, at temperatures higher than 450°C it has been seen that the $In_2Se_3$ film starts to form separated islands; loosing the more volatile Se, the material becomes In-rich, hence at high temperature it tends to liquefy and to divide into drop-like regions.
For this reason, the $In_2Se_3$ film is deposited at a substrate temperature of about 400°C, by R.F. magnetron sputtering, with a 3.3 W/cm$^2$ power density discharge and at $5*10^{-3}$ mbar pressure (1 nm/s deposition rate), using a 30 sccm Ar flux.
In fact, increasing the sputtering power from the 80 W used for Mo to 150 W, the $In_2Se_3$ films were more uniform, since with this high-power bombardment it is possible to obtain more easily a film with the same stoichiometry of the target, avoiding disproportions caused by the difference in elements' volatility. Polycrystalline films grown in these conditions results to be very well crystallized and uniform.
In order to produce an absorber layer of about 2-3 μm total thickness and considering the amounts of the other further constituents needed to reach the desired CIGS stoichiometry, a 1.5 μm thick $In_2Se_3$ is deposited.

Nevertheless, depositing a Cu layer on top of the $In_2Se_3$ film at 400°C substrate temperature, the obtained precursor and even the further selenized material normally present a lot of segregations. In fact, the $In_2Se_3$-Cu interaction has resulted to be very strong.
If this interaction happens during the deposition at high temperature, it makes the material lack in stoichiometry, since other phases different from CIS are allowed to form first.
For this reason, the Cu-deposition temperature has been lowered down to about 350°C, noticing that in this way the $In_2Se_3$-Cu interaction is more quiet, even if a partial mixing of constituents can however happen.

Moreover, in order to avoid the detrimental $Cu_xSe$ phases, it is necessary to grow the $CuInSe_2$ material (the same is true also for the further $Cu(In,Ga)Se_2$ ) with a bit less of Cu, with respect to the stoichiometric Cu/In = 1 ratio. Doing this, all the Cu atoms introduced into the absorber material can combine completely with the other constituents, preventing any Cu residual phase, keeping also in mind that with less Cu the probability of Cu-vacancies formation increases and even the *p*-type conductivity of CIGS.

To have a right amount of Cu for obtaining a good absorber material starting with a 1.5 μm thick $In_2Se_3$ film, a 200 nm thick Cu layer must be deposited.
After the Cu deposition an annealing in vacuum is performed and the produced structure is kept at 450°C for about 30 minutes, letting the materials mix more.

In fact, at this temperature these materials mix quite well and by their reaction a CIS precursor layer is formed. Nevertheless, as it can be seen by the X-ray diffraction (XRD) spectrum obtained in grazing incidence mode, this layer contains the <112> chalcopyrite $CuInSe_2$ phase with also residuals of $Cu_{11}In_9$ and $In_2Se_3$ phases (Figure 42). This is due to the fact that the deposition temperatures, but mainly the amount of Se introduced from the $In_2Se_3$ starting material, are not sufficient to make the deposited precursor material completely transform and reach the correct stoichiometry throughout its volume.

At the same time, it is also possible to see from this XRD spectrum that no Cu-peak is present and this confirms that all the introduced Copper has really reacted with the other constituents, leaving no elemental residual.

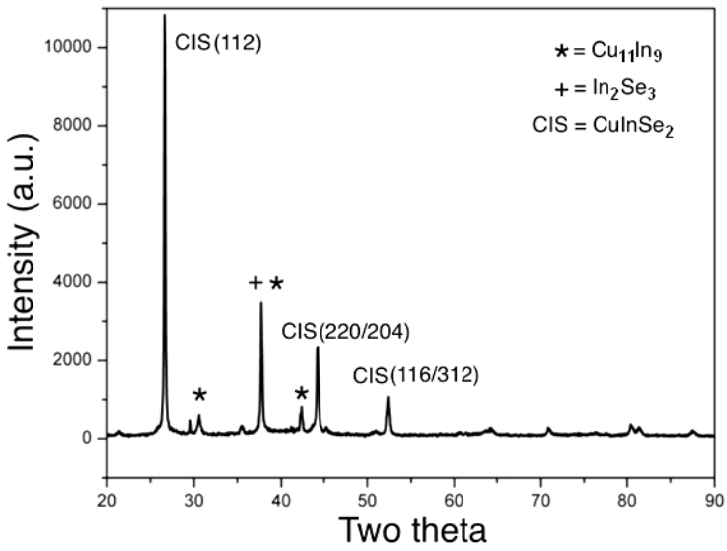


*Figure 42. XRD spectrum of $In_2Se_3$+Cu precursor layer, as deposited.*

In order to obtain a homogeneous $CuInSe_2$ film, without spurious phases the precursor is now selenized.
The selenization is performed by using the selenizator instrumentation described before.
After having heated the Se into the effusion cell up to 300°C and having produced a constant Se vapour flux, the precursor starts to be heated; the substrate heating ramp is very fast and it takes less than 4 minutes to reach 500°C, starting from room temperature.
In fact, the faster is the ramp for heating the precursor, the higher is the probability to prevent the formation of secondary phases at intermediate temperatures and this procedure is normally called rapid thermal annealing (RTA).

At the beginning the Se vapour is kept shuttered until the precursor reaches a temperature of at least 450°C, because just at these high temperatures, Se atoms can diffuse correctly into the whole precursor layer and the constituents start to react properly, going into their phase diagram. If the precursor is exposed to the Se vapour at lower temperatures, some other phases mainly with lower formation energy like, $Cu_2Se$ will form.
Once these spurious phases form, it will be difficult to remove them and, as already said, they are quite detrimental since they cause very easily short-circuit problems into the further *p-n* junction.

On the contrary, if the precursor reaches temperatures of about 500°C without receiving any new Se addition, the "old" Se present into the precursor structure will be not enough to mix completely all the In and Cu deposited and their residuals will tend to strongly interact, causing the formation of secondary phases and a bad crystallization of the absorber film.
Then, at 450°C the precursor is exposed directly to the Se vapour, letting at the same time its temperature increase quickly up to 530°C (the substrate softening-point limit), enabling its transformation into a uniform $CuInSe_2$ phase, which is the most reactive and stable at these high temperatures.

At the same time, as a consequence of the better interaction between constituents, the stoichiometry defects can be much reduced, improving the CIS film uniformity and crystalline quality.
In fact, Scanning Electron Microscopy (SEM) morphological characterizations have revealed that the CIS film after selenization results very well crystallized, with big grains of about 500 nm in size, very close one to each other and all with the same shape and these are really the consequences of a good growth mechanism (Figure 43).

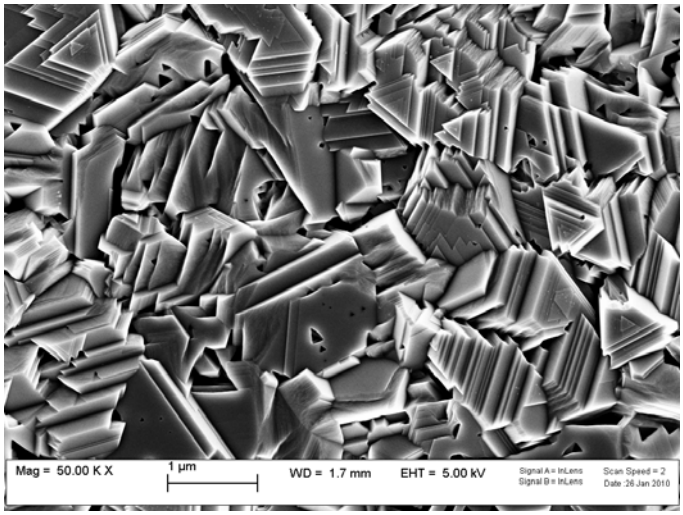


*Figure 43. SEM image of $CuInSe_2$ film morphology after selenization, obtained using $In_2Se_3$ , $Ga_2Se_3$ and Cu starting materials.*

At this point, in order to obtain the $Cu(In,Ga)Se_2$, Gallium needs to be added to the CIS material. For this reason the $CuInSe_2$ film is now covered by depositing in sequence a structure made of $Ga_2Se_3$ and Cu layers. As explained before, also in this case Cu is deposited last, in order to help the intermixing of these materials already during their depositions.
A 200 nm thick $Ga_2Se_3$ polycrystalline film (corresponding to a theoretical Ga/(In+Ga) ratio of about 12%) is deposited at the same 400°C temperature used for $In_2Se_3$, by R.F. magnetron sputtering with a 1.8 W/cm$^2$ power density discharge at $5*10^{-3}$ mbar pressure (0.4 nm/s deposition rate) and using a 30 sccm Ar flux. Immediately after, by keeping fixed the temperature, a 30 nm thick Cu film is deposited by D.C. magnetron sputtering with a 1.8 W/cm$^2$ power density discharge at $2*10^{-3}$ mbar pressure and using a 15 sccm Ar flux.

$Ga_2Se_3$ differs from $In_2Se_3$ deposition, because it can't be deposited with higher sputtering power, since as the bombardment power increases its local temperature increases too, causing a disproportion of the target material and the formation of Ga-rich liquid-like areas on its surface, which make the target no more usable for further sputtering depositions.

Even if Ga has been added, the material produced so far is not $Cu(In,Ga)Se_2$ yet, because at these temperatures $Ga_2Se_3$ results to be not able to set enough Ga free into the precursor structure to substitute In and also because the Se concentration introduced by $Ga_2Se_3$ is again too little to reach the correct stoichiometry with all the other constituents. For these reasons another selenization step is required in order to make this new precursor transform into CIGS.

Noticing the $Ga_2Se_3$ low chemical reactivity, in order to promote a better interaction of the constituents an annealing at 450°C in vacuum has been performed also on this second new precursor structure, for about 30 minutes.
As expected, the higher temperature of the annealing promotes the better intermixing of these stacked layers.

$Ga_2Se_3$ has revealed also that it can be well deposited directly on top of the CIS layer even up to 450°C, without losing too much Se and without disproportioning.
Since in this configuration the $Ga_2Se_3$ stands well the high temperatures, it has been deposited even the last Cu film at a higher temperature, of about 450°C, because the underneath layer is made of CIS, which is more stable than the starting materials and it can stand the Cu interaction at these high temperatures without damaging.
This higher temperature has resulted to let the $Ga_2Se_3$-Cu structure intermix from the very beginning with the beneath CIS layer, allowing also their better and easier reaction during the further selenization stage.
In this case, since last depositions have been performed already at 450°C, the annealing step is then no more necessary and so the process time length can be reduced.

Even if the intermixing of the starting materials has been improved at higher temperatures, their correct interaction hasn't happened yet and no CIGS-based material has been formed.
To make this new precursor structure completely transform into CIGS, it needs to be selenized again.

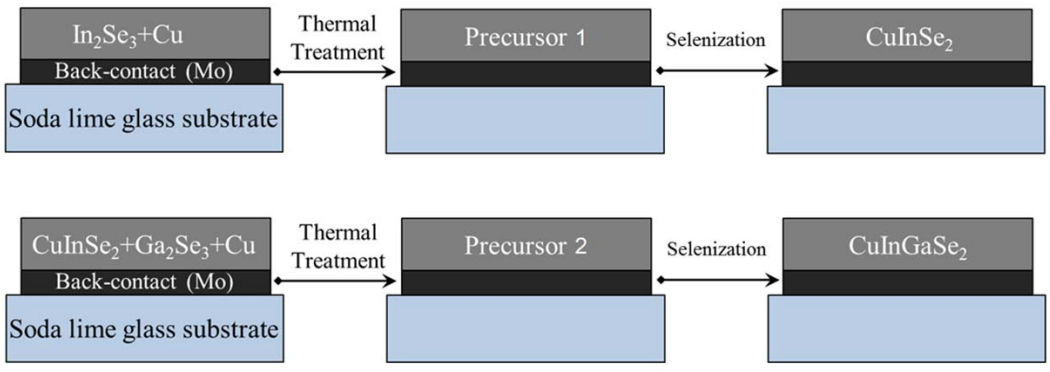


*Figure 44. Schematic image of the first method developed for CIGS film deposition, using InSe, $Ga_2Se_3$ and Cu starting materials.*

The higher selenization temperature, together with the simultaneous addition of Se, enable the Ga atoms to be set free from $Ga_2Se_3$ and to diffuse in the structure, promoting its interaction with the other constituents and the entry into the correct phase diagram.
Finally after the second selenization the CIGS material is formed.
Grazing incidence XRD spectra have confirmed that the precursor layer, or better its superficial portion, was really transformed into CIGS.
In fact, analyzing these spectra and comparing them with the CIS ones obtained before, it is easy to notice the characteristic peak-shift at higher angles, which is related to the transformation of CIS into CIGS, since this last one has smaller lattice parameters with respect to the CIS itself (Figure 45).

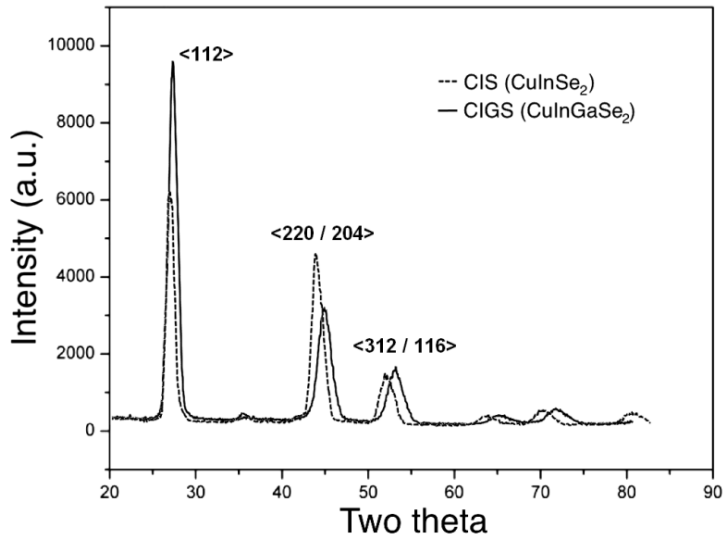


*Figure 45. Comparison between $CuInSe_2$* ***(dashed-line)*** *and $CuInGaSe_2$* ***(solid-line)*** *grazing incidence XRD spectra obtained with the first method, using $In_2Se_3$ , $Ga_2Se_3$ and Cu starting materials.*

By other XRD analysis, performed deeper into this material, it has been noticed that, in addition to the $Cu(In,Ga)Se_2$ characteristic peaks, into the absorber film there are also other peaks, related to phases like $CuInSe_2$ , $Cu(In,Ga)_3Se_5$ and $Ga_2Se_3$ (Figure 46).

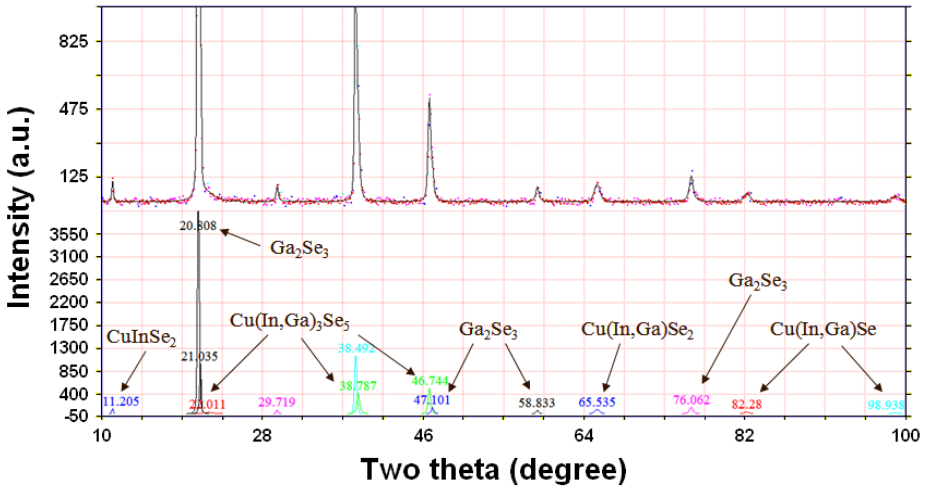


*Figure 46.* ***(up)*** *deep XRD spectrum of CIGS layer, obtained with the first method using $In_2Se_3$, $Ga_2Se_3$ and Cu starting materials, after the second selenization and* ***(down)*** *peacks deconvolution.*

Since some $CuInSe_2$ is still present into the material, this means that not all the absorber layer is transformed into CIGS.
On the other hand, the presence of the $Cu(In,Ga)_3Se_5$ phase into the absorber is very important, because this material tends to form when the CIGS tends to be Cu-poor. It demonstrates again that the absorber material lacks correctly a bit in Cu concentration, as desired, and hence that this process is suitable to produce a CIGS absorber material for solar cells.
As already said the $Cu(In_{3-x}Ga_x)Se_5$ is able to form a *p-n* pseudo-homojunction with the *p*-CIGS, which improves the electronic behavior of the junction itself. The same mechanism is thought to happen also into the film grain boundaries, which act as conduction-inversion centers and also as barriers for the carriers confinement into the CIGS columnar grains.
In this way, into the grain boundaries the carriers recombination mechanism is reduced, allowing to an increase of the device photovoltaic parameters [41].
Finally, the presence of residual $Ga_2Se_3$ phase means that not all the Gallium introduced by the $Ga_2Se_3$ starting material could be set free or reacted to form CIGS, probably because $Ga_2Se_3$ didn't interact completely at the thermodynamic conditions of this procedure.

After having grown this preliminary absorber material some solar cells have been completed, depositing onto the CIGS film a 80 nm thick CdS window layer, a 100 nm thick ZnO buffer layer and a 500 nm thick ITO front contact film. To improve the conductivity of the front contact and the device current collection, a Mo grid contact layer is also added; these steps will be described more in details later.

These solar cells have exhibited low open-circuit voltage ($V_{OC}$) in the range of 420-450 mV, low short-circuit current density ($J_{SC}$) in the range of 12-15 mA/cm$^2$ and fill factor (FF) in the range of 35-40%. These low parameters are due to the non-correct CIGS stoichiometry obtained and in particular the low $V_{OC}$ is related to the too little concentration of Ga introduced into the CIS material lattice, remembering also that a part of Ga couldn't react because it still fixed into the $Ga_2Se_3$ phase.

In order to supply more Ga to the CIS material and, as a consequence, to increase the devices $V_{OC}$, the $Ga_2Se_3$ film thickness has been increased up to 400 nm (a theoretical Ga/(In+Ga) ratio of about 22%) and correspondingly also the thickness of the Cu film up to 50 nm.
This absorber material has been tested again, producing some solar cells with the same latest procedure described above and they have exhibited $V_{OC}$ in the range of 500-520 mV, $J_{SC}$ in the range of 27-30 mA/cm$^2$ and fill factor of about 60%, with conversion efficiencies of about 11% (Figure 66).
Trying to increase more the solar cell $V_{OC}$, even thicker layers of $Ga_2Se_3$ have been deposited, with the corresponding Cu ones, but instead of seeing an increase in $V_{OC}$, the $J_{SC}$ started to decrease and in some cases with a consequential $V_{OC}$ reduction. This is due to the fact that as the $Ga_2Se_3$ film thickness increases, a higher concentration of residual $Ga_2Se_3$ remains into the absorber material and since it is quite an electrical-insulating material, over a certain amount it starts forming a too electrical-resistive layer, which introduces a series resistance into the solar cell. In fact, the J-V characteristics of these devices were really affected by a series resistance and they showed its typical effect.

Since it was not possible to increase the $V_{OC}$ just adding more $Ga_2Se_3$ into the structure, without causing a decrease in $J_{SC}$, EDS measurements in depth profiling mode have been performed on this absorber material, in order to check the distribution of constituents and principally the Ga concentration profile.
These EDS spectra have revealed that the Ga concentration was almost uniform, along the absorber thickness and with a small increase towards the back contact (Figure 47).
By these measurements it has been noticed that Ga tends more to diffuse towards the back of the precursor than to react near the surface and this has been ascribed to a low reactivity of the $Ga_2Se_3$ with the other starting materials.
$Ga_2Se_3$ seems to be too much stable for the thermodynamic conditions used and to set Ga free only at higher temperatures, at which the Ga diffusion is probably too high in comparison with its reactivity to allow the Ga to react locally in the proper way with the other constituents.

Near the absorber surface, where the *p-n* junction will establish, the Ga/(In+Ga) ratio is however too low with respect to the 25-30% optimal theoretical value, needed to obtain solar cells with better photovoltaic parameters and especially higher $V_{OC}$ and an approximate value of this concentration was estimated in about 10%.

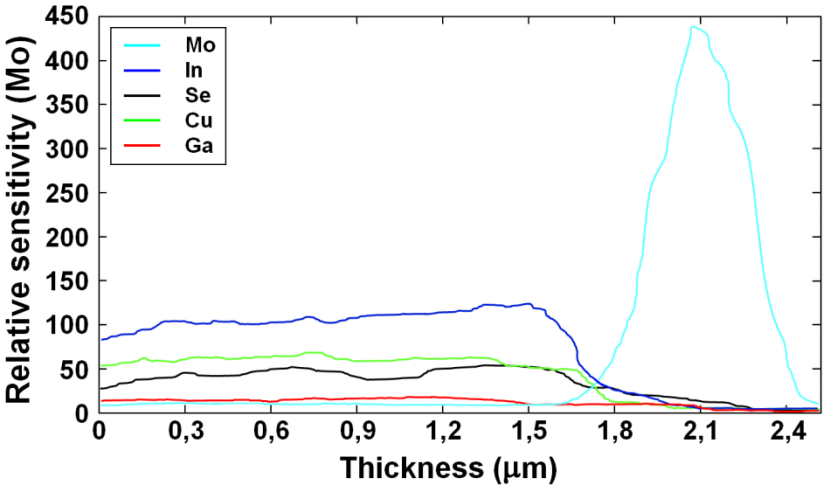


*Figure 47. EDS depth profiling spectra of constituent elements into the CIGS absorber material obtained with the first method, using $In_2Se_3$ , $Ga_2Se_3$ and Cu starting materials.*

Since Ga tends to diffuse from the surface into the precursor, before interacting properly with the other constituents, its diffusion has been limited by reducing the Ga concentration gradient towards the back of the precursor, in order to have a higher Ga concentration near the layer surface.
In this way of thinking it has been deposited on top of the "right" CIGS film a further second structure, composed of other $Ga_2Se_3$ and Cu layers.
At the same time, in order to avoid a too high concentration of residual $Ga_2Se_3$, the $Ga_2Se_3$ film thickness has been reduced in the first $Ga_2Se_3$-Cu structure.
In this way, on top of the CIS layer a 200 nm thick $Ga_2Se_3$ and a 30 nm thick Cu films have been deposited in the same conditions as before and the precursor has been then selenized and transformed into CIGS. Onto this layer other 200 nm thick $Ga_2Se_3$ and a 30 nm thick Cu films have been deposited always in the same conditions, and this new precursor has been selenized again.

With this new procedure, it has been possible to obtain solar cells with higher $V_{OC}$ up to 530 mV, with fill factor similar to the previous case, but with lower $J_{SC}$ .

Now, it seems that near the absorber layer surface there is really a higher Ga concentration. These results can be explained by thinking that the CIGS is very stable at the process conditions and this limits the diffusion of further Ga. In addition, the new added Ga can stay more near to the precursor surface, because it "feels" the presence of the Ga introduced before and so it can be really affected by a smaller concentration gradient.
In this way, a more Ga-rich superficial CIGS, with a higher energy gap, can form the *p-n* junction and it allows higher device $V_{OC}$ .
At the same time, since in this condition Ga can't diffuse very much into the precursor material, but stays more near its surface, also the $Ga_2Se_3$ residual remains there, even in higher concentration (less diluted into the CIGS), limiting the device photo-current.

Having in mind the idea of developing a process for producing high efficiency solar cells, which could be also easily scalable on industrial level, it is necessary to increase further the solar cell performances and think about other strategies, alternative to these very time-consuming ones.

Remembering the experimented high thermal stability of the $Ga_2Se_3$, this material has been used like a high temperature reaction "catalyst", in order to allow the constituent interaction to happen only at high temperatures, probably at more favourable conditions, at which all the constituents could really interact and form a better absorber material.
To reduce the time length of the process, the first selenization step has been eliminated, depositing the $Ga_2Se_3$ and Cu films directly on top of $In_2Se_3$-Cu structure, in the same conditions as before.

At this point, this whole new precursor structure is selenized, but after selenization the material has resulted to have a lot of segregations.
This has been explained considering again the high $In_2Se_3$-Cu reactivity. In fact, during the first selenization, thanks to the high temperature and the incoming Se, these materials could properly interact leading to the formation of the more stable CIS phase, which could correctly receive the further $Ga_2Se_3$-Cu structure.
Now, having added from the very beginning the $Ga_2Se_3$ to the as deposited $In_2Se_3$-Cu structure, the thermodynamic conditions of the system have been changed. Furthermore, performing a single selenization of this precursor structure, new chemical reactions tend to be promoted.
Taking into account that $Ga_2Se_3$ has a very low reactivity at these temperature conditions and that only near 500°C it starts setting Ga free, which can interact with the other constituents, it is easy to understand that as long as that temperature is not reached, all the constituents can't react properly.

At the same time, the reaction between $In_2Se_3$ and Cu could already happen, starting from about 400°C, but without receiving the correct amount of Se, since it is limited by the $Ga_2Se_3$ layer, they tend to form other more stable In-Cu phases.
This results in a new material, different from CIS or CIGS and rich in spurious phases.

### Second method using $In_2Se_3$ , $Ga_2Se_3$ and Cu

The solution consists in modifying the latest layer structure, depositing the starting materials in a different sequence.
Keeping all these results in mind, the $Ga_2Se_3$ film has been interposed between the $In_2Se_3$ and Cu ones (Figure 48).

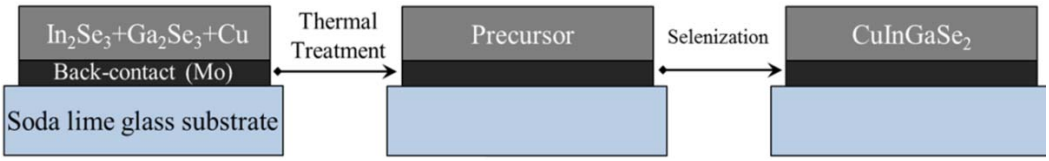


*Figure 48. Schematic image of the second method developed for CIGS deposition ,using $In_2Se_3$ , $Ga_2Se_3$ and Cu starting materials.*

The process has been changed, by depositing first the 1.5 μm thick $In_2Se_3$ film as usual and on top of it the $Ga_2Se_3$-Cu structure at a substrate temperature not higher than 400°C, in order to not cause thermal problems to the $In_2Se_3$ film and also paying attention on maintaining the good Cu/(In+Ga) and Ga/(In+Ga) ratios found with the previous method.
This precursor material is not as uniform as the one obtained in the previous configuration, but presents a lot of superficial segregations and a separation of grains.
Since it has been demonstrated that $Ga_2Se_3$ can be well deposited even at 450°C temperature, the problem should be related to the Cu film deposition.
It is well known that Copper is a very good diffuser and its diffusion increases as the temperature rises.
It is possible that, in these conditions, Cu has really a very high diffusivity, enough to partially penetrate into the $Ga_2Se_3$ layer. This is probably due to the fact that under the $Ga_2Se_3$ layer there is no more a Cu-containing CIS material and, as a consequence, Cu suffers from a strong concentration gradient, which enhances its diffusion.
At the same time, since $Ga_2Se_3$ doesn't interact at these temperatures but stays very stable, the Cu diffusion results so strong to provoke a partial separation of grains into the polycrystalline

$Ga_2Se_3$ film. This causes a bad film morphology and even a different local transformation into CIGS during the further selenization.
For this reason, Cu must be deposited on top of $Ga_2Se_3$ at a lower 350°C substrate temperature, in order to prevent these problems. Performing a further annealing in vacuum at 400°C, it is possible to improve more the film uniformity.
The precursor material is now good enough to be selenized in the same way as before.

Now, during selenization it is possible to notice that the starting point of the precursor transformation happens really at higher temperatures, with respect to the first method and only at about 480°C a changing in the precursor film morphology happens.
This can be really ascribed to the presence of $Ga_2Se_3$ between $In_2Se_3$ and Cu, which makes the constituents, mainly Indium and Copper, interact and mix only at higher temperatures leading to a better transformation of the precursor into CIGS.
This transformation can be seen in real time (through a window in the selenizator chamber) and it consists in an apparent smoothing of the of the film surface, which results more reflective.
This hypothesis has been confirmed to be true by a further SEM characterization.

The CIGS absorber material grown in this latest way is very similar to the material obtained with the first procedure, it is very well crystallized and its morphology is uniform along all the substrate area.
This morphology is similar to the CIS one, but as it can be seen by the SEM image (Figure 49), with a smaller grain size, which is representative of the transformation into CIGS. This is also the reason of the change seen in the film surface reflectivity, described before.

In this case it is necessary to point out that in general a good polycrystalline absorber material must be formed by grains big enough to guarantee the collection of most of the photogenerated carriers, allowing them to easily reach the *p-n* junction without coming up against too many grain boundaries, which tend to limit their transport.
In order to help these carriers to reach the junction before recombining, the absorber film grains must be bigger than the carrier diffusion length (of about 0.3-1 μm).
Nevertheless, the reduction of grains dimensions as a consequence of the CIS transformation into CIGS, which are however about 0.2-0.3 μm, mustn't be considered detrimental. On the contrary, the contraction of the grain dimension makes the film more compact, increasing the removal of micro-grain boundaries, which can exist between the starting grains, bigger but at the same time more rough.

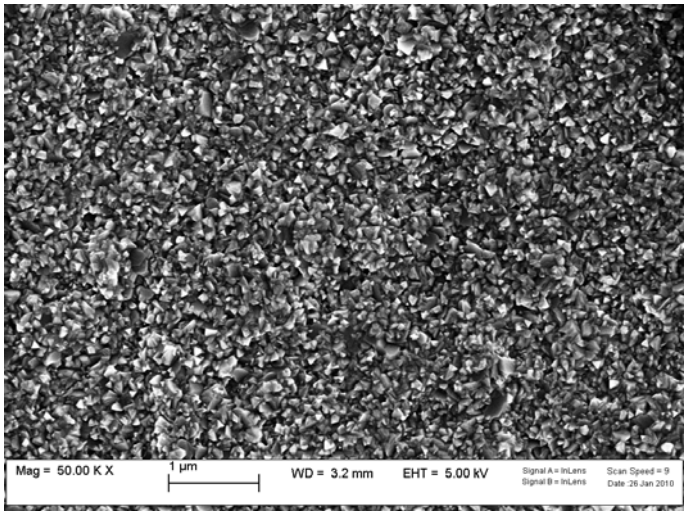


*Figure 49. SEM image of Cu(In,Ga)$Se_2$ film morphology after selenization obtained with the second method using $In_2Se_3$ , $Ga_2Se_3$ and Cu starting materials.*

This kind of CIGS material can be obtained in similar morphology and composition even if the annealing in vacuum is not performed on the precursor, before the selenization.
This is an important discover, because in this way the process time length can be further reduced.

The absorber material grown with this second method is similar to the CIGS produced with the first one, either in morphology, or in composition as confirmed by XRD spectra.
With this second method, best results have been obtained by depositing 500 nm thick $Ga_2Se_3$ and 270 nm thick Cu films.
Solar cells produced with this absorber material have exhibited best photovoltaic parameters of : $V_{OC}$ = 510 mV, $J_{SC}$ = 32 mA/cm$^2$, FF = 52% and efficiencies of about 11% (Figure 67).
The higher $J_{SC}$ obtained can be probably ascribed to the better interaction between $In_2Se_3$ and Cu, which happens at higher temperatures.
Maybe, in these latest thermodynamic conditions, a CIS matrix with a better crystal structure can form, preventing the lattice defects from trapping and limiting the photo-carriers flux, allowing their better collection and transport towards the junction.

In order to obtain higher efficiency CIGS solar cells it is very important that the Ga is distributed into the absorber material in a proper configuration.
For this reason, EDS depth profiling measurements have been performed also on this new absorber material obtained with the second method, checking the Ga distribution.

In this case, SIMS spectra have demonstrated that Ga concentration profile is still different from the desired distribution.
With this second method Ga diffused even more than in the previous one and in fact, this CIGS material has a much higher Ga concentration towards the bottom of the absorber near the Mo back contact, with respect to the surface, near the future interface with the CdS layer (Figure 50). This is quite similar to a Ga single-graded distribution, even if the Ga/(In+Ga) ratio near the CIGS surface is still about an approximate 10% and reaches the optimal 27% only in the bottom part of the absorber material.

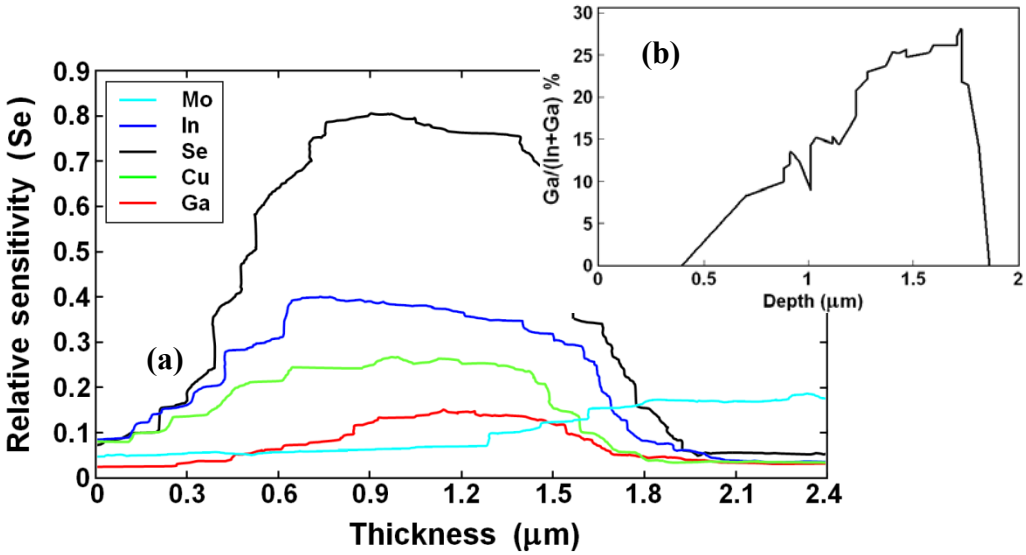


*Figure 50.* ***(a)*** *EDS depth profiling spectra of constituent elements into the CIGS absorber material obtained with the second method, using $In_2Se_3$ , $Ga_2Se_3$ and Cu starting materials and* ***(b)*** *detail of the Ga/(In+Ga) distribution along the CIGS layer thickness.*

Also for this second method many trials have been done to increase the Ga concentration near the absorber layer surface, but, as soon as the $Ga_2Se_3$ film thickness is increased over than the optimal value mentioned above of 500 nm, the $J_{SC}$ tends to decrease as well as the fill factor. This is probably due to the series resistance introduced by a too thick $Ga_2Se_3$ layers, the same described in the previous case.
Considering that $Ga_2Se_3$ tends to release Ga only at very high temperatures, it seems that Ga is set free in delay with respect to the reaction between Cu, In and Se, which instead have a high reactivity also at lower temperature, letting them very probably react sooner.

Taking into account that Ga has a very high diffusivity, once it is set free and that a more stable Cu-In-Se phase forms at lower temperatures, the reactivity between Ga and that phase is even lower, leaving the Ga to diffuse more along the precursor and to partially interact with it.
In this way, after having diffused so much into the precursor structure, just only a small part of that Ga, the one more near the Cu-In-Se phase, could react properly with the other constituents. Instead, staying deeper at bottom, most of it can interact there only with the incoming Se, forming a consistent electrical-insulating Ga-Se phase, like $Ga_2Se_3$ .
Moreover, the Ga concentration gradient into the precursor is probably still too strong and this could have even increased more the Ga diffusivity.
For these reasons, it is clear that as the $Ga_2Se_3$ film thickness increases, also the amount of $Ga_2Se_3$ residual increases too.
In addition, as the amount of the not bonded Ga (in the CIGS lattice) increases, it tends to form more Ga-Se phases like $Ga_2Se_3$ , causing the same problems of photo-current described before.
With this procedure the Ga diffusivity seems to keep however higher than its reactivity and despite increasing the $Ga_2Se_3$ film thickness, which means the amount of Ga introduced, any further enhancement in the solar cell performances can't be seen.

Despite the second method is faster, since only one selenization step is performed, the system is affected by a too strong Ga diffusion, which produces a not correct Ga concentration profile.
On the other hand, with the longer first method it is possible to regulate more precisely the Ga concentration gradient, mainly at the surface.
However, the efforts made with these procedures, in order to produce a good CIGS absorber characterized by a correct Ga graded profile with a higher concentration near the layer surface, didn't give the desired results.
Considering these results, it is clear that $Ga_2Se_3$ is not the ideal Ga-based starting material to allow the Ga to react correctly with the other constituents, taking into account that $Ga_2Se_3$ doesn't set easily enough Ga free for the correct stoichiometry of the absorber material.

With the aim to produce solar cells with better performances, the proper reactivity and consequently the Ga distribution into the absorber layer have to be improved.
To achieve these this condition, the $In_2Se_3$ and $Ga_2Se_3$ have been changed with other materials, which could better interact.
For this purpose, first the $In_2Se_3$ has been substituted with InSe.

InSe behaves like $In_2Se_3$ , at the sputtering conditions used, and so it can be deposited in a similar way.
Now, on top of the Mo back contact a 1.5 μm thick InSe polycrystalline film is deposited at 400°C substrate temperature, by R.F. magnetron sputtering with a 3.3 W/cm$^2$ power density discharge, at $5*10^{-3}$ mbar pressure (1.2 nm/s deposition rate), using a 30 sccm Ar flux.

### First and second methods using InSe, $Ga_2Se_3$ and Cu

Even in this case, both the two methods have been tested, depositing the same kind of structures in the optimized conditions described above, but paying attention in tailoring the thickness of $Ga_2Se_3$ and Cu films in order to obtain a good stoichiometry with the new InSe film (Figure 51).

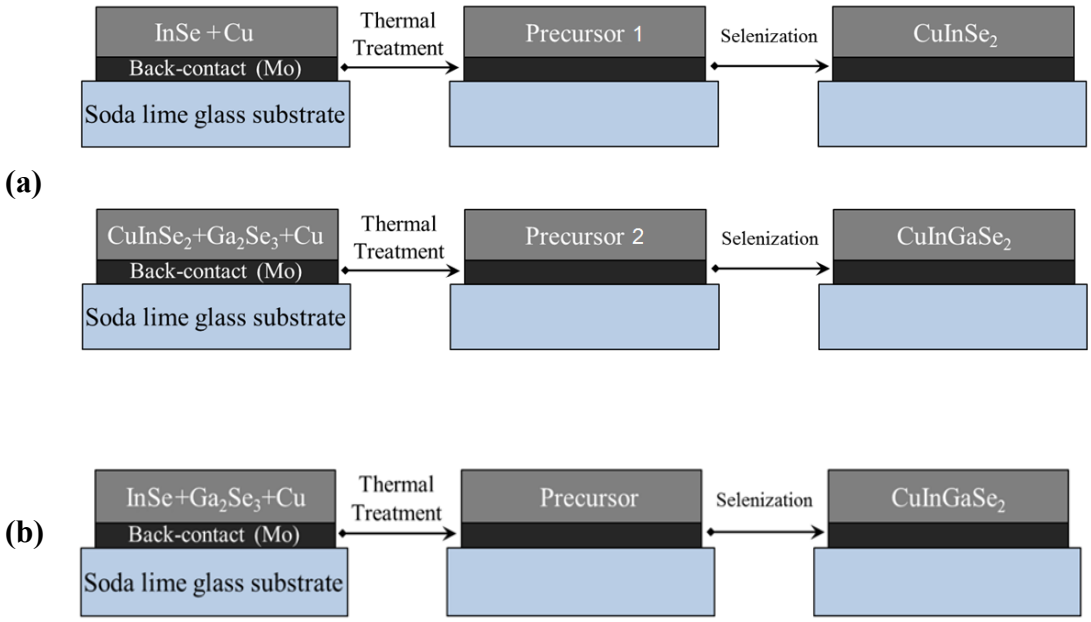


*Figure 51. Schematic image of the* ***(a)*** *first and* ***(b)*** *second method developed for CIGS deposition, using InSe, $Ga_2Se_3$ and Cu starting materials.*

In the first process method, in order to obtain a CIS precursor, it has been noticed that depositing Cu directly on top of InSe at the same 400°C temperature or even at 350°C, the reactivity of Cu with the InSe itself is already too stronger. In fact, it leads the surface of the precursor film to present a lot of phase defects, resulting in a inhomogeneous and rough precursor material.
To limit these segregations, Cu needs to be deposited onto InSe at a lower temperature of about 300°C.

Finally, it has been possible to complete the absorber material for both the two process options, in the same ways described above.

Solar cells prepared with this new precursor material have immediately exhibited, in both cases, higher $J_{SC}$, of about 34-35 mA/cm$^2$ (Figure 68).
This can be explained in terms of a better interaction between InSe and the other constituents, thanks to the temperatures and hence to the thermodynamic conditions used in the process.
In fact, being InSe more reactive than $In_2Se_3$, it can probably set In free into the absorber material in a more easy and uniform way. So, reacting with the other constituents and especially with Cu in a better way, it is feasible that InSe allows the formation of a better CIS matrix with the correct stoichiometry on a larger portion of absorber, enhancing both its optical and electronic properties.
Nevertheless, even if the $J_{SC}$ of the solar cells has increased up to very good values, any further increase in their $V_{OC}$ has been noticed and it is still quite low, around 480 mV.
This clearly demonstrates that the Ga interaction and distribution into the absorber material is not sufficient yet.

Once again, in order to improve the devices conversion efficiency the process needs to be modified.
Remembering that the major reason of the wrong Ga distribution into the absorber is the too low reactivity of $Ga_2Se_3$, it has been decided to change also this compound, with another Ga-based starting material, in order to enhance the reactivity. This new material has also to able to supply Ga in an easier way and in case also in a higher amount into the absorber for obtaining a better CIGS absorber material.
The selected material for this purpose is GaSe.
In fact, exhibiting a lower melting point than $Ga_2Se_3$ and decomposing at lower temperature, this material can probably more easily set Ga free, allowing a better interaction with the other elemental constituents, especially with Copper.
GaSe has revealed to have a thermal stability similar to $Ga_2Se_3$ and already at about 400°C deposition temperature uniform and homogeneous polycrystalline GaSe films can be obtained, without Se excess and then suitable for being processed.

GaSe is deposited by R.F. magnetron sputtering, with a 1.8 W/cm$^2$ power density discharge, at $5*10^{-3}$ mbar pressure (0.3 nm/s deposition rate), using a 30 sccm Ar flux.
Like $Ga_2Se_3$, GaSe can't be deposited with higher sputtering power, otherwise the target tends to suffer from a disproportion, segregating Ga-rich phases in form of drops into the bombarded region.

At his point both the two methods have been tested again, now using InSe and GaSe instead of $In_2Se_3$ and $Ga_2Se_3$.

## Second method using InSe, GaSe and Cu

To check mainly the effect of this latest substitution, the latest developed sequence has been used, but changing $Ga_2Se_3$ with a tailored GaSe film in order to keep the good constituents ratios found before.
The 1.5 μm thick InSe film is deposited first, always in the same conditions described before, and then it is covered by a sequence of GaSe and Cu layers (Figure 52).


*Figure 52. Schematic image of the second method developed for CIGS deposition, using InSe, GaSe and Cu starting materials.*

In this case, Cu has revealed that it can be deposited onto GaSe at the same 400°C and even at 450°C substrate temperature, without causing any morphology problem into the precursor, but instead improving the surface uniformity.
This reveals, since the beginning, the better behavior of GaSe at the process conditions.
Since the last deposition can be performed already at 450°C, it has been decided of removing the vacuum annealing step.
Just looking this new precursor material under the optical microscope, it is clear that constituents material have really reacted better than the previous cases. In fact, the precursor layer appears smoother and more uniform, without any phase separation onto the surface.

To test its morphology, SEM analyses have been performed on the precursor. As deposited, this precursor material is well crystallized, with arranged grains which present almost all the same shape and dimensions, in agreement with the smoothness of the film (Figure 54a).
At the same time with the electron microscope it has been noticed the presence of few small drop-like particles onto the film surface, probably Se-based compounds.

XRD measurements have been done on this new precursor material, to check its composition.
Grazing incidence XRD spectra confirmed that even during their depositions at 400-450°C constituents could already partially interact, forming the CIS phase.
In addition, as it can be seen in the spectrum, a part from CIS into the precursor material there are only InSe and GaSe residuals and no other intermediate phases were observed (Figure 53).
This is a consequence of a better reaction, especially between InSe and Cu, since all the Cu introduced has been "used" to form $CuInSe_2$ phase and not any other spurious phase.
The presence of residual InSe is due to the lower Cu amount introduced into the material, with respect to the stoichiometric Cu/(In+Ga) ratio equal to 1, in order to avoid $Cu_xSe$ phases caused in case by any Cu excess.
This result is another confirmation that the interaction and the ratio between constituents are now more correct.
However, very important is that Ga has not been set free at all from GaSe during the very deposition and didn't promote a partial transformation of the precursor into CIGS.
The selenization is still necessary to allow the CIGS growth.

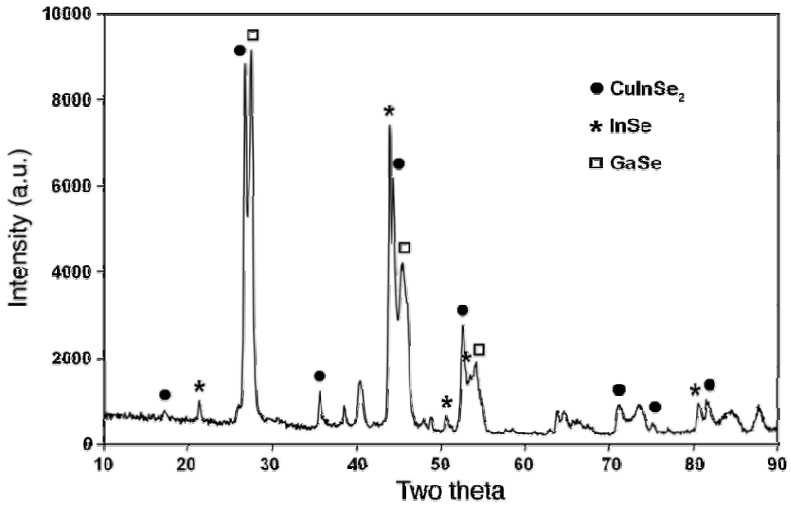


*Figure 53. XRD spectrum of the InSe-GaSe-Cu based precursor layer, as deposited.*

Similar results have been obtained by depositing all these layers at 400°C, making in this way any further annealing no more necessary.
This is another important discover, which allows to reduce further the process time length.

The precursor is then selenized in the usual way.
In this case the change in morphology of the precursor, as a consequence of the transformation into CIGS during the selenization, can be noticed already starting at about 450°C substrate temperature, as soon as the precursor received the Se vapour.
The fact that the precursor transformation happens at lower temperatures, than the previous cases, further reinforces the hypothesis of the higher reactivity of these latest starting materials.
The effects of the better behavior of the InSe, GaSe and Cu starting materials, at the process thermodynamic conditions, have been seen mainly by the SEM characterization of the so-obtained absorber material.

Looking at the SEM image below (Figure 54b), it is very evident that the crystallization of this film is the best one obtained so far, among all the methods performed before.
This CIGS film is more compact and dense and its grains are even much bigger than before, with an average dimension bigger than 1 μm.
These grains are also so tightly packed that the corresponding grain boundaries are considerably reduced.

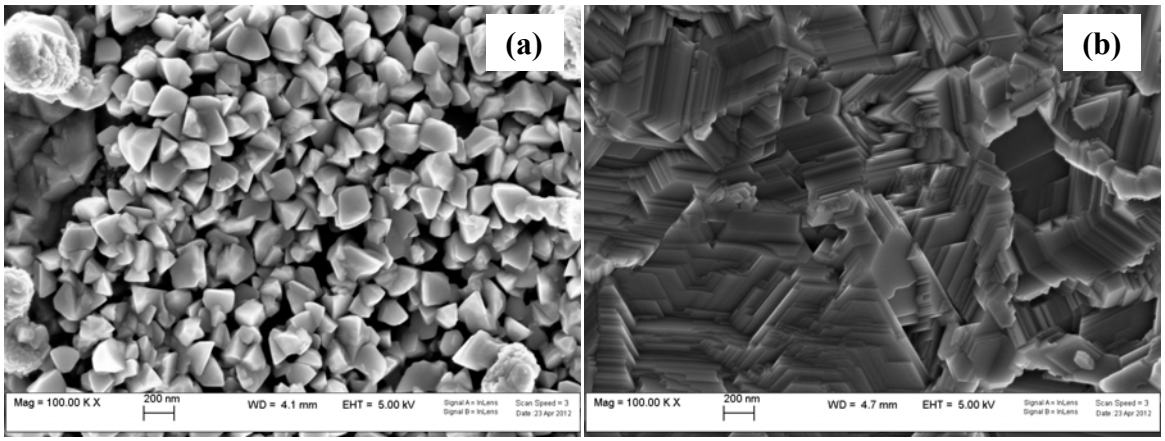


*Figure 54. SEM image of* ***(a)*** *the InSe-GaSe-Cu based precursor layer, as deposited, and* ***(b)*** *the co-respective CIGS layer after selenization.*

In order to check its compositional and stoichiometric quality, grazing incidence XRD measurements have been performed on the so-obtained absorber material (Figure 55).

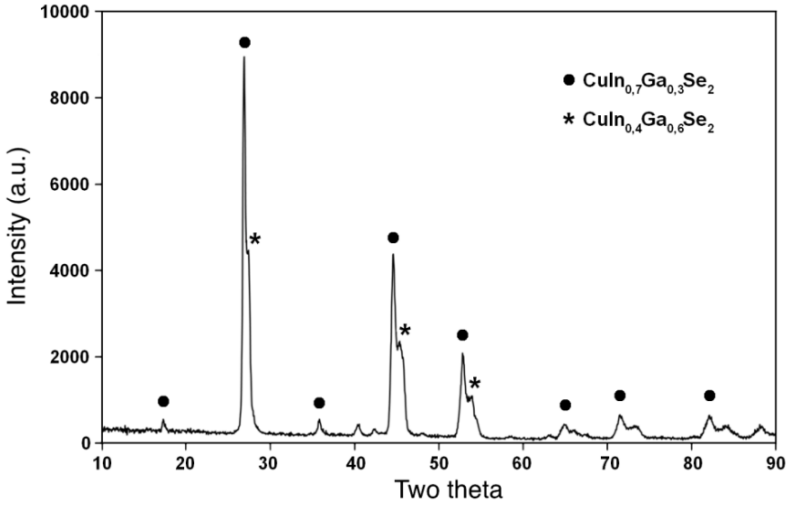


*Figure 55. Grazing incidence XRD spectrum of the CIGS layer after selenization, obtained using InSe, GaSe and Cu starting materials.*

This spectrum is very important, because it clearly shows that with this process a good CIGS material can be grown.
In fact, this CIGS absorber layer, or better its superficial part, is composed only of the $Cu(In_{0.7}Ga_{0.3})Se_2$ and $Cu(In_{0.4}Ga_{0.6})Se_2$ phases and this demonstrates the very good and better stoichiometry reached.
Moreover, the fact that in addition to the CIGS phase material with a 30% Ga/(In+Ga) ratio, there is also another CIGS phase with a 60% Ga/(In+Ga) ratio, it could be a good signal that the Ga concentration into the absorber has been really increased.
Even performing deeper XRD analysis, this material results to be very uniform and homogeneous, since it is composed almost completely of $Cu(In_xGa_{1-x})Se_2$ and $CuInSe_2$ phases. Only some secondary Ga-based phases are still present, but their contributes are so small that they can be considered negligible (Figure 56).

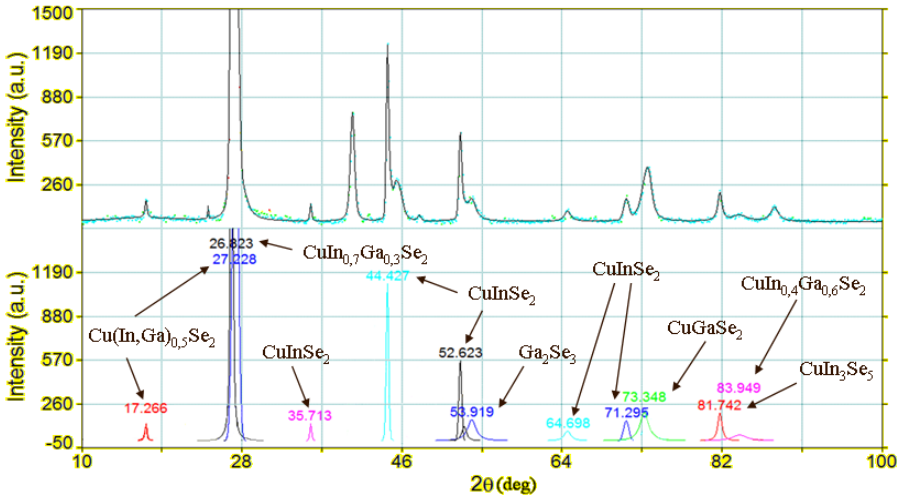


*Figure 56. Deep XRD spectrum of the CIGS layer after selenization, obtained with the second method using InSe, GaSe and Cu starting materials.*

The fact that almost all the Ga supplied from GaSe has been "used" to form the CIGS material and that no other Ga-based phases, or GaSe residuals remain into the absorber material, is another further confirmation that GaSe is more reactive than $Ga_2Se_3$ and that it can set Ga free in an easier way (no more Ga-Se residuals) and in a bigger amount (CIGS phases with 60% of Ga near the surface), for obtaining the desired CIGS stoichiometry.

All these features let consider this CIGS material a very promising absorber, more suitable to produce good solar cells.
Best results have been obtained by depositing 1.5 μm thick InSe film, covered with about 500 nm thick GaSe and about 280 nm thick Cu layers. Nevertheless, solar cells produced with this absorber and completed in the standard way described before, never show $V_{OC}$ higher than the cells made with the previous methods, of about 520 mV, but at the same time they exhibit good $J_{SC}$ in the range of 35-36 mA/cm$^2$ and fill factor in the range of 64-65% (Figure 69).
The fact that the devices $V_{OC}$ didn't enhance very much with respect to the previous cases, even if the interaction of these latest materials has been demonstrated to be much better, it makes think about a probably still not proper distribution of Ga into the absorber layer.

This has been checked by EDS depth profiling measurements, thanks to which it has been discovered that even if the Ga concentration has really increased, more than double, into the CIGS layer, reaching an approximate average value of about 24%, it is probably quite constant, with a small increase towards the bottom of the structure (Figure 57).

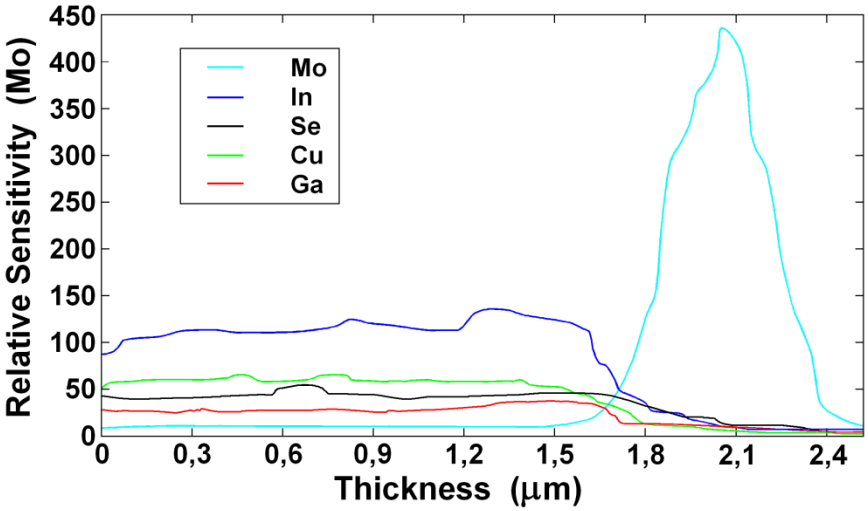


*Figure 57. EDS depth profiling spectra of constituent elements into the CIGS absorber material obtained with the second method, using InSe, GaSe and Cu starting materials.*

It is reasonable that, at the thermodynamic conditions used in the process, the mechanism of GaSe diffusion into the absorber material is still faster than its interaction with the other constituents.

Keeping fixed the InSe amount, but tailoring accurately the Cu film thickness for maintaining the right constituents ratios, neither increasing the GaSe film thickness up to 1 µm no enhancement in the photovoltaic parameters has been observed.
On the contrary, a strong reduction in $V_{OC}$ , $J_{SC}$ and fill factor happens. This is probably due to the introduced big amount of GaSe, which, remaining in a too consistent GaSe residual phase, or having let almost all the Ga diffuse towards the bottom of the absorber before reacting, it introduced a series resistance into the device.

First method using InSe, GaSe and Cu

In order to have a higher Ga concentration close to the surface of the absorber layer, the first method has been tested with the idea of adding GaSe to the CIS precursor material.
This time, after having deposited the InSe and Cu films, at their respective correct temperatures found before, this structure has been completed by directly depositing the further GaSe and Cu layers without any previous selenization or annealing, reminding the better reactivity of these starting materials and also in order to not increase the process time length.


*Figure 58. Schematic image of the first method developed for CIGS deposition, using InSe, GaSe and Cu starting materials.*

Also in this case the GaSe and the final Cu layers can be deposited at 400°C.
The structure is composed of a 1.5 μm thick InSe film, a 260 nm thick Cu one, a 400 nm thick GaSe one and a final 60 nm thick Cu layer.
A better precursor morphology can be even obtained by depositing the last Cu layer at a higher temperature, about 450°C, promoting a better partial intermixing.
After selenization the CIGS material is still well crystallized, similar to the latest case.

Solar cells produced with this absorber material show photovoltaic parameters very close to the previous ones.
Only with an increase in the InSe film thickness of up to 2 μm and tailoring the other constituents ratios by depositing on top of it a 330 nm thick Cu film, a 500 nm thick GaSe one and the final 60 nm thick Cu layer, it has been possible to have a further little increase in $V_{OC}$ up to 530 mV.
This small increase in $V_{OC}$ can probably be ascribed to a better crystallization of the InSe layer, felt also by all the further structure. In fact, it is feasible that, as the film thickness increases, a widening in grains dimensions can occur. For this reason, with a better crystallization the defective grain boundaries are reduced. This condition reduces the probability that a detrimental parallel resistance can form into the material.

In addition to this, if InSe film is more compact and with bigger grains, the diffusion of atoms or molecules coming from the near layers, mainly Cu, through its grain boundaries can be reduced. This can help the interaction between the starting materials to really happen between uniform and extended material layers and not between small-localized different phases, preventing the formation of islands with different composition and improving the homogeneity of the whole absorber layer.

Also in this latest case, the limitation in solar cells photo-voltage can be explained by EDS depth profiling analysis, in fact, it has demonstrated that the Ga distribution is still almost the same of before, with a quite constant concentration along the absorber thickness.

It is to be kept in mind that in the case of $In_2Se_3$ and $Ga_2Se_3$ the high $V_{OC}$ were obtained when the $Ga_2Se_3$-Cu structure was added to an already formed CIS layer and even higher when it was added to a CIGS layer.
For the CIS layer, the $Ga_2Se_3$ diffusion was regulated in part by the high stability and by the more compact structure of the underneath layer.
On the other hand, for the CIGS layer, the Ga diffusion was probably limited by a reduction in its gradient concentration towards the back, promoting only a little increase in the superficial Ga concentration and enabling the enhancement in $V_{OC}$ .
Even if in the previous cases there was a limitation in $J_{SC}$ , because of the $Ga_2Se_3$ residuals, the first procedure of the first method has been reproduced, but now using InSe and GaSe, since higher $J_{SC}$ were obtained with these materials.
For this reason, the InSe-Cu structure is deposited and then selenized in order to grow a CIS layer. After that the GaSe and the final Cu layers are added and the new precursor is then selenized again, allowing its transformation into CIGS.
Even in this case, solar cells prepared with this absorber material exhibit results similar to the previous ones, without any increase in $V_{OC}$ .

At this point, since probably the Ga diffusion can't be limited neither by the $CuInSe_2$, which is more stable and compact than any precursor material, it has been acted on the Ga concentration gradient.
It has been experimented the effect of adding other GaSe to the CIGS layer obtained in this latest way.
Another precursor structure has been made, by depositing on top of such a CIGS layer a 70 nm thick GaSe film and a 30 nm thick Cu layer at a substrate temperature of 450°C and then it has been selenized.

The so-obtained absorber material has been used to produce some solar cells and they have exhibited immediately an increase in $V_{OC}$ up to 560 mV and at the same time $J_{SC}$ in the range of 30-33 mA/cm$^2$ and fill factor in the range 60-62% (Figure 70).
Noticing this amazing jump in $V_{OC}$ it has been tested the effect of adding even more GaSe on top of that starting CIGS layer.
As foreseen, as the amount of GaSe added increases into the absorber layer, the $J_{SC}$ starts to decrease, but however depositing onto a similar starting CIGS a structure made of a 400 nm thick GaSe film and a 60 nm thick Cu one it has been possible to reach open circuit voltages up to 620 mV. Despite this very good voltage value, these solar cells exhibit low $J_{SC}$ of about 22 mA/cm$^2$ and also low efficiencies of about 8%.

It is clear that the gradient concentration is a very powerful instrument to limit the Ga diffusion into the precursor material, carrying out the correct reaction more near the surface of the precursor layer.
Despite the Ga concentration gradient approach has revealed to be efficient, this latest procedure results too long in terms of the process scalability and most of all it doesn't allow to obtain high efficiency devices.

To check if all these selenization steps are really necessary to obtain a good Ga distribution, it has been tested this latest procedure removing the intermediate selenization step.
Similar results have been obtained in both cases and the intermediate selenization, for the CIS layer formation, results to be not necessary for producing a good CIGS absorber material with the desired Ga concentration profile.
In this way, the time length of this procedure can be reduced, but the need to obtain higher conversion efficiencies remains.

For this reason, it has been limited the Ga concentration gradient into the precursor structure in other ways.
Introducing the GaSe in part at the bottom of the absorber structure and in part close to its surface, this last Ga would suffer from a smaller gradient "driving force" towards the bottom, keeping a higher Ga concentration near the surface.

### First option for limiting the Ga concentration gradient

In the first option, GaSe has been deposited first on top of the Mo back contact, at the standard 400°C temperature and then covering it by the usual InSe-Cu structure.

This new precursor seems to be even better than the latest ones, since it looks like more uniform and with a smoother morphology because it is made by smaller grains.
Since GaSe has been deposited as the first layer of the precursor structure, it is reasonable that any further annealing or selenization would make it diffuse more towards the back, modifying its local concentration.
Considering again all the previous results, the next step is then the deposition of the usual GaSe-Cu structure at 400°C, directly on top of the precursor and without any selenization.
The morphology of this new precursor is still very uniform and it doesn't show any considerable difference with respect to the previous stage.
This precursor needs to be selenized, in order to transform it into CIGS.

After selenization the CIGS material demonstrates almost the same morphology and crystallization quality of the latest films and for this reason it has been tested, producing some devices.
Solar cells produced in this way exhibit $V_{OC}$ of about 510 mV, but at the same time low $J_{SC}$ and low fill factor.
However, most important is that their J-V characteristics show the presence of a series resistance and a small roll-over effect and this has been ascribed mainly to problems related to the back contact.
Probably the GaSe put directly onto the Mo layer couldn't react properly with the other constituents, since its diffusion and intermixing was inhibited because of its position into the structure (taking into account the similar situation and results of before).
In this way, most part of all that GaSe film probably remains at the Mo/absorber layer interface, forming there an electrical resistive phase between, which limits the photo-current extraction.

Reducing the thickness of this bottom GaSe layer from 400 nm to 100 nm, an enhancement in $J_{SC}$ and fill factor has been observed, but the effect of a series resistance is still present.

The thickness of the first Cu film has been also increased, in order to promote a better intermixing with that GaSe, thanks to the very high reactivity and diffusion tendency of Cu.
At the same time, in order to prevent any Cu excess and the formation of spurious $Cu_xSe_2$ phases during selenization, the final Cu film has been removed from the structure.
No change in the device performances and in J-V characteristics has been seen, as a consequence of this variation.

Doing this and noticing that the final absorber material didn't suffer from consistent morphological problems, it has been understood that, thanks again to its good reactivity, GaSe can be even deposited as the final layer of the precursor structure, without any upper Cu film, still mixing and interacting properly.
The position of the GaSe films and then the sequence of the starting materials inside the precursor structure have resulted to be the process key points, since they affect very strongly the absorber growth and its photovoltaic properties.

Considering that neither with this procedure $V_{OC}$ can't overcome 510 mV, even in the latest case the Ga concentration gradient seems to be too strong, preventing Ga from staying more close to the absorber surface.
Probably the upper Ga can "feel" the presence of the Ga inside the GaSe layer at the bottom only after its diffusion into the beneath layers, making the surface of the absorber film be Ga-poor, preventing from obtaining higher $V_{OC}$ .
Hence, in order to further limit the Ga concentration gradient into the precursor, the process has been modified once again.

### Second option for limiting the Ga concentration gradient

For this reason, a precursor structure with a different sequence of the starting materials has been produced, by depositing on top of the Mo back contact first the InSe film, then on top of it a GaSe layer, which is followed by a Cu layer and this one is finally covered by another GaSe film, as showed in Figure 59.


*Figure 59. Scheme of the precursor structure final version.*

With such a sequence, the structure is composed of about a 2 μm thick InSe, a 200-300 nm thick GaSe, a 350-400 nm thick Cu and a final 400-500 nm thick GaSe films.
In this last configuration all the materials are deposited at 400°C and the so-obtained precursor still shows the same good morphology shown in Figure 54a and it is selenized as usual.
The CIGS grown with this layer structure is very uniform and well crystallized as in the previous best case (Figure 54b).

Grazing incidence XRD spectra performed on this latest CIGS material show again that the superficial part of the absorber layer is made just of CIGS phases, mainly with a Ga concentration of 30 and 60% respectively, allowing to think that the good composition condition hasn't changed too much.

Solar cells produced with this CIGS material have immediately exhibited good photovoltaic parameters and no more series resistance problems.
In very few trials it has been possible to obtain a big enhancement in $V_{OC}$ , jumping up to 560 mV and also in fill factor, up to 67% (Figure 71).

In order to understand better what has been changed into the absorber layer, EDS depth profiling measurements have been performed once again.
These EDS spectra result to be very different in the Ga distribution profile, with respect to the previous cases (Figure 60).
Having introduced Ga in two steps and mainly in two different portions of the precursor structure, it has probably fulfilled the idea of forming into the absorber three main regions, different in Ga concentration.
In fact, in such a way a multi-graded energy gap CIGS material seems to be produced.
This CIGS material seems to be also quite similar to the Ga double-graded system described above, in which its top and the bottom parts have a higher Ga concentration, while its middle part has a lower one.

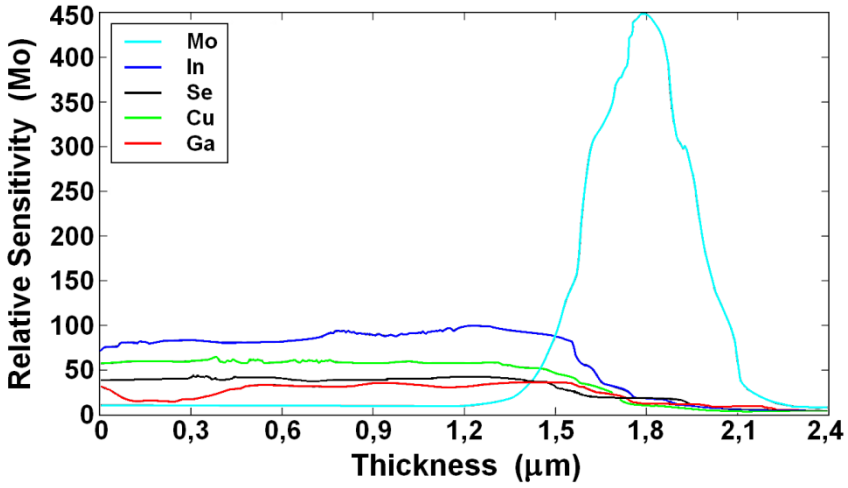


*Figure 60. EDS depth profiling spectra of the multi-graded CIGS layer after selenization.*

Tailoring the thickness of the starting materials and the constituents ratios, as well as their deposition temperatures, best results have been obtained composing a precursor structure by depositing directly in sequence a 2 µm thick InSe film and a first GaSe layer of about 360 nm, both at 400°C, then a 390 nm thick Cu film at 450°C and finally a second GaSe one of about 480 nm, at 400°C.

Solar cells produced with this CIGS absorber structure and completed in the usual way have exhibited in fact very good photovoltaic parameters, like : $V_{OC}$ = 576 mV, $J_{SC}$ = 38 mA/cm$^2$ , FF = 74% and conversion efficiency of about 16% (Figure 72).

## 5.3 Solar cell completion

As said before, after having grown a suitable absorber layer, in order to go on with the solar cell fabrication, it is necessary to complete the *p-n* junction by depositing the CdS window layer.
CdS can be deposited in polycrystalline thin films by R.F. magnetron sputtering, with a 35 W power discharge, at $2.5*10^{-3}$ mbar deposition pressure (0.6 nm/s deposition rate), using 20 sccm of Ar.
During CdS deposition, the substrate temperature is kept at about 200°C, in order to promote a good film uniformity. The thickness of the CdS layer is on the order of 80-120 nm.

Since the CdS layer must be quite thin, in order to not limiting the incident light which can be absorbed by the CIGS layer, it is very important to guarantee its uniformity and thickness on large area, in order to cover properly and completely the beneath CIGS film surface.
In fact, if the CdS layer is not able to cover all the CIGS surface but leaves some areas free, in these regions no Cd will be present and the CIGS superficial conductivity type inversion will not happen, worsening the total electronic behavior of the junction and hence the performance of the solar cell.
Moreover without the "shield" provided by a compact CdS layer, which acts also as a buffer, the CIGS can be in direct contact with the TCO layer and this increases very much its probability of being contaminated by metallic atoms (coming from the TCO).
CdS layers can be well deposited by the sputtering technique and already 80-120 nm thick films are uniform enough to cover the CIGS surface roughness in the right way.
Nevertheless, a proper coverage can't be guaranteed if CdS is deposited in thinner layers of about 50-60 nm, which is the typical range for CdS films deposited by chemical bath.

With a thick window layer, part of the incident light is blocked before arriving at the CIGS film and so a limitation in performances tends to occur.
In order to solve this problem it has been built up a different way for depositing CdS layers by sputtering and this is another aspect which makes this process innovative.
In fact, it has been thought that, optimizing the homogeneity and the uniformity of the CdS film, it is possible to enhance its transparency.
Essentially, to obtain these results it is necessary to remove the film's growth defects and this operation can produce the best effects if it is performed during the very deposition of the film.
In such a way it has been thought to use, in addition to the Ar, another sputtering gas, which can give place to set negative ions free during the plasma discharge (reactive sputtering).
If negative ions are produced, they will be accelerated by the electric field established in the deposition chamber (between target and substrate) in an opposite versus with respect to the Ar

positive ions, going towards the substrate and bombarding it. A limitation in choosing this gas consists in selecting gases which don't set free ions able to react with the film material, worsening its electronic or optical properties.
For this purpose, a gas containing Fluorine has been selected, the Trifluoromethane $CHF_3$ , which is used in addition to Ar.
Into the discharge $CHF_3$ is decomposed and ionized, setting $F^-$ ions free, which being negative charged tend to go towards the substrate (anode); these ions produce a bombardment of the film, which at the same time grows thanks to Ar ions bombardment onto the CdS target.
These collisions onto the surface of the growing film (back sputtering) are probably useful to remove the stoichiometry defects like Cd and S atoms weakly bonded, which normally act like light absorbing centers and cause a limitation in transparency.
Using $CHF_3$, CdS(F) thin films deposited by reactive sputtering result with a higher optical transparency, mainly at shorter wavelengths (Figure 61); it is like the energy gap of the CdS film is enhanced, allowing it to be more transparent.
This is probably due to a better crystalline quality and smoothness of the film, grown with a smaller concentration of light-absorbing defects.

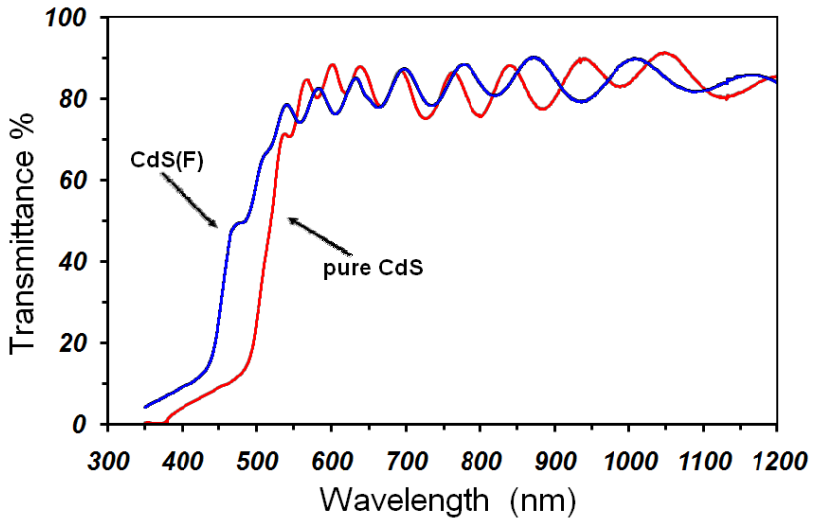


*Figure 61. Comparison between transmittance spectra of 80 nm CdS thin films deposited* ***(red line)*** *only by Ar and* ***(blue line)*** *by Ar+3% $CHF_3$ .*

Best results have been obtained depositing CdS(F) with a 0.8 $W/cm^2$ power density discharge, at about $2.5*10^{-3}$ mbar deposition pressure (0.4 nm/s deposition rate), using a 20 sccm Ar flux plus a 3-4% in flux of $CHF_3$ .

If less $CHF_3$ is used during the film deposition, the improvement in transparency tends to vanish. On the other hand, for more $CHF_3$, the back sputtering becomes too strong and it is able to excessively consume the film, making it too thin for a good CIGS coverage.

Moreover, no variation in electrical resistivity of CdS(F), with respect to the pure CdS, has been noticed and this can be considered as F is not a real dopant for CdS.
It has been also suggested that, during the deposition Fluorine can form with Cd atoms a $CdF_2$ compound, especially segregated probably into the grain boundaries, which is able to passivate them preventing the *p-n* junction from short-circuits, caused by the upper TCO layers [66].

In fact, for a CdS layer of about 100 nm thickness it has been often noticed that even different solar cells produced onto the same 1 $inch^2$ substrate with a sputtered pure CdS window layer exhibited very different performances and in some cases some of them were even short-circuited. It has been thought that after the further front contact deposition and the in-air heat treatment, which are both quite high temperature stages, because of the not proper thickness uniformity and stability of the deposited CdS layer (caused by the stoichiometry defects) the interaction between CIGS, CdS and TCO front contact could be different from region to region, causing a not uniform electronic behavior of the structure on the whole substrate area.
This hypothesis has been confirmed repeating the whole procedure, but depositing a thicker CdS film of about 200 nm thickness.
In this case the cells produced onto the same substrate exhibited more similar photovoltaic parameters, revealing that the CdS thickness and coverage were improved and were really important for the solar cell behavior.

The fact that already with about a 100 nm thick CdS(F) layer the solar cells exhibit no more big difference in performance, it can be ascribed to a more uniform coverage and a better stability of this material layer, which is able to better interact with the CIGS and to protect the junction from short-circuits, maybe thanks to the more compact structure of the film and the passivation of its grain boundaries.

So, with this technique it is possible to deposit CdS(F) by sputtering even in thin films of about 60-80 nm thickness, which are more transparent and at the same time uniform and stable so that to guarantee a proper coverage of the absorber.

After the CdS, next step consists in the deposition of the TCO front contact.
The front contact is made by depositing on top of CdS layer, first a ZnO thin film by R.F. magnetron reactive sputtering, with a 2.2 W/cm$^2$ power density discharge, at about $3*10^{-3}$ mbar deposition pressure (0.2 nm/s deposition rate), using a 20 sccm Ar flux plus a 7% in flux of pure $O_2$ .
The ZnO film is deposited by using a Zn metallic target, at about 200°C substrate temperature. The thickness of this film is about 100 nm.

The front contact is completed covering the ZnO layer by a further ITO thin film.
ITO is deposited by D.C. magnetron reactive sputtering, with a 3.3 W/cm$^2$ power density discharge, at about $2.5*10^{-3}$ mbar deposition pressure (1.2 nm/s deposition rate), using a 20 sccm Ar flux plus a 2.5% in flux of pure $O_2$ .
This film is deposited by using a 90% $In_2O_3$ +10% $SnO_2$ target, at the same 200°C substrate temperature as before and with a thickness of 400 nm.

The final step of the process is represented by depositing the metal grid contact onto the ITO film, thanks to which it is possible to collect better the power produced by the solar cell.
This metal contact reduces in fact the series resistance introduced by the 4-5 Ω/square sheet resistance of the ITO film, which the photo-carriers would meet if any metal contact is added and which would limit the solar cell performances.
This grid contact is made by using a metal foil mask and depositing through it a Mo thin film.
Mo is deposited at room temperature by R.F. magnetron sputtering with 3.3 W/cm$^2$ power density discharge, at about $2.5*10^{-3}$ mbar deposition pressure (0.8 nm/s deposition rate), using a 20 sccm Ar flux. In this way a 100 nm thick layer is obtained.

## 5.4 Treatments

### 5.4.1 The annealing in air

An annealing in air of all the device structure is normally done once the TCO front contact has been deposited.
This heat treatment is performed by inserting the structure into an oven at 220°C and keeping it at this temperature for a period ranging from 1 to 5 hours.
This heat treatment seems to be very useful for the formation of the *p*-CIGS/*n*-CIGS pseudo-homojunction, tanks to the interaction between CIGS and CdS and also to possible reactions between CIGS and Oxygen.

For example, about these last reactions it has been demonstrated by Hall effect measurements that into an In-rich CIGS film the holes concentration increases from $10^{16}$ $cm^{-3}$ up to $5*10^{18}$ $cm^{-3}$ as a consequence of an annealing performed in air.
It is thought in fact that Oxygen is able to modify the CIGS structure, by eliminating the double donor Se vacancies $V_{Se}$ and replacing them with the acceptors substitutionals $O_{Se}$ (O substitutes Se) and compensating also the interstitial Indium or the substitutionals $In_{Cu}$ , both donors, reducing the total number of the active donor energy-levels into the CIGS energy gap and increasing simultaneously its *p*-type conductivity [67].

To verify the formation of this probable homojunction, also C-V measurements have been performed onto the CIGS/CdS junction (T. Sakurai et all.), mainly studying the junction ideality factor dependence on the atmosphere in which the annealing has been performed.

To understand better the results of these experiments it is necessary to dwell for a while upon the meaning of the junction's ideality factor.
Remembering that the dark current density-voltage relationship of a generic *p-n* junction can be properly described by the Shockley equation

$$J = J_0 * \left( e^{\frac{q(V - I*R_S)}{nkT}} - 1 \right) \qquad (2)$$

where $J_0$ is the reverse saturation current density of the device, $(V - I*R_S)$ represents the voltage difference at the contacts of the device, $k$ is the Boltzman constant and $n$ is the **ideality factor** of the junction.

For an ideal homojunction $n = 1$ and it represents the situation in which the carrier transport happens into the junction essentially by the diffusion mechanism.
On the contrary, for a heterojunction $n \approx 2$ and this is due to the more complicated junction structure and to the many lattice defects generated at the interface between the two different materials.
In addition to the diffusion, in this latest case the carrier transport is governed also by recombination into the space charge region of the junction, caused by the defective interface-state energy levels introduced into the materials energy gap, which act like recombination centers for the photo-generated carriers.

By annealing the CIGS/CdS junction in different kinds of atmosphere, it has been noticed a big change in the junction ideality factor, which can reach values closer to 1 in the very case of annealing in $O_2$ and $N_2$ atmospheres (Figure 62).

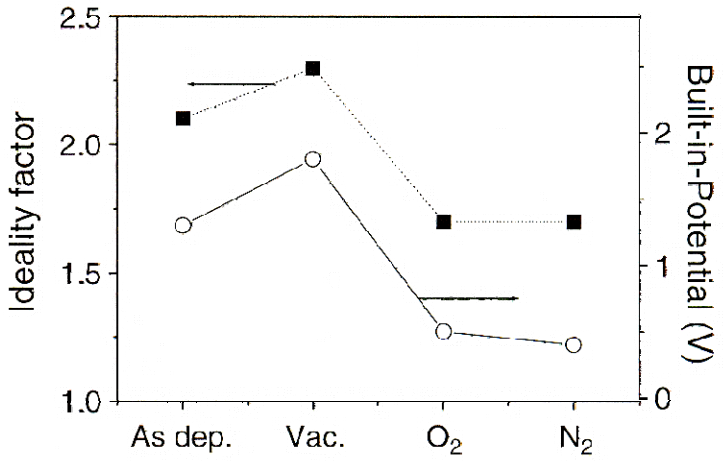


*Figure 62. Variation of the ideality factor and the built-in potential of an Al/CdS/CIGS heterojunction as a function of the annealing atmosphere, performed at 400°K for 30 minutes [68].*

In these latest conditions the junction seems to be improved, from an electronic point of view, and it looks like the defects at the interface are minimized, enabling the junction to behave more like a homojunction made with two materials with similar properties and in fact solar cells annealed in this way show better performances (Figure 63).

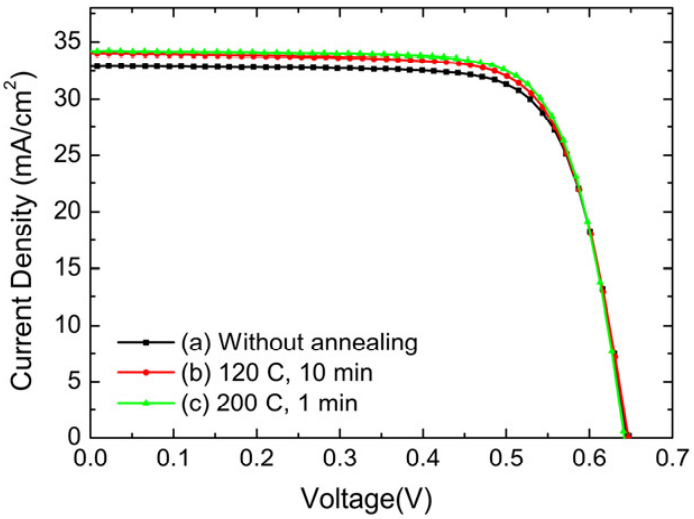


*Figure 63. J-V curve of CIGS/CdS solar cells **(a)** without annealing, **(b)** annealed at 120°C for 10 minutes, and **(c)** annealed at 200°C for 1 minute [69].*

Probably the better electronic behavior of the junction is related to a better distribution of Cd into the superficial atomic layers of the CIGS material and to its proper doping activation into the absorber lattice, which can both promote a more uniform formation of the *p-n* pseudo-homojunction on a larger area of the CIGS film surface.
The fact that the junction ideality factor is reduced towards $n$ equal to 1 also in the case of an annealing performed in an inert $N_2$ atmosphere, emphasizes the hypothesis that the pseudo-homojunction is mainly promoted by the Cd atom diffusion, coming from the CdS layer, and not by some reaction with the Oxygen.

## 5.4.2 The light soaking

When the solar cell is completed it can receive another treatment, the **light soaking** (LS), which consists in an annealing of the device during its illumination.
LS is performed by illuminating the solar cell from the front contact side, using a intense light source, letting at the same time it warm up and reach a superficial temperature of about 80-100°C, for a period between 30 and 60 minutes.
Light soaking promotes the reduction of the devices reverse current and at the same time the increase in their open circuit voltage, in their short-circuit current, in their fill factor and hence in their efficiency.

An example is given by one of the solar cells produced in laboratory with this described process. This is a 0.3 $cm^2$ solar cell and on it has been performed a light soaking using an halogen lamp for about one hour, making the device reach a 90°C superficial temperature.
As a consequence of the treatment, it has been noticed the variation in its photovoltaic parameters:

| | | | |
|---|---|---|---|
| $V_{OC}$ | 520 mV | → | 530 mV |
| $J_{SC}$ | 33.2 mA/$cm^2$ | → | 34.5 mA/$cm^2$ |
| FF | 0.62 | → | 0.64 |
| $\eta$ | 13.4 % | → | 14.4 % |

The explanation of these phenomena is still not very clear, nevertheless it is thought that this treatment promotes a partial filling of the electrons traps, mainly introduced by interface defects, but also by the native defects present into the materials of the solar cell layers, which act like channels for the reverse current transport [40].
In fact, by performing capacitance-voltage investigations, after light soaking the capacitance normally results to be changed (Figure 64).

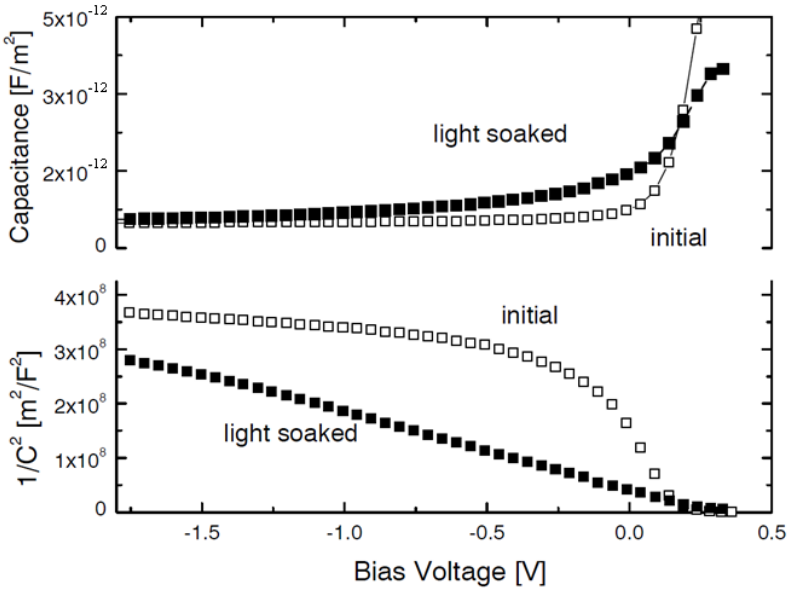


*Figure 64. Capacitance-voltage (**above**) and Mott-Schottky $1/C^2$-voltage (**below**) characteristics of a solar cell before and after the light soaking. The measurement has been performed in dark conditions and at a 40 kHz frequency applied bias.*

The Mott-Schottky plot (F.-J. Haug et all.) shown gives a reasonably straight line corresponding to a uniform carrier concentration of about $1.5*10^{15}$ $cm^{-3}$, which is one order of magnitude higher than the initial carrier density present in the CIGS before light soaking [70].
This increase in carrier concentration is probably due to a persistent entrapment of electrons in the bulk of the absorber, then a saturation of trap states in the CIGS band gap and a corresponding release of trapped carriers [71].

At the same time it can be thought that those electrons, if trapped in the SCR, act as an additional space charge and thereby diminish the total width of the space charge region.
The maximum electric field between the SCR edges thus tends to increase by illumination, since new charge carriers are further added.
So, in case the device is limited by the Shockley-Read-Hall space charge recombination, this effect leads to a gradual decrease of recombination during the further illumination and hence during its working life [72].
In this way the photovoltaic parameters can be enhanced, allowing the solar cells to exhibit higher performances.

# Results

With this innovative process for producing all thin film CIGS-based solar cells, very promising results have been obtained.
During this PhD thesis work many solar cells have been produced, studying their performances as a function of the changes done in the process parameters, like the deposition conditions of the starting materials, the ratios between the elemental constituents into the absorber material and the sequences of the stacked layers into the precursor structure, in order to obtain the best photovoltaic performances.

For example, in the case of the Mo back contact, without the bi-layer configuration, Mo doesn't seem to be the proper material to be used in thin film $Cu(In,Ga)Se_2$-based solar cells.
For Ar deposition pressures higher than about $7*10^{-3}$ mbar, the Mo film adhesion couldn't be obtained and the lift-off of the cell structure happened almost always.
The same results were obtained even for Ar deposition pressures lower than $6*10^{-3}$ mbar.
In this way the pressure range, for depositing the first Mo layer, has been set and the best adhesion results have been obtained using the D.C. magnetron sputtering technique with a 1.8 $W/cm^2$ power density discharge, depositing a 30 nm thick layer at $6.5*10^{-3}$ mbar (0.2 nm/s deposition rate), using a 45 sccm Ar flux.

It has been studied also the effect of the Mo film thickness on its adhesion onto the glass substrate. Even in the best deposition conditions described above, depositing Mo films thinner than 20 nm, sometimes the lift-off of the further cell structure happened during or even before the selenization step.
This phenomenon has been explained by EDS depth profiling measurements, by which it was discovered that, as a consequence of a high temperature annealing , Mo partially had diffused into the glass substrate for some hundreds of nanometres (Figure 50).
In this condition the substrate's surface couldn't be covered in a sufficient and uniform way to allow the second Mo layer to stick properly.

On the other hand, increasing its thickness from 30 nm up to 50 nm this problem is avoided but no consistent improvement was produced, revealing that a 30 nm Mo film is already thick enough for a good adhesive layer.

A second 200 nm thick Mo film, deposited by D.C. magnetron sputtering technique, with a 1.8 W/cm$^2$ power density discharge and at pressures higher than $2.5*10^{-3}$ mbar, revealed an ohmic-poor behaviour and solar cells produced with this bi-layer back contact resulted to have a roll-over in their J-V characteristic, which is a typical effect of a bad "ohmic quality" of the back contact itself.
Good results have been gained by depositing the second Mo layer at $2*10^{-3}$ mbar (0.4 nm/s deposition rate), using a 15 sccm Ar flux. With this Mo bi-layer structure, the roll-over started to decrease.
The alternative strategy has been to increase the thickness of the second Mo layer, in order to improve its crystalline quality and for 500 nm thick films the roll-over disappeared (Figure 65). This is probably due to an increase in Mo film's columnar grain dimensions, corresponding then to a reduction of its grain boundary size.

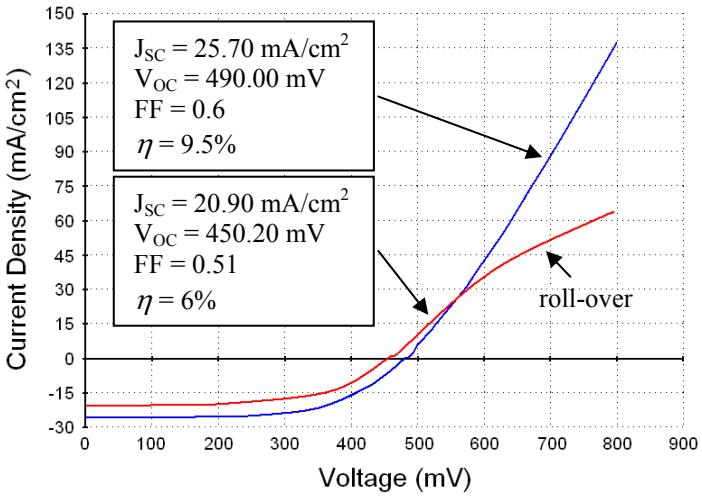


*Figure 65. J-V characteristics of 0.5 cm$^2$ CIGS solar cells with an electrical resistive back contact (**red curve**) and with a good ohmic back contact (**blue curve**). (measure performed in A.M. 1.5 condition, 25°C, 80 mW/cm$^2$ light irradiance).*

With this Mo bi-layer structure, it has been possible to produce a good back contact, suitable for Cu(In,Ga)$Se_2$-based thin film solar cells, which well stands the high temperature steps during the production process.

Another important aspect is that, in these conditions, it is possible to deposit the whole back contact in a thinner structure, even at quite high deposition rates and in a short time, contributing to reduce the time length of the process and to improve its scalability.

The $In_2se_3$ and $Ga_2Se_3$ starting materials have demonstrated to be a good alternative to the common elemental Indium and Gallium, respectively.
To use these materials correctly, it has been necessary to understand the correlation between their interaction and the thermodynamic conditions of the process.

It has been seen that for $In_2se_3$ a quite high deposition temperature, of about 400°C, improves the film crystallinity.
If this material is deposited at lower substrate temperatures, the film tends to grow with a Selenium excess, causing superficial segregations which, reacting with Copper, can form $Cu_2Se$ and then short-circuit the solar cell.
At temperatures higher than 400°C the film looses instead too much Se, starting to be more In-rich and to separate into islands.
The optimal conditions for the $In_2Se_3$ film deposition have been found by using the R.F. magnetron sputtering technique, with a 3.3 $W/cm^2$ power density discharge, at $5*10^{-3}$ mbar pressure (1 nm/s deposition rate), using a 30 sccm Ar flux, at a substrate temperature of 400°C.

The first method developed for the CIGS absorber layer growth consisted in growing a $CuInSe_2$layer and then adding the Ga in a second time, with the idea of having a more Ga-rich superficial material.
Considering the amount of the other further constituents, in order to have a 2-3 μm thick absorber layer, the$In_2Se_3$ has been deposited with a thickness of about a 1.5 μm.
By depositing a 200 nm Cu thick film, corresponding to a Cu/In ratio of about 75%, a good precursor material was obtained, strictly following the correct deposition parameters described in the previous chapter.
After Cu deposition an annealing in vacuum, at a substrate temperature of about 450°C, revealed to be effective in improving the Cu diffusion into the beneath $In_2Se_3$ layer and their intermixing.

As foreseen, grazing incidence XRD measurements showed that, despite the good morphology, the so-obtained material was not completely a CIS layer, but in addition to the $CuInSe_2$ phase there were also the $Cu_{11}In_9$ and the $In_2Se_3$ secondary phases (Figure 42).

It has been noticed that the best precursor transformation into $CuInSe_2$ happens at very high selenization substrate temperatures, at about 530°C if the correct amount of Se is supplied during the growth.
Moreover, if the precursor received Se instead at a too low substrate temperature, other phases would form, like $Cu_xSe$.
On the contrary, if the precursor reached the high temperatures, without any addition of new Se, it would go out the correct stoichiometry, suffering from a lot of spurious phases.
Grazing incidence XRD measurements confirmed that after a correct selenization, a more homogeneous $CuInSe_2$ layer was obtained, without any considerable secondary phase (Figure 45).

Depositing onto the 1.5 μm thick $In_2Se_3$ layer a Cu film thinner than 150 nm, which means a Cu/In ratio lower than 60%, the precursor material showed some superficial segregation, which remained even after selenization.
These segregations have been thought to be due to an increasing amount of $In_2Se_3$ residual as a consequence of a lack in Cu.
On the other hand, for Cu films thicker than 250 nm, corresponding to a Cu/In ratio of about 95%, an elemental-like Cu film seemed to start forming onto the precursor surface.
In this last case the amount of Cu put into the precursor was too high and in fact during selenization it provoked the formation of superficial $Cu_xSe$.
In this way it has been set the correct Cu/In ratio in the range of 75-85%, to obtain a good CIS material.

It has been studied also how to deposit and how to add the $Ga_2Se_3$ to the CIS layer, in order to obtain the desired $Cu(In,Ga)Se_2$ absorber material.
After the $Ga_2Se_3$ layer deposition, another film of Cu is needed, in order to keep the right 75-85% total Cu/(In+Ga) ratio.
Then, having deposited onto the CIS layer a 200 nm $Ga_2Se_3$thick film (a theoretical Ga/(In+Ga) ratio of 12%) and a corresponding 30 nm Cu thick layer, another selenization is requested to enable the intermixing between all the constituents with the consequent transformation into CIGS.

XRD measurements performed on this final layer confirmed that a CIGS material was obtained, but with some other secondary phases, among which the most intense contribute was given by a $Ga_2Se_3$ residual (Figure 46).

Solar cells produced in this way exhibited low $V_{OC}$ in the range of 420-430 mV, low $J_{SC}$ in the range of 12-15 mA/cm$^2$ , fill factor in the range of 35-40% and efficiencies around 2-3%, showing also the effect of a series resistance in their J-V characteristic.

However, by depositing onto the CIS layer a thicker 400 nm $Ga_2Se_3$film (a theoretical Ga/(In+Ga) ratio of 22%) and a corresponding 50 nm thick Cu layer, in order to have more Ga in substitution of Indium into the absorber material lattice, it has been really seen an improvement in the device performances.
With this procedure it has been possible to produce solar cells, which, once completed in the usual way, has exhibited $V_{OC}$ in the range of 500-520 mV, $J_{SC}$ in the range of 27-30 mA/cm$^2$ , fill factor of about 58-60% and efficiencies from 10 to 11% (Figure 66).

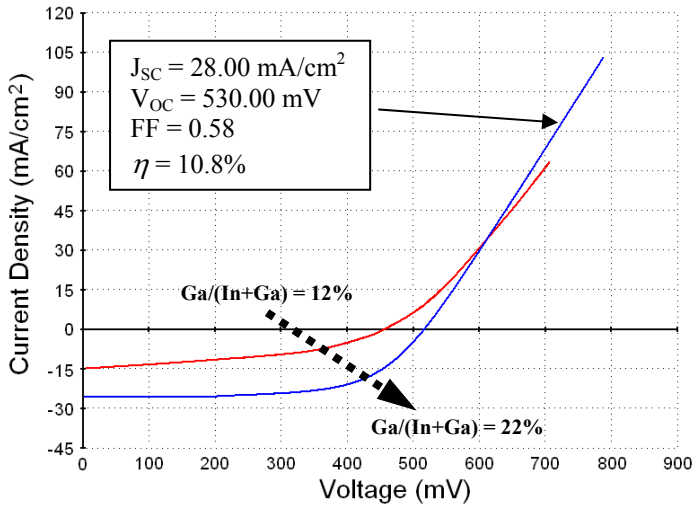


*Figure 66. J-V characteristics of 0.5 cm$^2$ solar cells produced with the first method using $In_2Se_3$ , $Ga_2Se_3$ and Cu starting materials, with different Ga/(In+Ga) ratios (measure performed in A.M. 1.5 condition, 25°C, 80 mW/cm$^2$ light irradiance).*

With this procedure, for $Ga_2Se_3$ films thicker than 400 nm (a theoretical Ga/(In+Ga) ratio higher than 26%) no further enhancement in the photovoltaic parameters has been seen, but, on the contrary, a decrease in $J_{SC}$ started to happen.
Increasing further the $Ga_2Se_3$ film thickness, the amount of Ga into the precursor increases too, but at the same time even the amount of $Ga_2Se_3$ residual increases, causing the introduction of a high series resistance into the device, limiting the photo-current collection.

EDS measurements have been performed on these absorber materials, in order to check the distribution of constituents and most of all of Ga.
These EDS spectra have revealed that the Ga concentration was constant along the absorber thickness, with only a small increase towards the Mo back contact.
The Ga/(In+Ga) ratio was however too low with respect to the theoretical 25-30% value, near the superficial *p*-*n* junction region and an approximate value of this concentration was probably about 10% (Figure 47).
Because of the limited quantity of Ga present into the CIGS, in this case results couldn't overcome 500-520 mV $V_{OC}$ and 10-11% conversion efficiencies.

For this reason, a second method has been developed.
The $Ga_2Se_3$ layer was interposed between $In_2Se_3$ and Cu films, with the idea of enabling their interaction only at higher and more favorable temperatures.
It has been found that depositing directly $Ga_2Se_3$ and Cu films at 450°C onto the same $In_2Se_3$-Cu structure as before, without any intermediate selenization, the final absorber material presented a lot of segregations.
Probably, during selenization the more stable $Ga_2Se_3$ tends to obstruct the diffusion of the incoming Se into the precursor, making $In_2Se_3$ and Cu react at high temperature without the right amount of Se for forming a unique stoichiometric $CuInSe_2$ phase. This causes then a too strong interaction between them and probably the formation of other secondary phases.
Instead, depositing the $Ga_2Se_3$ layer between the $In_2Se_3$ and Cu films this mechanism is avoided, but, since there is no Cu under the $Ga_2Se_3$ layer, the Cu deposited on top of this structure feels a too strong concentration gradient towards the bottom.
Combining the strong diffusion driving force of Cu and the low reactivity of the $Ga_2Se_3$ at these 450°C "low" temperatures, the effect results in a wrong intermixing and in a grain separation of the polycrystalline $Ga_2Se_3$ film, affecting also the morphology of the final material after the selenization.
It has been discovered that, by depositing Cu on top of $Ga_2Se_3$ at lower temperatures, about 350°C, this mechanism is avoided and, after selenization, the so-obtained CIGS material shows a good morphology and a composition similar to that produced with the first method (Figure).

Experiments revealed that, even without performing any annealing in vacuum before selenization, similar results could be obtained and this has represented another important aspect for reducing the process time length.
For $Ga_2Se_3$ film thicknesses up to 400 nm, corresponding to the theoretical optimal Ga/(In+Ga) ratio of 22%, $V_{OC}$ couldn't overcome 480 mV.

It has been necessary to increase its thickness up to 500 nm, reaching a theoretical Ga/(In+Ga) ratio of about 26%, and the corresponding Cu layer up to 270 nm, in order to see a small improvement.
Solar cells produced with this CIGS absorber have exhibited $V_{OC}$ in the range of 500-510 mV, $J_{SC}$ of about 32 mA/cm$^2$ , fill factor in the range of 50-52% and efficiencies from 10 to 11% (Figure 67).

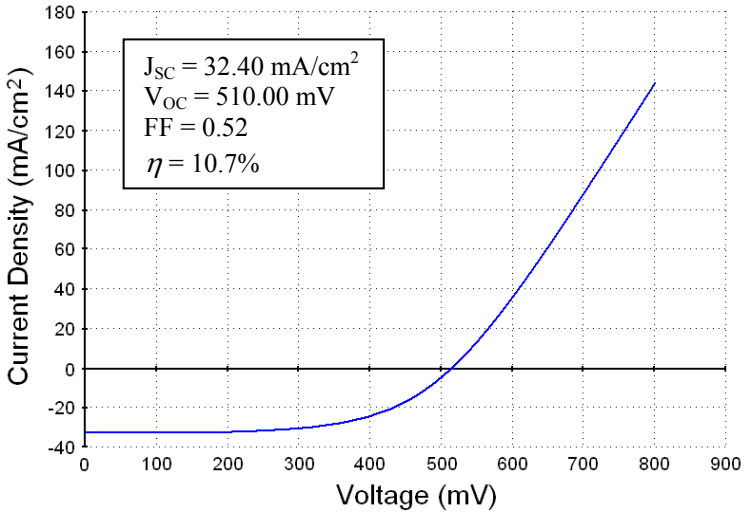


*Figure 67. J-V characteristic of a 0.5 cm$^2$ solar cell produced with the second method using $In_2Se_3$ , $Ga_2Se_3$ and Cu starting materials (measure performed in A.M. 1.5 condition, 25°C, 80 mW/cm$^2$ light irradiance).*

Even in this case a theoretical Cu/(In+Ga) ratio of 75% has resulted to be the optimal one.
For a Cu concentration lower than 70% the $J_{SC}$ started to decrease, probably because of an increase in the content of In-Se and Ga-Se electrical-resistive residuals, while, for Cu concentrations higher than 80%, solar cells were short-circuited and this is easily ascribed to the shunt resistances introduced by the Cu-Se segregations.
The fact that it was necessary to introduce a higher concentration of $Ga_2Se_3$, with respect to the previous case, in order to obtain similar open-circuit voltages, but without seeing at the same time any important enhancement, it led to think about a different distribution of Ga into the absorber material.

In fact, performing depth profiling EDS measurements it has been seen that Ga was diffused again and it was even more confined into the back of the absorber layer, with respect to the case of the first procedure, at an approximate value of about 27% and still remaining in a low concentration, below 10%, near its free surface (Figure 50).

Neither increasing the $Ga_2Se_3$ film thickness up to 800 nm, any further enhancement in $V_{OC}$ was seen, but on the contrary the problem of $J_{SC}$ reduction appeared.
Not even with this second method it has been possible to obtain the desired Ga concentration profile into the absorber. In fact the Ga concentration near the absorber surface was still too low to allow solar cells to exhibit $V_{OC}$ higher than 500-520 mV. At the same time with a proper $Ga_2Se_3$ film thickness, higher $J_{SC}$ have been obtained probably thanks to the better interaction between $In_2Se_3$ and Cu at higher temperatures.

Comparing these results, the second method has resulted to be faster, since it needs only one selenization, but produces a not correct Ga concentration profile, while with the longer first method it is possible to regulate better the Ga concentration, mainly at the surface of the absorber.
Moreover, it has been demonstrated that for these process conditions $Ga_2Se_3$ is not the ideal Ga based starting material to allow constituents to react correctly in order to form the desired absorber layer, since it has a very low reactivity and it doesn't set easily enough Ga free for reaching the right stoichiometry of the CIGS absorber material.

To improve the Ga distribution into the absorber layer, the $In_2Se_3$ and $Ga_2Se_3$ have been substitute with InSe and GaSe.
InSe has resulted to behave in a quite similar way to $In_2Se_3$ . In fact, it can be deposited in the same conditions.

Performing the first process method procedure with this latest material, it has been discovered immediately that at the usual 400°C and even at the 350°C processing temperature, the interaction between InSe and Cu was too strong.
It has been necessary to deposit Cu onto the InSe at a lower temperature of about 300°C in order to prevent the formation of phase defects.

The main difference noticed in using InSe has been an immediate jump of $J_{SC}$ , up to values of about 35 mA/cm$^2$ (Figure 68).

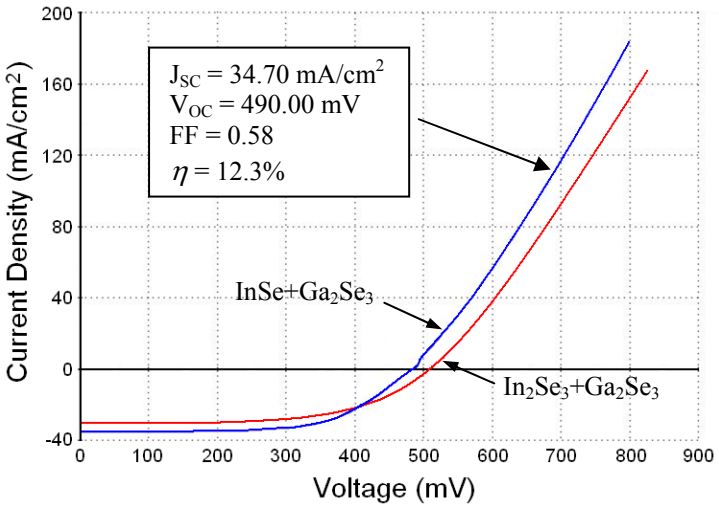


*Figure 68. Comparison between J-V characteristics of 0.5 cm$^2$ solar cells produced with an absorber material made of $In_2Se_3$+$Ga_2Se_3$+Cu and InSe+$Ga_2Se_3$+Cu respectively (measure performed in A.M. 1.5 condition, 25°C, 80 mW/cm$^2$ light irradiance).*

Despite the good improvement in $J_{SC}$ , solar cells didn't exhibit any changing in $V_{OC}$ , which remained at values ranging about 480-490 mV.
This has been another confirmation of the hypothesis that the main reason of low $V_{OC}$ was indeed due to the bad interaction between $Ga_2Se_3$ and the other starting materials.

For this reason the $Ga_2Se_3$ has been substituted with GaSe and it was checked its behaviour at the process conditions.
GaSe has revealed to have a thermal stability similar to $Ga_2Se_3$ and it can be well deposited in the same conditions.
To test the effect of this substitution, it has been used the latest developed sequence and the 1.5 µm thick InSe film was covered by a sequence of a GaSe film and a Cu layer.
Keeping the good theoretical Ga/(In+Ga) ratio of before, equal to 26%, the corresponding Cu/(In+Ga) concentration was needed to be reduced from 75% to 60-65%.
In addition it has been discovered that with this procedure Cu can be deposited onto the GaSe even at higher temperature up to 450°C, without causing morphology problems in the precursor and by depositing all the starting materials at 400°C it is already possible to obtain a good material.

In fact, by SEM microscopy it has been seen that the so obtained precursor is very well crystallized, with grains presenting almost all the same shape and dimensions (Figure 54a).

More important is that the grazing incidence XRD measurements have revealed that this precursor was only constituted of $CuInSe_2$ , InSe and GaSe and no any other spurious phases were present (Figure 53).

However GaSe didn't react completely during the deposition, setting some Ga free and for this reason the selenization step has resulted to be still necessary.
After selenization, the so-obtained CIGS layer has been characterized by SEM microscope investigation. This material has revealed the best crystal structure, among all the previous ones. In these conditions the CIGS material was grown in a very compact and dense way, with tightly packed grains and then smaller grain boundaries (Figure 54b).

The better nature of this CIGS material has been seen also performing grazing incidence XRD measurements, which revealed that, near the surface, the absorber layer, was only composed of $Cu(In_{0.7}Ga_{0.3})Se_2$ and $Cu(In_{0.4}Ga_{0.6})Se_2$ phases.
Moreover, the fact that, in addition to the CIGS phase with a 30% Ga/(In+Ga) ratio, there is also another CIGS phase material with a 60% Ga/(In+Ga) ratio, could be a signal that the Ga concentration near the absorber surface has been really increased (Figure 55).

Even performing deeper XRD analysis, this material has resulted to be very uniform and homogeneous, which is composed almost completely of $Cu(In_xGa_{1-x})Se_2$ and $CuInSe_2$ phases. Only some secondary Ga-based phases are still present, but their contributes are so small that they can be considered negligible (Figure 56).
This has been another confirmation that the GaSe is much more reactive than $Ga_2Se_3$at the process conditions and that it can set more Ga free for obtaining the desired CIGS stoichiometry.

Tailoring the InSe, GaSe and Cu films thicknesses, best results have been obtained depositing a 1.5 μm thick InSe film, covered with a GaSe layer of about 500 nm and a Cu one of about 270 nm.

Nevertheless, solar cells produced with this absorber and completed in the usual way have exhibited $V_{OC}$ never higher than 520 mV, but at the same time they exhibited good $J_{SC}$ in the range of 35-36 mA/cm$^2$ and fill factor in the range of 64-65% (Figure 69).

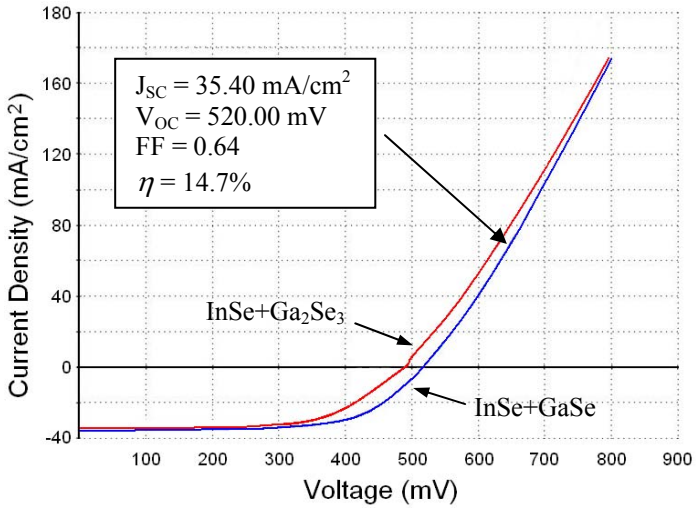


*Figure 69. Comparison between J-V characteristics of 0.5 cm$^2$ solar cells produced with an absorber material made of InSe+$Ga_2Se_3$+Cu and InSe+GaSe+Cu respectively (measure performed in A.M. 1.5 condition, 25°C, 80 mW/cm$^2$ light irradiance).*

Neither with GaSe films up to 1 μm thickness, corresponding to a Ga concentration higher than 40%, it has been possible to further enhance the solar cell $V_{OC}$ ; on the contrary, there was a strong reduction in all photovoltaic parameters.

EDS measurements performed on these CIGS films showed that, even if the Ga concentration was really increased more than double into the CIGS, with a approximate value of about 24%, it was quite constant along the layer, with only a small increase towards the bottom (Figure 57). This phenomenon has been considered due to a too fast Ga diffusion mechanism, with respect to its interaction with the other elemental constituents and for the settled thermodynamic conditions.
Then, a CIGS absorber layer with a "correct", but uniform amount of Ga along its thickness has resulted to be not enough to obtain higher efficiency solar cells.
At this point, the first procedure has been used again, in order to have more Ga close to the surface of the absorber layer.

Taking into account the previous results and keeping almost the same constituents ratios, this time the precursor structure was made by depositing at 400°C first a1.5 μm thick InSe film, then a 230-260 nm thick Cu layer at 300°C, a 380-400 nm thick GaSe film at 400°C and a final 60-80 nm thick Cu layer at 450°C in sequence.
Similar results were obtained either with, or without any previous annealing or selenization of the InSe-Cu structure and this represented a very important aspect for reducing the time-length of the process.
After selenization the CIGS material obtained was well crystallized, like in the latest case.
Solar cells produced with this absorber material have showed however photovoltaic parameters very similar to the previous case.
Increasing the InSe film thickness from 1.5 up to 2 μm and consequentially also the other layers, ranging about 300-350 nm for the Cu film, 450-550 nm for the GaSe layer and 60-70 nm for the final Cu film, it has been obtained a little further increase in $V_{OC}$ , up to 530 mV.

This limitation in solar cell photo-voltage was explained again by EDS depth profiling analyses, since they demonstrated that Ga distribution was still almost the same as with the previous procedure, with a constant profile.

In order to limit the Ga diffusion into the precursor layer, it has been tried also to add the GaSe-Cu structure to an-already selenized CIS material, but similar results have been obtained.
Since Ga diffusion can't be limited by the more stable $CuInSe_2$ , it has been acted on the Ga concentration gradient.
For this reason some solar cells have been produced adding to this obtained CIGS material one further GaSe-Cu structure, composed of a 70 nm thick GaSe layer and a 30 nm thick Cu film.
In his way it has been possible to gain immediately an increase in $V_{OC}$ , up to a range of 550-560 mV, at the same time $J_{SC}$ in the range of 30-33 $mA/cm^2$ and fill factor ranging about 60-62% (Figure 70).

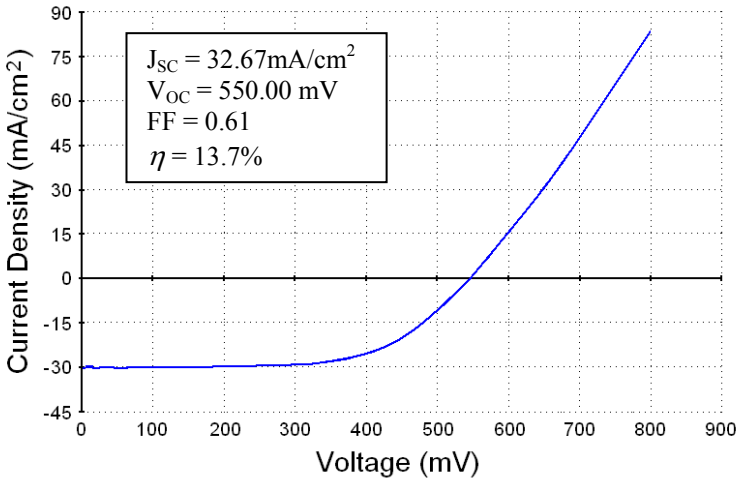


*Figure 70. J-V characteristic of a 0.5 cm$^2$ solar cell produced with the first method using InSe, GaSe and Cu starting materials (measure performed in A.M. 1.5, at 25°C and with 80 mW/cm$^2$ incident light irradiance conditions).*

As foreseen, increasing the Ga concentration near the top of the absorber layer, the $J_{SC}$ started to decrease with respect to latest results.

With these experiments it was demonstrated that the Ga diffusion into the precursor can't be proper limited only by more stable and compact layers like $CuInSe_2$ , but that a higher and efficient control on it can be obtained, instead, acting on the Ga concentration gradient.

For this purpose the process has been modified once again.
Finally, by depositing a precursor structure made by a sequence of InSe, GaSe, Cu films and a final GaSe layer, keeping almost the same constituents ratios as before it has been obtained immediately a great improvement in the solar cell $V_{OC}$ .
For example, solar cells produced with an absorber material made by a sequence of a 2 µm thick InSe, a 240 nm thick GaSe, a 360 nm thick Cu and a final 360 nm thick GaSe films (reaching a total theoretical Ga/(In+Ga) ratio of about 25%), all deposited at 400°C substrate temperature, have exhibited photovoltaic parameters like $V_{OC}$ of about 530 mV, $J_{SC}$ in the range of 36-37 mA/cm$^2$ , fill factor in the range of 64-65% and efficiency from 15 to 15.5%.
Just increasing the thickness of the top GaSe layer up to 480 nm, reaching a Ga/(In+Ga) ratio of about 28% and keeping all the other parameters fixed, a jump in $V_{OC}$ and hence in fill factor up to 560 mV and 67% respectively has been immediately noticed (Figure 71).

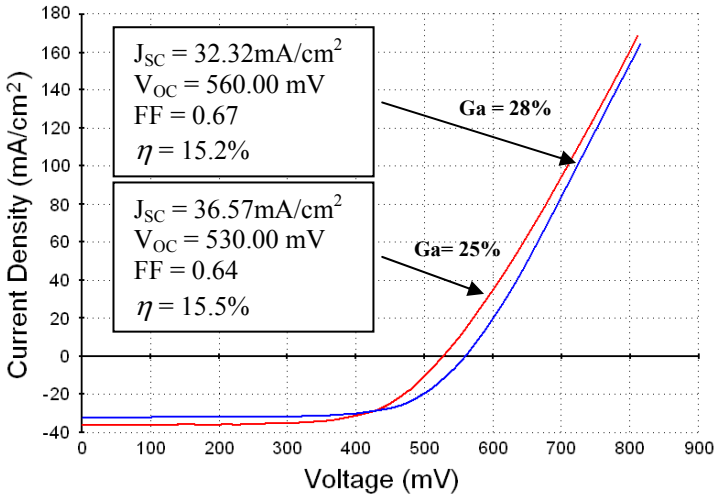


*Figure 71. J-V characteristics of 0.5 cm$^2$ solar cells produced with the last configuration using InSe, GaSe and Cu starting materials and with different Ga/(In+Ga) ratios (measure performed in A.M. 1.5 condition, 25°C, 80 mW/cm$^2$ light irradiance).*

In general, by increasing the superficial Ga concentration into the absorber layer, it is possible to enhance the $V_{OC}$, but if this top GaSe film exceeded the 600 nm thickness (a theoretical Ga/(In+Ga) ratio of about 32%) a decrease in $J_{SC}$ and even in $V_{OC}$ would happen.

In order to increase the superficial Ga concentration, without depositing thicker top GaSe films and avoiding any decrease in the photo-current, the Ga concentration gradient has been further limited by increasing the thickness of the bottom GaSe film.
Nevertheless, just increasing the first GaSe film thickness, up to 360 nm, and keeping fixed the other film thicknesses, as in the case of the latest good results (reaching a Ga/(In+Ga) ratio of about 32%), it was not sufficient and a problem of series resistance effect appeared again in these solar cells.

It has been necessary to increase the Cu deposition temperature in order to promote a better interaction of constituents and by producing solar cells with an absorber material composed of a similar sequence of thicker first GaSe and Cu layers, deposited at about 400°C and 450°C respectively, higher performances have been obtained.

For example, best results have been obtained by depositing the sequence of a 2 μm thick InSe film and a 360 nm thick GaSe layer, at 400°C and then covering this structure with a 400 nm thick Cu film, deposited at 450°Cand another 480 nm thick GaSe layer, deposited at 400°C (a theoretical total Ga/(In+Ga) ratio of about 31%).
With such an absorber layer and completing these devices in the usual way it has been possible to produce solar cells, which have exhibited higher photovoltaic parameters, up to $V_{OC}$ of about 576 mV, $J_{SC}$ of about 38 mA/cm$^2$ , fill factor of about 74% and conversion efficiency of 16.2% (Figure 72).

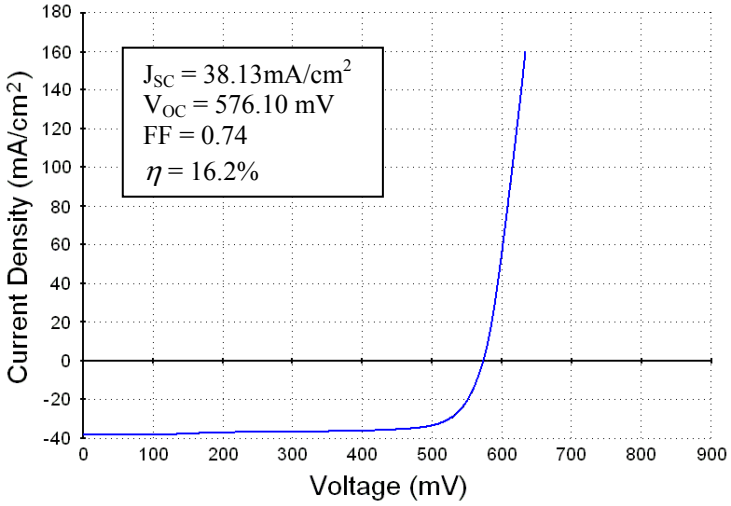


*Figure 72. J-V characteristic of a 0.5 cm$^2$ (0.3 cm$^2$ aperture) solar cell produced with the last configuration using InSe, GaSe and Cu starting materials and depositing Cu at 450°C (measure performed in A.M. 1.5 condition, 25°C, 80 mW/cm$^2$ light irradiance).*

Checking by EDS depth profiling measurements which was the compositional change introduced into the absorber, it has been seen a considerable different Ga concentration profile with respect to the previous cases, very similar to the double graded one (Figure 60).

Increasing more the first GaSe film thickness up to 480 nm, reaching a theoretical Ga/(In+Ga) ratio of about 35% in order to further reduce the Ga concentration gradient and allowing more Ga to stay near the surface, no further increase in $V_{OC}$ has been obtained.
On the contrary, the so-produced precursor material started to show some Ga-Se segregations, which were responsible of worsening the film homogeneity and of the photo-voltage decrease.

With this procedure it seems that the idea of producing a CIGS absorber material divided into three regions, different in Ga concentration, has been fulfilled.
Probably, all the volume of this final absorber material has a bottom portion with a high Ga concentration, a middle region with a lower Ga concentration and a surface with again a higher amount of Ga, both with a concentration profile similar to the detected one, which justify these good results.

Moreover, it has been also found out a new strategy to deposit good CdS buffer layers by sputtering, in alternative to the common used chemical bath.
Depositing CdS(F) by R.F. magnetron sputtering, in an atmosphere of Ar plus a 3-4% in flux of $CHF_3$, it has been possible to produce films more transparent than the pure CdS films deposited in the same conditions but in just pure Ar, especially in the UV region (Figure ).
These results have been explained considering that during the sputtering discharge the $CHF_3$ molecules can be ionized and can produce negative $F^-$ ions, promoting a back-sputtering action onto the growing film, improving its compositional homogeneity and then its transparency.
If less $CHF_3$ is used during the film deposition, the improvement in transparency vanishes as well as the beneficial effect on large-area performance.
Instead, for more $CHF_3$, the back sputtering becomes too strong and it excessively consumes the film, making it too thin for a good CIGS coverage.

Completing the solar cells with a CdS(F) film of about 60-80 nm thickness, good and very reproducible results have been obtained onto the whole substrate area, probably thanks to a better interaction between the CIGS and the CdS(F).

The most important aspect of this strategy is the possibility to deposit a uniform buffer film onto a more extended substrate area, enabling to produce larger solar cells with high performances.
The second important feature of this deposition procedure consists in growing CdS(F) films, suitable for CIGS-based solar cells, thinner than the corresponding pure CdS layers needed, limiting the amount of the used material.
This technique represents then a good alternative to the conventional chemical bath deposition, since the thickness of these CdS(F) films tends to be more comparable to the 50-60 nm thick ones, normally deposited by chemical bath and at the same time, being the sputtering a more safety, hence cheaper technique, it can make the solar cell production be more scalable in case of a large scale industrial production.

Even if the so-developed process can already be scalable at the industrial level, since only the sputtering and the selenization techniques are used, the selenization performed by evaporation has been substituted with another even more scalable technique, which is the closed space sublimation (CSS).
In fact, as described above the selenization stage consists in an annealing of the precursor while some Se evaporates from an effusion cell. This evaporation is performed in vacuum conditions and the Se vapour produced can't be confined only near the precursor material, but on the contrary a big portion of that vapour flux is totally free to go and condense far away from the precursor surface.
Considering that during the selenization a Se flux of about 1 μm/s is produced and only a small part of it reaches the precursor promoting its transformation, it is easy to understand that with this method a quite important amount of evaporated Se is not used, but wasted.

Instead, the CSS technique is based on the evaporation of a target material, put very close to the substrate and in a controlled "high"-pressure deposition condition.
By introducing a certain pressure of an inert gas, like for example Ar, into the deposition chamber, if the gas pressure is higher than the vapour pressure of the evaporating material, the vapour coming from the target material will stay near the evaporating surface in a "cloud-like" state.
In this way the vapour is confined near the source and doesn't reach the substrate.
Only if the inert gas pressure is reduced below the material vapour pressure, this vapour will be able to move away from the target surface and to reach the substrate. At the same time, since the distance between crucible and substrate is very small, about some millimetres, most of the necessary vapour will reach immediately the substrate.

The CSS technique would be a better substitute to the classic selenization method, increasing further the process scalability for a potential large scale production.
With this technique the selenization stage has been optimized in a period of only 2 minutes, starting from the correct temperature and only a small amount of the evaporated Se is used, thanks to its better confinement.

This new selenization procedure has been tested on $In_2Se_3$ , $Ga_2Se_3$ and Cu based precursors. Preliminary good results have been obtained with a precursor material produced by depositing a sequence of a 1.5 μm thick $In_2Se_3$ layer at 400°C, a 450-500 nm thick $Ga_2Se_3$ film at 400°C and a 250-260 nm thick Cu layer at 350°C, performing a further annealing in vacuum at 400°C before selenization.

Despite keeping almost the usual values of temperatures for the Se vapour and for the substrate, a quite different precursor transformation has been obtained with the CSS selenization (Figure 73).

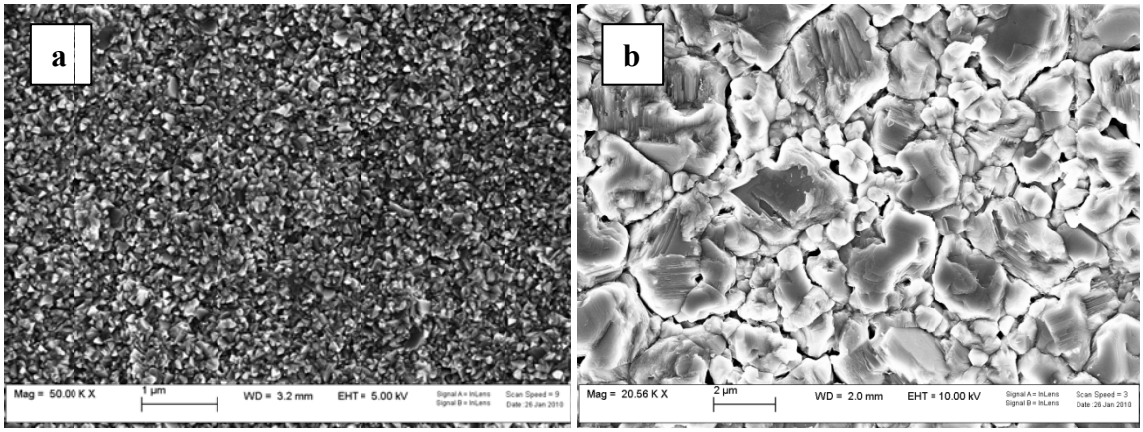


*Figure 73. Comparison between SEM images of $Cu(In,Ga)Se_2$ films morphology after selenization performed by* ***a)*** *evaporation and* ***b)*** *CSS, obtained using $In_2Se_3$ , $Ga_2Se_3$ and Cu starting materials.*

With this new procedure the absorber film tends to grow with grains much bigger and less faceted than the corresponding ones obtained with the Se evaporation.
The reason of this result has not been well understood yet, but however with that kind of absorber material it has been possible to produce solar cells which exhibited photovoltaic parameters like $V_{OC}$ in the range of 460-480 mV, $J_{SC}$ in the range of 17-23 $mA/cm^2$ , fill factor in the range of 59-60% and efficiency from 6 to 8% (Figure 74).

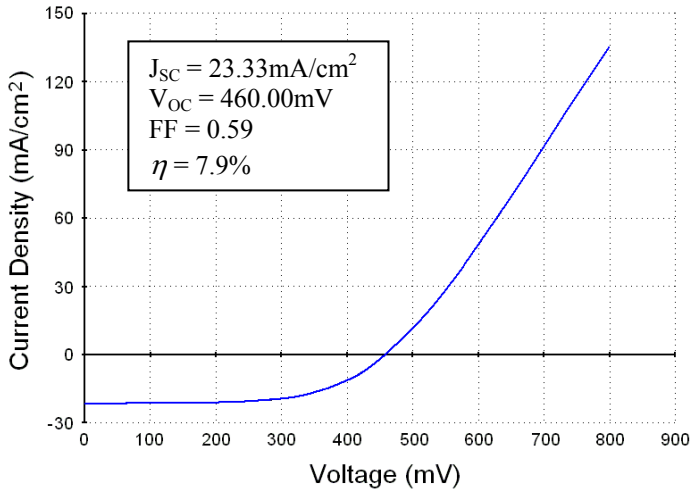


*Figure 74. J-V characteristic of a 0.5 cm$^2$ solar cell selenized by CSS produced using $In_2Se_3$ , $Ga_2Se_3$ and Cu starting materials (measure performed in A.M. 1.5 condition, 25°C, 80 mW/cm$^2$ light irradiance).*

As said in the introduction, recently the topic of improving the photovoltaic architectonic integration (BIPV) has become very important. Nowadays more emphasis has been put on the possibility of producing photovoltaic modules able to be integrated, or even to be directly assembled to form the so-called ventilated walls, which are special walls able to minimize the thermal exchange between indoor and outdoor, saving energy, used for the indoor heating or cooling.

This integration can be improved and accelerated using for example other kind of materials for the substrate or for the final "box" in which the solar cells are encapsulated.
A more integrable substrate material is, for example, the ceramic.
In order to not increase the future cost of the device, it has been thought not to use a special or personalized kind of ceramic, but the cheap commercial tiles.

The optimized process described before, using $In_2Se_3$ , $Ga_2Se_3$ and Cu, has been experimented also onto some ceramic substrates.

Best ceramics have resulted to be the ones produced with very small grain-size, about 10 µm powder sized.
In fact, as the starting powders are finer, the final ceramics tend to become smoother. Nevertheless, even the smoothest "raw" commercial ceramic resulted to have a too high roughness and very extended superficial disuniformities (Figure 75).

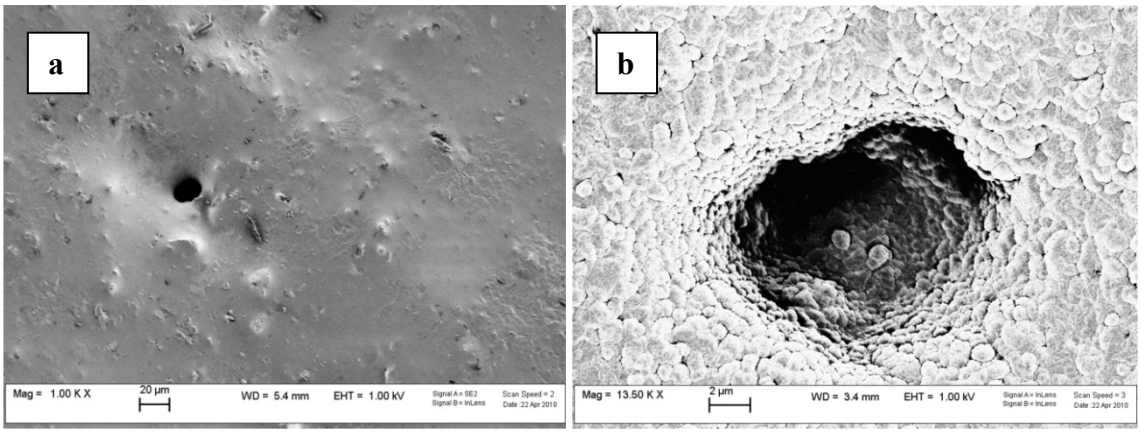


*Figure 75. SEM image of the superficial morphology of* ***a)*** *a raw ceramic substrate and* ***b)*** *a CIGS film, made using $In_2Se_3$ , $Ga_2Se_3$ and Cu starting materials, deposited onto it.*

If the ceramic surface is covered by a glassy enamel, with a similar composition to the soda-lime glass, it results much smoother, making the ceramic a suitable substrate for thin film deposition.

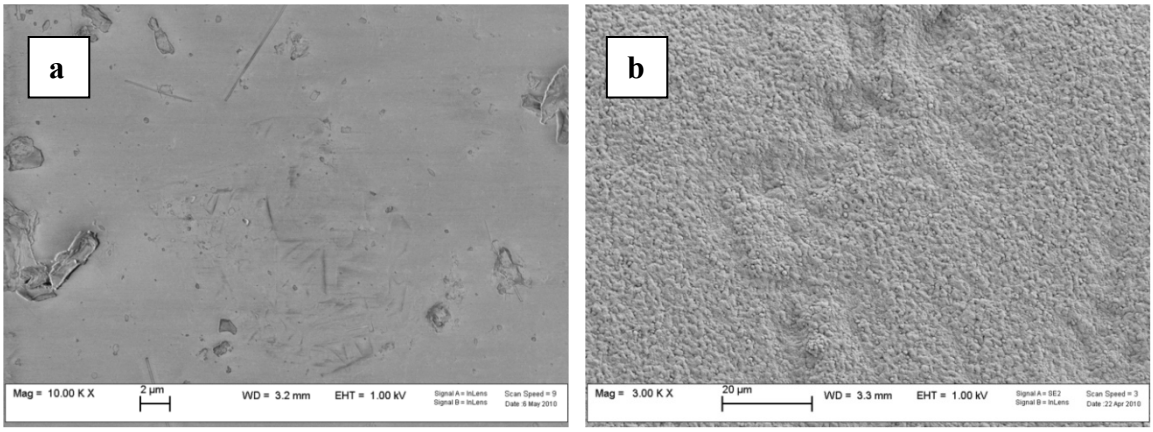


*Figure 76. SEM image of the superficial morphology of* ***a)*** *an enamelled ceramic substrate and* ***b )*** *a CIGS film, made using $In_2Se_3$ , $Ga_2Se_3$ and Cu starting materials, deposited onto it.*

With this kind of substrate it is very difficult to deposit and to grow $Cu(In,Ga)Se_2$ thin films, with an acceptable and a suitable structural morphology.
In fact, the substrate superficial voids and prominences are higher than the thickness of deposited films and so these films can't fill or cover them completely (Figure 76).
In this way a good film continuity can't be obtained and the probability to have pin-holes or electrical insulation problems becomes very high.

Moreover, in general ceramic doesn't contain enough Sodium to dope properly the CIGS material, but on the contrary the enamel contains enough Na inside to avoid any other further addition.
The enamelled ceramic has resulted to be a good alternative to S.L.G. substrate since it stands very well to the process thermodynamic conditions, even in a better way and it doesn't suffer from problems related to the substrate thermal bending, characteristic of the soda-lime glass.

For these reasons, the process technology has been transferred also on this new kind of substrate and some solar cells have been produced.
Preliminary experiments have been performed and good results have been obtained so far with a precursor material produced by depositing a sequence of a 1.5 µm thick $In_2Se_3$ layer and a 500-600 nm thick $Ga_2Se_3$ film, both at 400°C and a 260-270 nm thick Cu layer at 350°C, performing a further annealing in vacuum at 400°C before selenization.

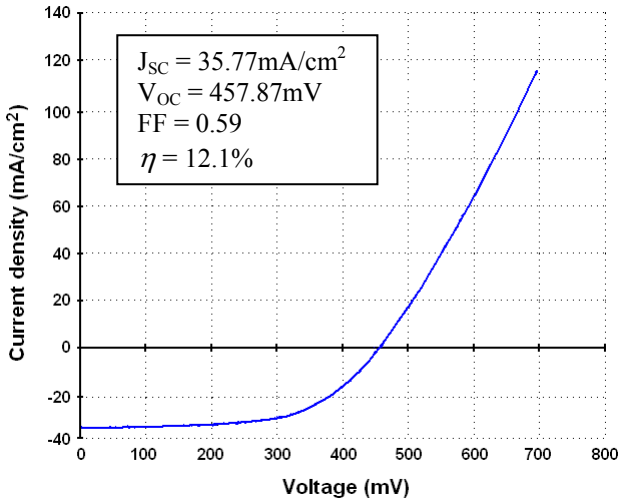


*Figure 77. J-V characteristic of a 0.5 cm$^2$ solar cellmade using $In_2Se_3$ , $Ga_2Se_3$ and Cu deposited on an enameled ceramic substrate. (measure performed in A.M. 1.5 condition, 25°C, 80 mW/cm$^2$ light irradiance).*

Best solar cells produced with this kind of absorber, have exhibited photovoltaic parameters like $V_{OC}$ in the range of 440-460 mV, $J_{SC}$ in the range of 30-36 mA/cm$^2$ , fill factor in the range of 59-61% and efficiency from 10 to 12% (Figure 77).

All the aspects, which let this process be considered innovative, have already been described. However, another important feature of this process, which makes it be much more different from the conventional ones used nowadays, is the introduction of the constituent atomic species into the growth system. They are introduced, in fact, by independent and consecutive depositions of the starting-material layers.

Normally, the most common kind of process used to grow a CIGS absorber layer, consists in depositing more constituents simultaneously, sometimes even all the four, by crossed depositions (mainly evaporations).
Nevertheless, these co-depositions lead the precursor material to grow with local differences in stoichiometry.
The particular geometry of the deposition system (different distances between crucibles and the substrate and also different incident angles of the arriving particles, coming from the different crucibles) and also the different behaviour of the chemical species used, easily cause a not uniform spatial distribution of the constituents and, in some cases, even localized agglomerations of different materials (segregations).
Starting from these conditions, the desired right mixing of constituents can't happen and a uniform precursor layer is difficult to be obtained. In addition, this interaction becomes very sensitive to the changes felt by the growth system, making the results not reproducible.
In this way only CIGS-based crystal islands can be obtained, surrounded by secondary phase agglomerations, which make this absorber material be not suitable for photovoltaic applications. Only if very precise and expensive controls are performed on the main deposition parameters, these problems can be solved and very good absorber materials can be obtained, for producing record solar cells.

In this new kind of process the peculiarity of depositing superposed layers, one after each other, guarantees instead that the substrate's surface, as well as every further layer are completely covered by the next material in a more uniform way, avoiding local differences in composition. During the selenization, which happens after the material depositions, the mix and the interaction of constituents occur between layers and no more between agglomerations of different materials, resulting more uniform and homogeneous.

This strategy allows to obtain, quite easily, a polycrystalline CIGS absorber layer, spatially uniform and suitable for solar cells, characterised by a very small, in some cases almost absent, amount of segregations.
Moreover, adding severally the constituents to the system lets the growth process be much more simplified, since the thermodynamic and compositional variables active during the material growth are reduced in number.
In these conditions the growth mechanism can be more precisely controlled, promoting a high reproducibility in the results.

# Future perspectives

It is clear that in order to obtain higher-efficiency CIGS-based thin film solar cells, it is really necessary to produce a $Cu(In,Ga)Se_2$ absorber material with better morphological and compositional properties.

The basics of a suitable process for the production of CIGS thin films have been established and very good results have been obtained, but there is still much work to do, to optimize and to improve these results.

For example, by spectroscopic or compositional investigations focused onto Sodium concentration and mainly on its distribution into the CIGS layer, as a function of the process conditions, it could be possible to understand how it can eventually affect the CIGS growth mechanism, its doping level and how to modify the Na concentration, to improve the electrical properties of the growing material.

By checking, with morphological and compositional measurements, how the substrate temperature, the Se amount and the time-length of the selenization process influence the transformation of the growing material, it could be possible to adjust both the method of providing Se and also its concentration into the precursor, in order to let it transform into CIGS in the best way.

So far, only few experiments have been performed with the CSS selenization method, but this technique could allow to obtain even better results, thanks to the more confined and uniform interaction between the precursor material and the Se vapour.
Moreover, substituting the selenization by evaporation with the CSS technique, the process will be even more scalable from the industrial production point of view.

Even if the Gallium graded profile produced into the absorber layer has given very good results, it is just a preliminary outcome.
Optimizing its concentration profile, mainly adjusting the Ga concentration at the back and at the top of the CIGS layer, it is expected to improve more the solar cell performances.
Testing even other In-, Ga- and Cu-based starting materials, like for example In-S and Ga-S based compounds, it could be eventually promoted a better matching between the solar light spectrum and the energy gap of the absorber material, increasing even more the device photovoltaic conversion efficiency.
At that point the process will be perfectly suitable for being transferred on large scale production.
Therefore, with a better and more uniform composition of the CIGS material, the absorber could be produced in thinner films, giving rise to a new generation of very thin devices.
Moreover, by using less material, the production costs would strongly decrease and, as a consequence, the final price and the energy pay-back time of these devices would be reduced, allowing to reach the grid parity condition more easily.

So far, only Cu coupled with $In_2Se_3$ and $Ga_2Se_3$ have been tested onto ceramic substrates.
It would be fascinating to experiment also the InSe and the GaSe, to check their different behaviour, in order to obtain even better photovoltaic parameters, which could lead to an improvement in the building integration potential of these devices.

In the next future, it is thought to experiment metallic foils as substrates, with the aim of producing flexible solar cells.
Transferring this simple process onto flexible substrates, the competitiveness of this technology will be further enhanced, increasing also the potential applications of these devices especially on curved or not stiff surfaces.

A laser scribing procedure is going to be set-up, by which the series electrical interconnection of adjacent solar cells produced onto the same full-area substrate can be made.
This system seems to fit very well the so-developed process, dividing the films deposited onto the whole substrate in a special pattern, making these interconnections completely integrate into the final device.

Next step will be the construction of a bigger deposition machine, suitable to host 30x30 $cm^2$ area substrates, with which mini-modules either on glass, ceramic tiles or even metal foils can be produced.
In fact, up to now the main limit of CIGS technology is the difficulty of producing uniform and homogeneous films onto big area substrates.
This will be an intermediate, but very important stage, since it will check the real possibility of obtaining good and uniform photovoltaic materials onto more extended-area substrates, in order to further transfer this process to an industrial scale, for the production of high efficiency photovoltaic modules.

# Conclusion

In this PhD thesis work it has been developed an innovative process for the deposition of $Cu(In,Ga)Se_2$ thin films, suitable for the production of high efficiency solar cells.

This process requires only simple and easily scalable techniques, like sputtering and selenization with pure Selenium.
Moreover, it is a completely-dry process, which doesn't need any use of wet solutions or hazardous chemicals for the material deposition or treatment.
From an industrial production point of view this is a very important aspect, since it prevents from the storage and the handling of wet chemicals, helping the reduction of the production costs.

It has been found the correct procedure to deposit a good Mo bi-layer back contact, overcoming the usual problems of sticking and electrical conductivity.

It has been possible to deposit and to grow CIGS thin films with a high morphological and compositional uniformity onto the whole 1 inch square area soda-lime glass substrates, obtaining many solar cells onto the same substrate, which are able to exhibit similar photovoltaic parameters.

It has been found out an alternative strategy for depositing the buffer CdS layer by sputtering on larger areas, overcoming the common troubles related to its thickness and compositional homogeneity.

By sputtering starting materials like $In_2Se_3$ $Ga_2Se_3$ and Cu it has been possible to produce good solar cells, which exhibit $V_{OC}$ in the range of 510-530 mV, $J_{SC}$ in the range of 28-32 $mA/cm^2$ , fill factor in the range of 52-58% and energy conversion efficiencies from 11 to 12%.

This technology has been well transferred also onto ceramic substrates, obtaining solar cells, which have exhibited $V_{OC}$ in the range of 440-460 mV, $J_{SC}$ in the range of 30-36 $mA/cm^2$ , fill factor in the range of 59-61% and efficiencies from 10 to 12%.

Substituting the $In_2Se_3$ and the $Ga_2Se_3$ with InSe and GaSe respectively, it has been possible to promote a better interaction between the constituents materials, obtaining an absorber material with a superior crystallization quality and a higher superficial Ga concentration, which has resulted in devices with higher open-circuit voltages.
Solar cells produced with this CIGS material have exhibited higher photovoltaic parameters. Typical values are : $V_{OC}$ of about 550 mV, $J_{SC}$ of about 35 mA/cm$^2$ , fill factor of about 65% and energy conversion efficiencies of 15%.

Finally, by depositing at well-defined substrate temperatures a specific sequence of the starting materials, it has been possible to regulate the Ga concentration profile, into the absorber layer, by acting on the precursor structure. In this way a Ga multi-graded absorber layer is obtained.
The best results have been obtained by depositing in sequence films of InSe, GaSe, Cu and GaSe, in proper thickness ratios and performing a unique selenization stage.
Solar cells produced with such an absorber material, constituted by sequence of a 2 μm thick InSe film, a 360 nm thick GaSe layer, a 400 nm thick Cu film and a 480 nm thick GaSe layer and further selenized in pure Se, have exhibited the following photovoltaic parameters: $V_{OC}$ of about 576 mV, $J_{SC}$ of about 38 mA/cm$^2$, fill factor of about 74% and energy conversion efficiencies higher than 16%.

In conclusion, this process has demonstrated to have all the qualifications for being successfully transferred to the industrial scale level, making real the possibility to produce high efficiency photovoltaic modules which could be very competitive even in the global photovoltaic market.

# REFERENCES


[1] EIA, U.S. Energy Information Administration, International Energy Outlook 2011, DOE/EIA-0484, 2011

[2] EPIA, Solar Generation 6, Solar photovoltaic electricity empowering the world, February 2011

[3] IEA, Technology Roadmap, Solar photovoltaic energy, 2010

[4] V. M. Fthenakis, P. D. Moskowitz, "Photovoltaics: Environmental, Health and Safety Issues and Perspectives", Prog. Photovolt. Res. Appl. 8, pp. 27-38, 2000

[5] SolarBuzz, Solar Market Research and Analysis, January 2012

[6] Europe's Energy Portal, October 2012

[7] M.A. Green, "The Path to 25% Silicon Solar Cell Efficiency: History of Silicon Cell Evolution", Prog. Photovolt: Res. Appl. 17, pp. 183-189, 2009

[8] O. Schultz, S.W. Glunz, G.P. Willeke, "Multicrystalline silicon solar cells exceeding 20% efficiency", Progress in Photovoltaics: Research and Applications 12, pp. 553-558, 2004

[9] S. Benagli, D. Borrello, E. Vallat-Sauvain, J. Meier, U. Kroll, J. Hötzel, J. Spitznagel, J. Steinhauser, L. Castens, Y. Djeridane, "High-efficiency amorphous silicon devices on LPCVD-ZnO TCO prepared in industrial KAI-M R&D reactor", 24th European Photovoltaic Solar Energy Conference, Hamburg, September 2009

[10] X. Wu, J.C. Keane, R.G. Dhere, C. DeHart, A. Duda, T.A. Gessert, S. Asher, D.H. Levi, P. Sheldon, "16.5%-efficient CdS/CdTe polycrystalline thin-film solar cell", in: Proceedings of the 17th European Photovoltaic Solar Energy Conference, Munich, pp. 995-1000, 22-26 October 2001

[11] First Solar, http://investor.firstsolar.com/releasedetail.cfm?ReleaseID=639463

[12] S. Wagner, J.L. Shay, P. Migliorato, H.M. Kasper, Appl. Phys. Lett. 25, p. 434, 1974

[13] W.E. Devaney, R.A. Michelsen, W.S. Chen, 18th IEEE Photovoltaic Specialists Conference, IEEE Publishing, NY, p. 173, 1985

[14] P. Jackson, D. Hariskos, E. Lotter, S. Paetel, R. Wuerz, R. Menner, W. Wischmann, M. Powalla "New world record efficiency for Cu(In,Ga)$Se_2$ thin-film solar cells beyond 20%", Prog. Photovolt: Res. Appl. 19, pp. 894-897, 2011

[15] E.A. Alsema, M.J. de Wild-Scholten, V.M. Fthenakis, "Environmental impacts of PV electricity generation - a critical comparison of energy supply options", Presented at the 21st European Photovoltaic Solar Energy Conference, Dresden, Germany, 4-8 September 2006

[16] http://www.trefis.com/stock/fslr/articles/60278/first-solar-can-hit-144-with-rock-bottom-production-costs/2011-07-01

[17] EPIA, Global Market Outlook for Photovoltaics until 2016, May 2012

[18] M. Gloeckler, J.R. Sites, "Band-gap grading in Cu(In,Ga)$Se_2$ solar cells", Journal of Physics and Chemistry of Solids 66, Issue 11, pp. 1891-1894, November 2005

[19] M.A. Green, "Solar cells : operating principles, technology, and system applications", c1982, Englewood Cliffs, N.J. : Prentice-Hall, ISBN: 0138222703

[20] S.M. Sze, "Physics of Semiconductor Device", Wiley Interscience Publication, New York, 1981, pp. 848-849

[21] A. Luque, S. Hegedus, "Handbook of Photovoltaic Science and Engineering", 2nd edition, 2011, Wiley, Chichester, West Sussex, United Kingdom, ISBN 978-0-470-72169-8

[22] R.H. Bube ," Photovoltaic Materials", Properties of Semiconductor Materials Volume 1, 1998, Imperial College Press, London, ISBN: 1-86094-065-X

[23] M.-R. A. Magomedov, Dzh. Kh. Amirkhanova, Sh. M. Ismailov, P.P. Khokhlachev, R.Z. Zubairuev, Tech. Phys. 42 (3), March 1997

[24] S.B. Zhang, S.-H. Wei, A. Zunger, H. Katayama-Yoshida, "Defect physics of the $CuInSe_2$ chalcopyrite semiconductor", Phys. Rev. B 57, N. 16, pp. 9642-9656, 1998

[25] M.A. Contreras, B. Egaas, P. Dippo, J. Webb, J. Granata, K. Ramanathan, S. Asher, A. Swartzlander, R. Noufi, "On the Role of Na and Modifications to Cu(In,Ga)$Se_2$ Absorber Materials Using Thin-MF (M=Na, K, Cs) Precursor Layers", Presented at the 26th IEEE Photovoltaic Specialists Conference, Anaheim, California, September 29-October 3, 1997

[26] D. Braunger, D. Hariskos, G. Bilger, U. Rau, H.W. Schock, "Influence of sodium on the growth of polycrystalline Cu(In,Ga)$Se_2$ thin films", Thin Solid Films 361-362, pp. 161-166, 2000

[27] D.J. Schroeder, A.A. Rockett, "Electronic effects of sodium in epitaxial $CuIn_{1-x}Ga_xSe_2$", J. Appl. Phys. 82, p. 4982, 1997

[28] D. Wolf, G. Müller, W. Stetter, F. Karg, J. Schmid, H.A. Ossenbrink, P. Helm, H. Ehmann, E.D. Dunlop, "In-situ investigation of Cu–In–Se reactions: impact of Na on CIS formation", in: Proceedings of the 2nd World Conference on Photovoltaic Solar Energy Conversion, Vienna, pp. 2426-2429, 1998

[29] S.-H. Wei, S.B. Zhang, A. Zunger, J Appl. Phys. 85, 7214, 1999

[30] R. Kimura, T. Mouri, T. Nakada, S. Niki, A. Yamada, P. Fons, T. Matsuzawa, K. Takahashi, and A. Kunioka, "Effects of Sodium on $CuIn_3Se_5$ Thin Films", Jpn. J. Appl. Phys., vol. 38, pp. L899-L901, 1999

[31] J.F. Guillemoles, L. Kronik, D. Cahen, U. Rau, A. Jasenek, H.W. Schock, J. Phys. Chem. B 104, p. 4849, 2000

[32] T. Wada, N. Kohara, S. Nishiwaki, T. Negami," Characterization of the Cu(In,Ga)$Se_2$/Mo interface in CIGS solar cells", Thin Solid Films, Volume 387, Issues 1-2, pp. 118-122, 29 May 2001

[33] D. Schmid, M. Ruckh, H.W. Schock, Sol. Energy Mater. Sol. Cells 41/42, p. 281, 1996
[34] H.W. Schock, U. Rau, Physica B 308-310, p. 1081, 2001
[35] J.F. Guillemoles, P. Cowache, A. Lusson, K. Fezzaa, F. Boisivon, J. Vedel, D. Lincot, J. Appl. Phys. 79, p. 7293, 1996
[36] R.J. Schwartz, J.L. Gray, Conf. Rec. 21st IEEE Photovolt. Spec. Conf., p. 570, IEEE, 1990
[37] J.H. Scofield, A. Duda, D. Albin, B.L. Ballard, P.K. Predecki, "Sputtered Molybdenum Bilayer Back Contact for Copper Indium Diselenide-Based Polycrystalline Thin-Film Solar Cells", Thin Solid Films, Volume 260, Issue 1, pp. 26-31, 1 May 1995
[38] S.-H. Wei, A. Zunger, J. Appl. Phys. 78, p. 3846, 1995
[39] K. Ramanathan, J. Keane, R. Noufi, " Properties of High-Efficiency CIGS Thin-Film Solar Cells", 31st IEEE Photovoltaics Specialists Conference and Exhibition, Lake Buena Vista, Florida January 3-7, 2005
[40] R. Herberholz, V. Nadenau, U. Rühle, C. Köble, H.W. Schock, B. Dimmler, "Prospects of wide-gap chalcopyrites for thin film photovoltaic modules", Solar Energy Materials and Solar Cells 49, p. 227-237, 1997
[41] A. Bosio, N.Romeo, A. Podestà, S. Mazzamuto, V. Canevari, "Why $CuInGaSe_2$ and CdTe polycrystalline thin film solar cells are more efficient than the corresponding single crystal ?", Crystal Research and Technology, Vol. 40, 2005
[42] M.J. Hetzer, Y.M. Strzhemechny, M. Gao, M.A. Contreras, A. Zunger, L.J. Brillson, "Direct observation of copper depletion and potential changes at copper indium gallium diselenide grain boundaries", Applied Physics Letters 86, 162105, (2005)
[43] S.R. Kodigala, "Thin films and nanostructures, $Cu(In_{1-x}Ga_x)Se_2$ Based Thin Film Solar Cells", Volume 35, 2010, Elsevier, ISBN: 978-0-12-373697-0
[44] S. Schleussner, U. Zimmermann, T. Wätjen, K. Leifer, M. Edoff, "Effect of gallium grading in $Cu(In,Ga)Se_2$ solar-cell absorbers produced by multi-stage coevaporation", Solar Energy Materials and Solar Cells, Volume 95, Issue 2, pp. 721-726, February 2011
[45] T. Dullweber, U. Rau, M.A. Contreras, R. Noufi, H.W. Schock, "Photogeneration and Carrier Recombination in Graded Gap $Cu(In, Ga)Se_2$ Solar Cells", IEEE Transactions on electron devices, Vol. 47, No. 12, December 2000
[46] R. Chakrabarti, B. Maiti, S. Chaudhuri, A.K. Pal, "Photoconductivity of $Cu(In,Ga)Se_2$ films", Solar Energy Materials and Solar Cells 43, p. 237, 1996
[47] T.B. Massalski, "Binary Alloy Phase Diagrams", 2nd edition, Vol. 2, 1990, American Society for Metals, pp. 1410-1412
[48] Z. Bahari, E. Dichi, B. Legendre, J. Dugué, "The equilibrium phase diagram of the copper-indium system: a new investigation", Thermochimica Acta Volume 401, Issue 2, pp. 131-138, 2003
[49] C.H. Chang, A. Davydov, B.J. Stanbery, T.J. Anderson, Conf. Record of the 25th PVSC, pp. 849-852, 1996

[50] T.J. Anderson, O.D. Crisalle, S.S. Li, P.H. Holloway, "Future CIS Manufacturing Technology Development", NREL, Final Report 1998-2001

[51] M. Edoff, C. Platzer-Björkman, "Co-Evaporation of CIGS and Alternative Buffer Layers for CIGS Devices", in Thin Film Solar Cells: Current Status and Future Trends, 2010, Nova Science Publisher, Inc., ISBN: 978-1-61668-326-9

[52] M.A. Contreras, M.J. Romero, B. To, F. Hasoon, R. Noufi, S. Ward, K. Ramanathan, "Optimization of CBD CdS process in high-efficiency Cu(In,Ga)$Se_2$-based solar cells", Thin Solid Films 403-404, pp. 204-211, 2002

[53] K. Ramanathan, H. Wiesner, S. Asher, D. Niles, R.N. Bhattacharya, M.A. Contreras, R. Noufi, "High-Efficiency Cu(In,Ga)$Se_2$ Thin Film Solar Cells Without Intermediate Buffer Layers", Presented at the 2nd World Conference and Exhibition on Photovoltaic Solar Energy Conversion, Vienna, Austria, 6-10 July 1998

[54] A. Rockett, D. Liao, J.T. Heath, J.D. Cohen, Y.M. Strzhemechny, L.J. Brillson, K. Ramanathan , W.N. Shafarman, "Near-surface defect distributions in Cu(In,Ga)$Se_2$", Thin Solid Films 431-432, pp. 301-306, 2003

[55] T. Nakada, A. Kunioka, "Direct evidence of Cd diffusion into Cu(In,Ga)$Se_2$ thin films during chemical-bath deposition process of CdS films", Appl. Phys. Lett. 74, p. 2444, 1999

[56] Z.R. Khan, M. Zulfequar, M.S. Khan, "Effect of thickness on structural and optical properties of thermally evaporated cadmium sulfide polycrystalline thin films", Chalcogenide Letters Vol. 7, No. 6, pp. 431-438, June 2010

[57] S. Ray, R. Banerjee, N. Basu, A.K. Batabyal, A.K. Barua, "Properties of tin doped indium oxide thin films prepared by magnetron sputtering", J. Appl. Phys. 54, p. 3497, 1983

[58] Y. Shigesato, S. Takaki, T. Haranou, Appl. Surf. Sci. 48/49, p. 269, 1991

[59] R. Bel Hadj Tahar, T. Ban, Y. Ohya, Y. Takahashi, "Tin doped indium oxide thin films: Electrical properties", J. Appl. Phys. 83, pp. 2631-2645, 1998

[60] Z. Qiao, "Fabrication and study of ITO thin films prepared by magnetron sputtering", PhD dissertation, 2003, http://duepublico.uni-duisburg-essen.de/servlets/DerivateServlet/Derivate-11635/Dissertation_Qiao.pdf

[61] T.A. Gessert, Y. Yoshida, C.C. Fesenmaier, T.J. Coutts, "Sputtered $In_2O_3$ and ITO thin films containing zirconium", J. Appl. Phys., 105, 083547/1-7, 2009

[62] S. Uthanna, T.K. Subramanyam, B. Srinivasulu Naidu, G. Mohan Rao, "Structure-composition-property dependence in reactive magnetron sputtered ZnO thin films", Optical Materials 19, pp. 461-469, 2002

[63] B.E. McCandless, K. Dobson, Solar Energy 77, pp.839-856, 2004

[64] J. Vossen, W. Kern, "Thin Film Processes", New York: Academic Press, Inc., 1978

[65] N. Romeo, A. Bosio, S. Mazzamuto, D. Menossi and A. Romeo, "CIGS Thin Films Prepared by Sputtering and Selenization by using $In_2Se_3$, $Ga_2Se_3$ and Cu as Sputtering Targets", in: Proceedings of 35th Photovoltaic Specialists Conference (PVSC), Honolulu, Hawaii, IEEE, pp. 786-788, 20-25 June 2010

[66] N. Romeo, A. Bosio, V. Canevari, in Proc. of 3rd World Conference on Photovoltaic Energy Conversion, WCPEC-3, Osaka, Japan, pp. 469-470, 11-18 May 2003

[67] F. Börner, J. Gebauer, S. Eichler, R. Krause-Rehberg, I. Dirnstorfer, B.K. Meyer, F. Karg, "Defects in CuIn(Ga)$Se_2$ solar cell material characterized by positron annihilation: post-growth annealing effects", Physica B: Condensed Matter, Volumes 273-274, pp. 930-933, 1999

[68] T. Sakurai, N. Ishida, S. Ishizuka, M.M. Islam, A. Kasai, K. Matsubara, K. Sakurai, A.Yamada, K. Akimoto, S. Niki, "Effects of annealing under various atmospheres on electrical properties of Cu(In,Ga)$Se_2$ films and CdS/Cu(In,Ga)$Se_2$ heterostructures", Thin Solid Films 516, pp.7036-7040, 2008

[69] Y.D. Chung, D.H. Cho, N.M. Park, K.S. Lee, J.K., "Effect of annealing on CdS/Cu(In,Ga)$Se_2$ thin-film solar cells", Current Applied Physics, Volume 11, Issue 1, Supplement, pp. S65-S67, January 2011

[70] F.-J. Haug, H. Zogg, A.N. Tiwari, "11% efficiency on CIGS superstrate solar cells without sodium precursor", 29th Photovoltaic Specialists IEEE Conference - PVSC, pp. 728-731, 2002

[71] F. Engelhardt, M. Schmidt, T. Meyer, O. Seifert, L. Bornemann, R. Harney, J. Parisi, W. Riedl, F. Karg, M. Schmidt, U. Rau, "Reversible changes in the electrical transport properties of Cu(In,Ga)$Se_2$ thin films and solar cells", in: Proceedings 14th European Photovoltaic Solar Energy Conference, Barcelona, pp. 1234-1237, 1997

[72] V. Nadenau, U. Rau, A. Jasenek, and H.W. Schock, "Electronic properties of $CuGaSe_2$-based heterojunction solar cells. Part I. Transport analysis", J. Appl. Phys. 87, p. 584, 2000